# High Resolution Infrared Spectroscopy
# of
# Molecular Clusters

A thesis submitted to
The Australian National University
for the degree of Doctor of Philosophy

Glenn Walter Ross Bryant

July 1989

## Statement

I hereby declare that this thesis is my own work and that, to the best of my knowledge and belief, it contains no material previously published or written by another person, nor material which to any substantial extent has been accepted for the award of any other degree or diploma of a university or other institute of higher learning, except where due acknowledgement is made in the text of the thesis.

Glenn Bryant

Glenn Walter Ross Bryant

3 July 1987.

## Acknowledgements

I would like to thank my supervisor, Prof. R.O. Watts, for his patience, tolerance and encouragement during my time with him.

I am also indebted to Prof. R.W. Crompton for allowing me to study in his group at the Research School of Physical Sciences, ANU, and for his constant interest and assistance with my progress.

There are a number of other people at the Research School who I would like to thank for their assistance and encouragement: Dr. T. Rhymes and all the other members of the Electronics Unit, Mr. K. Jackman, Mr. K. Roberts and the technical staff, and Dr. S. Buckman.

Special thanks to Prof. B. Orr for his hospitality, support, and suggestions. Also to Prof. D.F. Eggers for our many enlightening trans-Pacific discussions, and providing band-contour analysis programs. The provision of high-resolution data on the acetylene bands by Dr. W.J. Lafferty is also gratefully acknowledged.

Financial support from a Commonwealth Postgraduate Research Award is gratefully acknowledged.

I owe my family many thanks for their patience, understanding and support.

Finally to my wife Sue, and our son Nicholas, my deepest thanks for their constant encouragement and thoughtfulness, and their endurance over this rather protracted period of our lives.

## Abstract

The tuning of a single-mode F-centre laser has been placed under the control of a microcomputer, and this has been used to measure the infrared spectra of acetylene clusters in the 3250-3300 $cm^{-1}$ region with high resolution (0.0004 $cm^{-1}$). These clusters were formed in a supersonic expansion, and their dissociation upon vibrational excitation was detected via the optothermal method.

The rotational structure of two of the observed bands has been assigned and is found to arise from the acetylene dimer, in a T-shaped configuration. Transitions within these bands show a number of perturbations through Fermi or Coriolis interactions with unidentified states. In addition, each transition has three components, which have been explained elsewhere (i.e. not in this work) by an interconversion tunnelling motion in the dimer.

Another band was analysed and assigned to the acetylene trimer, with a planar, cyclic structure, while two more bands are identified as belonging to the acetylene tetramer with a similar cyclic structure, although it is non-planar. Finally, one band has been assigned to the pentamer, again having a cyclic, non-planar configuration.

All of the structures are consistent with a weak hydrogen bonding interaction between acetylene molecules.

This work has been presented in part in the following publications :

G.W. Bryant, D.F. Eggers and R.O. Watts, High-resolution infrared spectroscopy of acetylene clusters *J.Chem.Soc.Farad.Trans.2*, **84** (1988) 1443.

G.W. Bryant, D.F. Eggers and R.O. Watts, High-resolution infrared spectrum of acetylene tetramer, *Chem.Phys.Lett.*, **151** (1988) 309.

# Addendum

My apologies to Ludwig Boltzmann and Peter Vohralik for consistently misspelling their surnames throughout this thesis.

p55, 1st paragraph - "consequential" should be "consequently"

p62, 1st paragraph - "3265.0477 $cm^{-1}$" should be "3266.0477 $cm^{-1}$"

p84, 3rd paragraph - the units of the C-H bond length changes are Å

p85, 2nd paragraph - "Reduction of" should be "Increasing"

A number of the Figures showing spectra are plotted without an *x*-axis label. This label should be "Wavenumber /$cm^{-1}$".

## On hydrogen-bonding in acetylene clusters:

Despite the large amount of theoretical and experimental work on molecular complexes, the definition of what constitutes a hydrogen-bond remains rather *ad hoc*. A universal, albeit broad, definition might be that hydrogen bonding is an attractive interaction involving a hydrogen atom in the vicinity of the intermolecular bond. Using this definition alone, the structures of acetylene clusters presented in this work, which are supported by *ab initio* calculations on the dimer and trimer performed elsewhere, can be considered hydrogen-bonded: in each case a hydrogen atom of one molecule can be found near a line joining the molecular centres. It therefore seems logical to look for other signatures of hydrogen-bonding.

The observation of large shifts in the of the $\nu_s$ (A-H) stretching vibration to lower frequencies, along with an increase in the intensity of this band, is indicative of systems undergoing hydrogen-bonding. The explanation of this behaviour involves electrostatic interactions with the binding partner that reduce the A-H bond force constant and increase the bond length. Often the magnitude of the shift can be correlated with the strength of the interaction. This red shift is observed in the acetylene cluster spectra (and in the spectrum of crystalline acetylene), adding support to the conclusions based on a purely structural interpretation.

Whilst the increase in the red shift of $\nu_s$ (C-H) with increasing cluster size fits nicely with the *ab initio* result that the binding energy per monomer increases from dimer to trimer, there are other effects that may play a role in shifting this vibrational frequency. These include possible coupling to the newly created intermolecular bond vibrations, as well as to internal vibrations, such as the symmetric C-H stretch, in the lower symmetry environment found in the cluster. Relating the increasing red shifts to reductions in C-H force constants relies on a thorough to analysis of the vibrations of each cluster in order to account for such couplings. The statements found in the Conclusion (p84) on the possibility of hydrogen-bonding in acetylene clusters are thus an oversimplification.

# Table of Contents

# Table of Figures

# Table of Tables

# Chapter 1: Introduction

The condensation of gases to form liquids and solids is perhaps the most obvious manifestation of the forces of attraction between molecules. Since the equation of state proposed by van der Waals can be interpreted in terms of both repulsive and attractive intermolecular interactions, the latter have become known as "van der Waals forces". The elucidation of the nature of these forces and their implications on the bulk properties of matter has long been one of the central themes of chemical physics, and to that end the study of van der Waals (vdW) clusters - aggregates of atoms and molecules held together by weak interactions - holds much promise. Indeed, as well as information on intermolecular potentials, one might hope that by studying systems of increasing degrees of aggregation, the gap between molecular and solid state physics might be bridged, and an understanding of such things as solvation and surface structure may be achieved on the molecular level. In addition, the weak nature of the binding in these systems has important dynamic implications, since only moderate excitation is sufficient to break the cluster apart. Thus vdW clusters have become an important tool in the investigation of energy transfer and redistribution in unimolecular reactions.

Such is the interest in these systems that the literature on them is extensive, and has fortunately been the subject of a number of excellent reviews. The article of Beswick and Jortner (1981) contains a comprehensive bibliography of the earlier work on vdW molecules, while that of Castleman and Keesee (1986) presents examples of the many directions cluster research has taken.

It has been the development of the supersonic free jet and complementary spectroscopic techniques that created such intense activity in the field. Spectroscopy of simple systems (atom-atom and atom-diatom complexes) has brought new information on the details of the relevant interaction potentials (well depth and anisotropy for example), while for larger systems equilibrium structures and binding energies have been determined, which can be compared with the predictions of model intermolecular interactions (Buckingham 1986).

The spectroscopic study of vdW systems can also yield information on the time-dependent behaviour of excited states (Beswick 1981). The vibrational energies of constituent molecules, and even the rotational energy of the complex as a whole, are sufficient to overcome the binding energy of the cluster. The excited cluster can be viewed as being in a kind of resonance state (see, for example, the articles in (Truhlar 1984)) and the study of the decay of such states - the processes of rotational and vibrational predissociation - has become an area of intense theoretical and experimental investigation, (Janda 1985, Celii 1986, Brumer 1985). The quantities of interest are the energy of the state, it's lifetime and the branching ratios to possible decay channels.

Theoretically the resonance states are associated with poles in the scattering matrix with total energy

$$W = E - ih/4\pi\tau$$

where $E$ is the energy of the state and $\tau$ it's lifetime. The latter determines the position of the spectral feature, while the state lifetime is related to the energetic width of the state $\Gamma$ by

$$\tau = h/2\pi\Gamma$$

which in turn manifests itself as an homogeneous broadening of the observed lines if $\tau$ is sufficiently small. Thus two of the characteristics of these states can be derived from spectroscopic measurements. The calculation of these quantities is amenable to techniques used in scattering theory (Truhlar 1984), but at present the complexity of a fully quantum mechanical treatment of the problem limits such work to atom-diatom complexes. For polyatomic systems recourse is made to approximate calculations, such as the "Energy Gap" model of Ewing (Ewing 1982). Here the propensity for dissociation is related to the amount of energy that must be transferred from the internal degrees of freedom to translational motion in the vdW coordinate - the larger this amount of energy is for a particular decay channel, the slower the decay rate.

Where the resonances are well separated, i.e. narrow and/or widely spaced, quantum numbers may be assigned to the metastable state (in particular $v$ and $J$), so that the standard methods of spectroscopic analysis become applicable (Herzberg 1945). In other words, if the metastable states are long lived relative to characteristic times of the complex (vibrational and rotational periods, for instance), they may be treated as bound for the sake of analysing the spectral features, and the latter are a source of structural information.

## 1.1 Spectroscopic Studies of van der Waals Molecules

The small inertial constants of van der Waals systems results in the congestion of spectral features into relatively narrow regions. Consequently high-resolution spectroscopic techniques must be used to examine the energy level structure of these species in detail, particularly when one is interested in the widths of these levels.

The earliest studies of van der Waals molecules were performed in low pressure, low temperature gas cells, using Long Path Length IR absorption spectroscopy. Such experiments are generally complicated by interfering absorptions of monomeric species, collisional effects and sequence congestion due to the low frequency vibrations of the vdW bonds (Sandorfy 1984, Legon 1986). Despite these difficulties the utility of this method for simple systems has been demonstrated in a number of cases :

McKellar and co-workers (McKellar 1982), using a conventional grating spectrometer with instrument resolution < 0.1 $cm^{-1}$, have examined the spectra of rare gas-hydrogen complexes, which appear as fine-structure on top of the broad, collision-induced band of the $H_2$ fundamental. They were able to resolve line splitting caused by the anisotropy of the intermolecular potential, and these results have been used in conjunction with other experimental data to determine an accurate, three-dimensional potential-energy surface (LeRoy 1987). The availability of this surface has in turn lead to these systems becoming the testing ground for methods of calculating the widths and energies of predissociating states (LeRoy 1982). However, only in the case of HD-Ar, and one transition of $H_2$-Kr, has the lifetime broadening been sufficient to be observable at the resolution of the experiments, to allow a direct comparison of theory and experiment (Kidd 1986). More recent work on this system can be found in the articles in (Weber 1987).

A difference-frequency laser has been used by Pine and co-workers to obtain the spectra of $(HF)_2$ and $(DF)_2$ (Pine 1984), $(HCl)_2$ (Ohashi 1984), Ar-HCl (Howard 1985) and X-HF, where X=Xe,Kr & Ar (Fraser 1986) with Doppler-limited resolution (about 100MHz). The HF dimer was the first system to display mode-specific vibrational predissociation lifetimes : no excess broadening was observable in "free" HF stretching region, while the "bound" HF stretch has a lifetime component in it's linewidth of some 300MHz (see Figure 1.1). This was not observed in the HCl dimer. Halberstadt *et.al.* (1985) have subsequently performed calculations on the linewidth and final rotational state distribution of the excited proton donor monomer in $(HF)_2$, and obtained a value for the linewidth that is comparable to the experiment. Pine and Howard (Pine 1986) have been able to obtain estimates of the well depths and dissociation energies of the HF and HCl dimers from the line strengths in the infrared bands. The spectra of X-HCl and X-HF provide information about the interaction potentials - specifically the well depth, and to some extent the anisotropy.

Bevan *et.al.* have used FTIR to examine HCN-HF (Wofford 1986a, Legon 1986) and DCN-DF (Jackson 1987), and the HCN dimer (Wofford 1986b) with an instrument resolution of about 150MHz. The HCN-HF complex is the most extensively studied H-bonded system to date, and all the intramolecular vibrations have been examined at this resolution. A great deal has thus been learned about the IR spectroscopy of this complex, which has also been found to display predissociation lifetimes that depend on the vibrational mode excited. A study of the $\nu_1$ (H-F stretch) band using a continuously tunable F-centre laser (Bender 1987) displayed broad lines (FWHM = 3GHz), and the effects of Coriolis perturbations from nearby (combination) vibrational states manifest themselves as changes in the positions, intensities, linewidths and number of lines observed for a given rotational quantum number *J*.

In all of the above examples the determination of the excess broadening due to vibrational predissociation required the deconvolution of instrumental, Doppler and pressure broadening effects from the observed lineshapes. The advent of free jets and molecular beams provided a new source of vdW molecules to which a wide range of spectroscopic techniques have been applied. Beams offer a number of advantages over gas-cells :

- the concentration of clusters can be made relatively high;
- a wide range of cluster sizes and types can be produced;
- the cooling that occurs during the expansion substantially reduces the number of populated states, which in turn reduces the spectral congestion;
- the use of well collimated beams offers a substantial reduction in the contribution of the Doppler effect to the spectral linewidth, which opens up the possibility of high resolution spectroscopy using tunable, narrow-band sources.

One complicating factor is the distribution of cluster sizes that can be produced in an expansion. Unless the spectral features of the different clusters are well separated, some sort of mass discrimination must be employed to examine the spectrum of a cluster of a particular size. Alternatively very dilute seeded beams may be used to ensure that only the lower order clusters are present. The dependence of the spectra on source backing pressure and component concentrations might also be used to assign features to a cluster of a particular size. The low temperatures obtained in an expansion mean that only the deepest parts of the potential minimum are probed in beam experiments. In addition, level populations can have non-Boltzman distributions which can complicate the analysis of spectral line intensities.

We can divide up the molecular beam spectroscopic techniques used to study these systems according to the excited state energy levels they probe:

### 1.1.1 Rotational Spectroscopy

Rotational spectroscopy of clusters formed in a molecular beam generally involves the study of bound-bound transitions in the ground vibrational state, so that predissociation is not observed. The two principle techniques used to examine the radio-frequency and microwave spectra of vdW and hydrogen-bonded complexes have been outlined several times (Dyke 1984, Legon 1986, Legon 1983, Klemperer 1974).

The use of Molecular Beam Electric Resonance (MBER) in cluster spectroscopy was pioneered by Klemperer and co-workers, and first used to examine the spectrum of the HF dimer (Dyke 1972); it offers some degree of cluster selectivity by using a mass spectrometer to detect the molecular beam. Pulsed Molecular Beam Fourier Transform Microwave Spectroscopy was developed by Flygare (Balle 1981) and has been used by Legon and Millen to

examine hydrogen-bonded heterodimers. The main results of these studies are the structural parameters for dimeric systems, and the articles of Legon and Millen (1986) and Peterson *et.al.* (1985) contain summaries of such parameters for many of the systems studied using these techniques. These methods rely on the species under investigation having a dipole moment, and since "homogeneous" clusters (i.e. only one type of molecule in the cluster ) larger than the dimer have generally been found to be non-polar, such systems have eluded scrutiny with these powerful techniques. This is not the case for "heterogeneous" clusters and Gutowsky *et.al.* (1987) have begun to extend the size of such systems studied, examining the $Ar_2$-HF and $Ar_3$-HF systems using the Flygare method. Since no mass selectivity is available with this technique, spectral features belonging to each species had to be extracted from the total beam spectrum.

## 1.1.2 Vibrational Spectroscopy

Ro-vibrational spectroscopy offers similar possibilities for structure determination as the methods above, and is not restricted to polar species. In addition it provides a method of investigating the process of predissociation.

Again there are a number of reviews of the study of the infrared spectra and vibrational predissociation of vdW molecules in the literature (Nesbitt 1988, Miller 1986, Celii 1986). These provide good summaries of a great deal of the work in the field.

**Direct Absorption:** This is generally applied to a free jet rather than a collimated beam, because of the latter's longer optical path, and the higher density achievable in a pulsed nozzle (for a given pumping speed) makes them the preferred choice. Howard *et.al.* (in Weber 1987) have used a diode laser spectrometer to examine the spectra of X-OCS, X=Ne,Kr,Ar with an instrument width of 120MHz. They were not able to perceive any broadening due to lifetime effects at this resolution, but analysed the observed ro-vibrational structure to confirm the structure derived from microwave studies.

Nesbitt *et.al.* have used a combination of a slit source, to increase the path length, and a difference frequency laser spectrometer to obtain high resolution spectra of $N_2$-HF (Lovejoy 1986), Ar-HF (Lovejoy 1987a), and $CO_2$-HF (Lovejoy 1987b). Only in the last case did they observe broadening in excess of the apparatus resolution (25MHz). In addition, they have been able to observe hot bands of the low-frequency intermolecular vibrations.

Barnes and Gough have reported using FTIR to examine $(CO_2)_n$ (1987) and $(SF_6)_n$ (1987) clusters in a free jet at rather low resolution, with the aim of inferring structural details about them from the observed spectra.

**Laser-Induced Dissociation:** Klemperer (1974) proposed that the vibrational predissociation of $(HF)_2$ might be observed as the depletion of the relevant ion peak when a molecular beam detected by a mass spectrometer is crossed with an infrared laser of an appropriate wavelength. This proposal has been put into practice with $CO_2$ lasers to study a number of systems, as summarized in the article by Gentry in (Truhlar 1984). In particular, ethylene clusters have received a great deal of attention. One problem with using a mass spectrometer to detect clusters is that these weakly bound species can fragment upon ionization, so that larger clusters may contribute to the mass peaks of smaller ones. To overcome this, Huisken and Pertsch (1987) applied the scattering technique developed by Buck and Meyer (1986a) to observe the dissociation spectra of $(C_2H_4)_n$, n=2-5, free from the fragmentation problem. They concluded that earlier work was complicated by this effect, but that the spectra were structureless and had the same width and peak position for each n. However, their earlier work suggests that not all of the linewidth is due to lifetime effects.

In addition to the $CO_2$ laser work, Lisy and co-workers have used an OPO to examine a number of systems in the 3μm region, including water clusters (Vernon 1982), the benzene dimer and trimer (Vernon 1981), the HF trimer (Michael 1986) and complexes of HF and $N_2$, $C_2H_2$ and $C_2H_4$ (Kolenbrander 1986). Only in the mixed-cluster cases was the resolution ($0.06cm^{-1}$) sufficient to observe rotational structure, although no detailed analysis was undertaken. In the case of $(HF)_3$, while no sharp rotational structure was resolved, it's geometry was determined by isotopic substitution experiments, which indicate the trimer has a cyclic form.

**MBER:** This method has been adapted to the study of vibrational spectra, by introducing IR laser radiation between the two focussing fields. The method is sensitive to both absorption (as in the microwave experiments) and dissociation. Thus DeLeon and Muenter (1984) examined the free HF stretching region of $(HF)_2$ using a color-center laser, with considerably reduced Doppler broadening than the gas-cell experiments discussed earlier. Fraser *et.al.* (1985) looked at the spectra of complexes of $NH_3$ with various partners, using both $CO_2$ laser and microwave radiation, in some cases together to make IR-MW-double resonance measurements. Marshall *et.al.* (1985) have used a far-infrared laser to examine the low-frequency van der Waals modes of Ar-HCl.

**The Optothermal Method:** This technique is similar to the method above, where the mass spectrometer is replaced by detector sensitive to the energy of the molecular beam (and is discussed in more detail in the next section ). It has the advantage that it can also detect absorption as well as dissociation, but a spectrum obtained by this method has contributions from the whole cluster distribution in the beam.

The review of Miller (1986) lists much of the earlier work using this technique.

Snels *et.al.* (1986) and Baldwin and Watts (1987) have observed sharp structure in the ethylene cluster dissociation spectra by tuning their $CO_2$ laser frequency across the gain profile of the lasing transition. The evidence suggests that this can be attributed to the ethylene dimer, indicating that the excited state of this species has a lifetime no shorter than 10ns.

Miller and co-workers have demonstrated the power of this method when combined with a tunable, high-resolution IR laser. Using a computer-controlled F-centre laser, with an instrumental linewidth of 15MHz (5MHz with a single molecular beam-laser crossing) they have examined infrared spectra of a large number of homogeneous and heterogeneous clusters, particularly those containing hydrogen fluoride. This work has been summarized in the article by Miller (1988). In cases where the species are polar, Stark spectroscopy has produced values for the dipole moments in the vibrationally excited states. A similar apparatus has been established by Pine *et.al.* (Pine 1988a). Some of the work done by both groups will be discussed in the chapters that follow.

**CARS:** The CARS method has been applied to examine the spectra of clusters in a free jet, such as $(CO_2)_n$ (Pubanz 1985) and HCN complexes (Maroncelli 1985). In the case of the carbon dioxide dimer a staggered parallel structure was inferred from a comparison of IR and the Raman spectra.

### 1.1.3 Electronic Spectroscopy

One of the first techniques used in this region of the spectrum was that of Laser Induced Fluorescence, pioneered by Levy and co-workers to study the He-$NO_2$ complex (Levy 1981). The relatively simple spectroscopy of iodine has allowed a detailed study of the predissociation of the electronically excited He-$I_2$ complex as a function of the vibrational quantum number $v$ in the $I_2$ sub-unit. Lifetimes were found to decrease quadratically with $v$, and this behaviour has been the subject of a number of theoretical investigations (Janda 1985).

The other well-used technique is Multi-Photon Ionization, coupled with Time-of-Flight mass spectrometry. Castleman and Keesee (1986) discuss the large number of experiments that have been performed using this method to study the effects of complexation on spectral features (specifically the shifts and widths of vibronic bands). Aromatic systems are most often studied by these methods, usually in complexes with small molecules or rare gas atoms.

While for simple systems the spectral broadening observed can usually be associated with predissociation, this distinction is not as clear in clusters of larger (polyatomic) molecules.

Apart from possible inhomogeneous effects such as unresolved rotational structure, other sources of homogeneous broadening need to be identified and accounted for. A distinction should be drawn between the dissociation lifetime and the lifetime of the state in general, which may be limited by other effects such as vibrational dephasing when broadband excitation is used (Brumer 1985). In this regard, time-resolved measurements of the dissociation process have the potential to make such a distinction, and due to the availability of fast, pulsed lasers in the visible region, most experiments of this type on van der Waals systems have looked at vibronically excited states (Casassa 1988). Mitchell *et.al.* (1985) have examined the dissociation of the ethylene dimer in real time using a pulsed $CO_2$ laser. They concluded that the dimer fragments in a time less than 10ns, the upper limit of the instrument resolution.

Although the widths and energies of the resonance states of van der Waals molecules have been the subject of numerous investigations, the rather more difficult task of examining the importance of possible decay channels has received less attention. Because the process of vibrational predissociation of a vibronically excited cluster leaves the product molecule electronically excited, the emission of these products can be analysed to obtain final state distributions if their spectroscopy is well known. Thus Levy *et.al.* (1981) determined that the $\Delta v = -1$ channel is dominant in the decay of $HeI_2$. King and co-workers, in their study of the vibrational predissociation of the NO dimer (Casassa 1986), have examined both the rotational-state distributions and the velocity distributions of the NO fragments, and this perhaps represents the most detailed study of the vibrational predissociation process to date.

## 1.2 The Optothermal Method

Cavallini, Gallinaro and Scoles (1967) first reported the use of a conventional liquid helium cooled semiconductor bolometer (of the type described by Low (1961)) as a molecular beam detector and subsequently these devices have proved useful in crossed-beam differential cross-section measurements (Danielson 1987, Boughton 1986, Boughton 1985). The semiconductor physics underlying the operation of these elements has been given by Zwerdling *et.al.* (1968). In short, when a single crystal of p-type semiconductor, for example, germanium doped with an acceptor impurity like gallium is cooled to liquid helium temperatures, the only mechanism for low frequency (d.c.) conduction arises from the hopping of holes from a filled to an empty acceptor site - so called "impurity hopping conduction". This hopping is thermally activated, or phonon assisted, and results in an electrical resistance that is strongly temperature dependent:

$$R = R_0 exp[\varepsilon/kT]$$

where ε represents an activation energy for the conduction mechanism. Such a strong dependence makes these devices very sensitive to IR radiation, particularly when bonded to an absorbing substrate. The bolometer resistance is usually measured in a bridge circuit and phase sensitive detection employed. The figure of merit for a bolometer is the Noise Equivalent Power (NEP), which for typical, commercially available devices is of the order of $10^{-14}$ W $Hz^{-1/2}$. In the case of molecular beam detection, atoms and molecules impinging on the cold bolometer surface are adsorbed onto it, giving up practically all of their kinetic and internal energy. The bolometer signal is given by :

$$S_B = n\langle v\rangle[E_{kin} + E_{int} + E_a]$$

where $n\langle v\rangle$ is the flux of molecules, $E_{kin}$ their kinetic energy, $E_{int}$ their internal energy (rotations and vibrations), and $E_a$ is the heat of adsorption of the molecule onto the cold surface. Typical minimum detection capabilities are $10^{12}$-$10^{14}$ molecules $m^{-2}$ $s^{-1}$.

Gough, Miller and Scoles (1977), by realising that a change in the internal energy of the molecules in the beam would produce a change in the bolometer signal, devised what has become an extremely sensitive spectroscopic technique. Ro-vibrationally excited molecules are produced by crossing the molecular beam with an IR laser, and the extra energy is carried to the bolometer in a time that is short compared to the fluorescence lifetime. This in turn produces a change in the bolometer resistance that is detected by chopping the laser and using phase-sensitive detection. The method is thus somewhat akin to the photoacoustic method, since the absorption of radiation is detected directly, which lowers the detection limit imposed on normal absorption spectroscopy by laser intensity fluctuations (Demtröder 1982).

The resolution offered by laser-molecular beam techniques, combined with the high sensitivity of what has become known as the optothermal method, has led to it's use in a wide range of spectroscopic investigations. These include :

- Laser-Stark Spectroscopy of HF and HCN (Gough 1981b) and $CO_2$ (Gough 1983) .
- Studies of coherent transients - Ramsey fringes in $SF_6$ (Bordé 1984).
- High vibrational overtone spectroscopy of $H_2O$ (Douketis 1985)
- Electronic spectroscopy of $I_2$ (Buck 1986)

In addition to semiconductor bolometers, a number of other thermally sensitive devices have been used to perform optothermal spectroscopy. Bassi *et.al.* (1985) have reported using a superconducting bolometer to examine the IR multiphoton excitation spectrum of $CF_3Br$. Such devices may prove to be useful with the advent of new high $T_c$ compounds, eliminating the need for liquid helium. Pyro-electric detectors have been used both in beam (Miller 1982)

and gas-cell experiments (Kornilov 1985, Hartung 1979) and a platinum filament has been used to study the multiphoton absorption spectrum of $NH_3$, $C_2H_4$ and $SF_6$ in a gas cell (Li 1984).

The molecular beam optothermal method is also sensitive to processes whereby laser excitation results in dissociation and a reduction of the flux of a particular species reaching the bolometer. Thus Gough, Miller and Scoles (1978, 1981a), using this method, reported the first studies of the vibrational predissociation of vdW clusters formed in a molecular beam. Subsequently the technique has been used to study the dissociation spectra of a wide range of clusters, as discussed in the previous section.

As an example of the use of this technique, Figure 1.1 shows scans through ro-vibrational features in the "bound" and "free" HF stretching bands of the HF dimer, using an F-center laser (the apparatus used to obtain these scans is discussed in the next chapter); a scan through the $P(1)$ monomer line is also given, plotted in the same sense as the dissociation signal for comparison. The difference between the dissociation lifetimes in the two vibrational states is obvious, and the comparison uncomplicated by the Doppler broadening seen in the gas-cell work of Pine *et.al.* (Pine 1984). A careful study of the dependence of the lifetime on the vibrational, rotational and tunnelling state of the dimer has been performed, using the molecular beam optothermal technique (Pine 1988b).

## 1.3 Clusters of Acetylene

Miller *et.al.* chose to investigate the C-H stretching vibrations of acetylene clusters formed in a molecular beam, with the hope of resolving rotational structure in the infrared vibrational predissociation spectra. In Figure 1.2 the dissociation spectrum they obtained using a rather concentrated mixture of acetylene (11%) in helium has been reproduced (Fischer 1985).

In all the spectra presented in this work, the signal corresponding to a decrease in the bolometer signal, caused by the dissociation of excited clusters in a time that is less than the flight time from the interaction region to the detector ($\approx$ 0.2ms), is plotted as positive as a function of the laser frequency. The sharp negative features are ro-vibrational transitions in the bands of the monomer found in this region. Because the laser was not running single-mode, and was tuned in a discontinuous fashion, many of the monomer transitions are missed. The broad cluster dissociation signals to the red of the monomer absorptions were less dependent on the laser mode structure. As the size of the clusters formed in the beam is increased by raising the source pressure, new features emerge close to the absorption frequencies of the low-temperature phase of crystalline acetylene. The structure in the high-pressure spectra is the result of the cluster size distribution, as well as the different environments in which an absorbing species may find itself in a cluster of a given size (Miller 1984a).

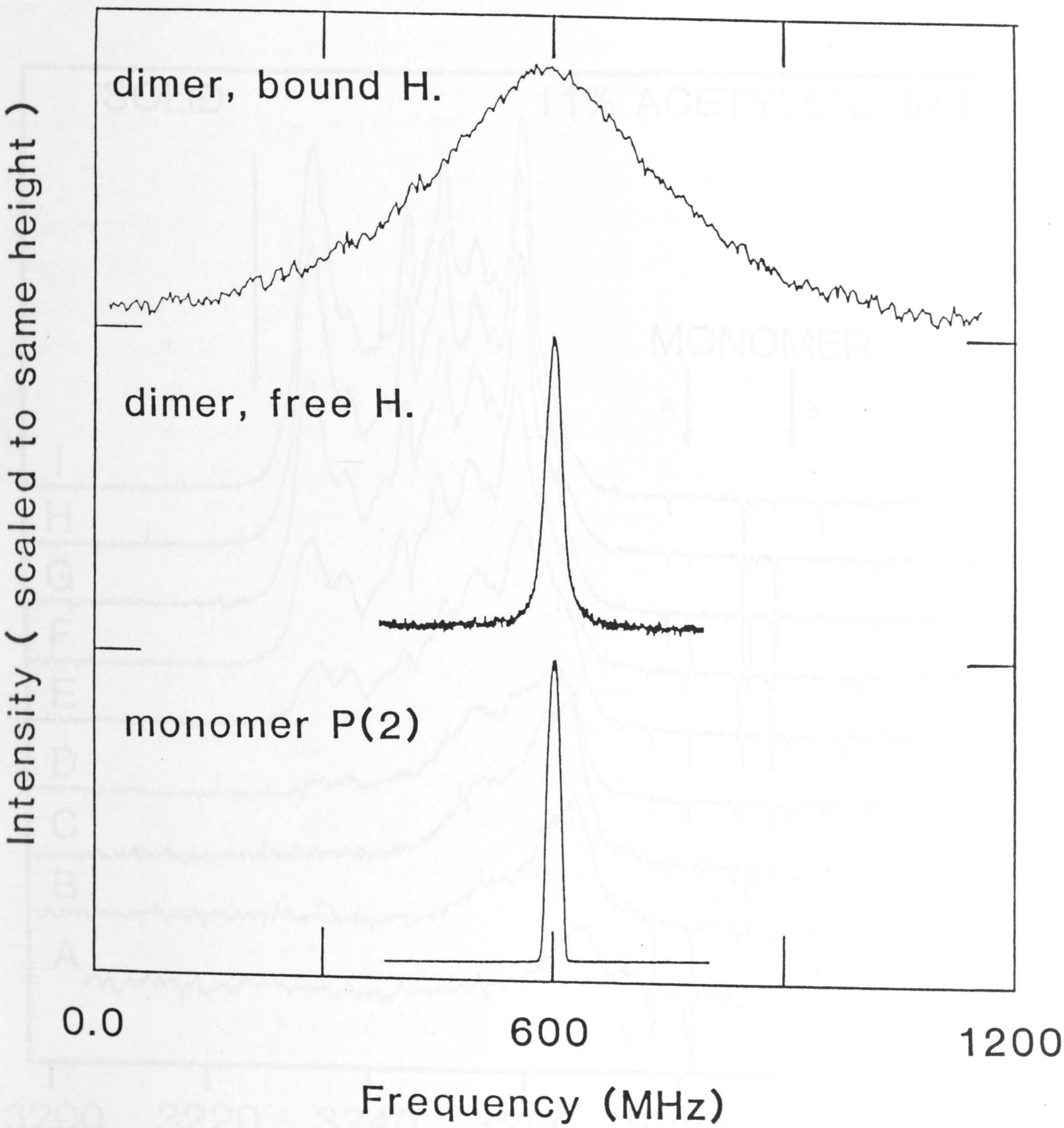


**Figure 1.1:** Ro-vibrational transitions in the "bound" and "free" HF stretching vibrations of $(HF)_2$, seen as dissociation signals using the optothermal method. The bolometer signal decreases in these cases, and increases in the case of the $P(2)$ absorption of the HF monomer in the beam, which is shown to indicate the instrumental resolution.

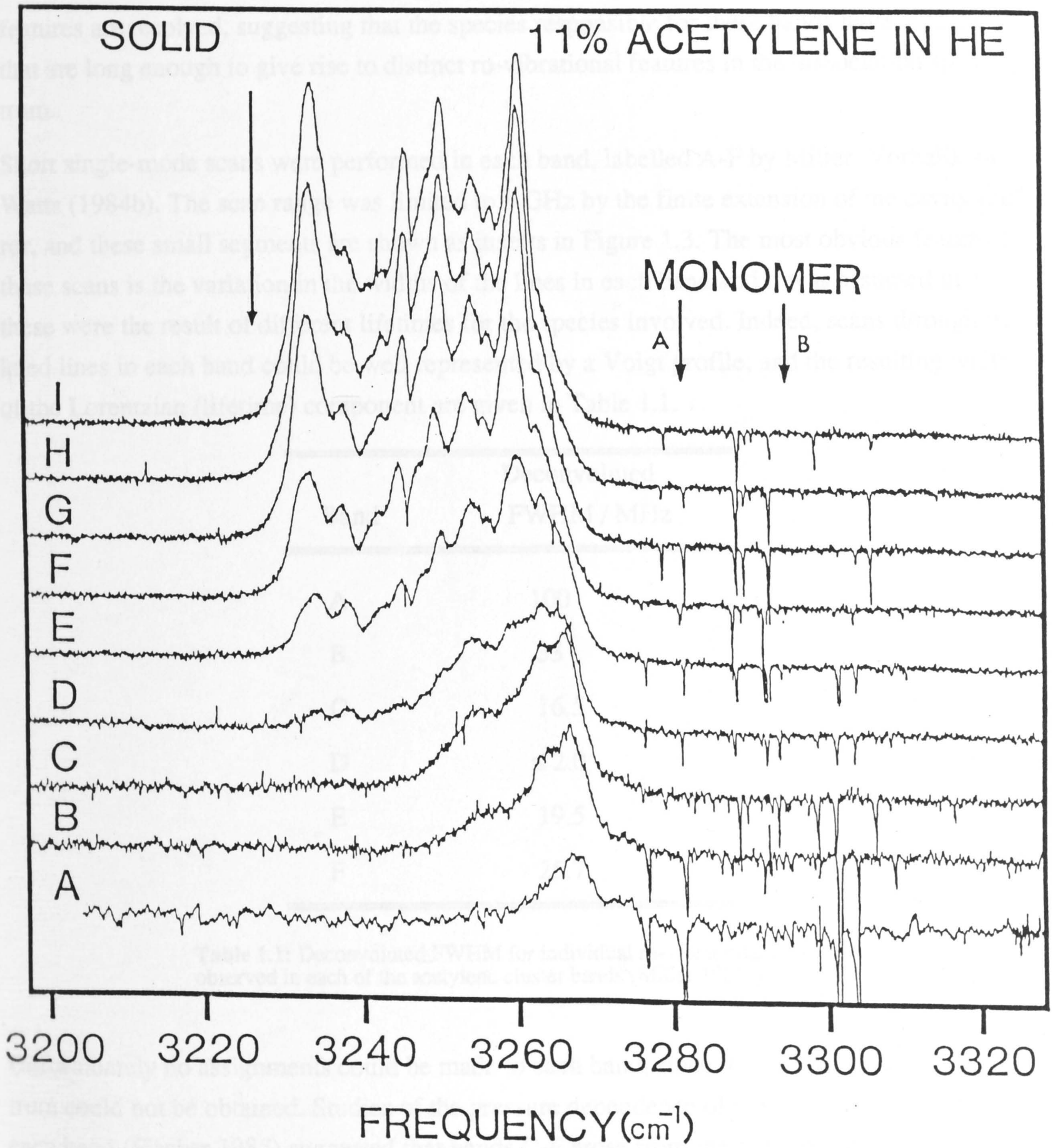


**Figure 1.2:** Dissociation spectra of acetylene clusters using an 11% mixture of acetylene in helium (Fischer 1985). The source pressures are A:480 B:685 C:800 D:915 E:1100 F:1240 G:1490 H:1680 and I:1890 kPa. The arrows mark gas phase and solid absorptions discussed the Appendix.

Even at the lowest source pressure there was no evidence of sharp features in these dissociation spectra. Upon diluting the mixture the spectrum changed considerably, as shown in Figure 1.3. At a concentration of 1% the spectrum has broken up into 6 distinct bands, and sharp features are resolved, suggesting that the species responsible for these bands have lifetimes that are long enough to give rise to distinct ro-vibrational features in the dissociation spectrum.

Short single-mode scans were performed in each band, labelled A-F by Miller, Vorhalik and Watts (1984b). The scan range was limited to 3 GHz by the finite extension of the cavity mirror, and these small segments are shown as inserts in Figure 1.3. The most obvious feature of these scans is the variation in the widths of the lines in each band and it was assumed that these were the result of different lifetimes for the species involved. Indeed, scans through isolated lines in each band could be well represented by a Voigt profile, and the resulting widths of the Lorentzian (lifetime) component are given in Table 1.1.

| Band | Deconvoluted FWHM / MHz |
|---|---|
| A | 100 |
| B | 33 |
| C | 16.5 |
| D | ≤ 2.0 |
| E | 19.5 |
| F | 25.7 |

**Table 1.1:** Deconvoluted FWHM for individual ro-vibrational transitions observed in each of the acetylene cluster bands (Miller 1984b)

Unfortunately no assignments could be made to each band, since the full ro-vibrational spectrum could not be obtained. Studies of the pressure dependence of the relative intensities in each band (Fischer 1985) suggested that bands C-F arose from the acetylene dimer (or, at least, from a species formed from just two atoms or molecules), band B from the trimer and band A the tetramer or pentamer. While this provides some indication of possible assignments an unequivocal determination of the species responsible for each band requires an analysis of the full ro-vibrational spectrum. Only then can the questions about the origins of the different linewidths start to be answered.

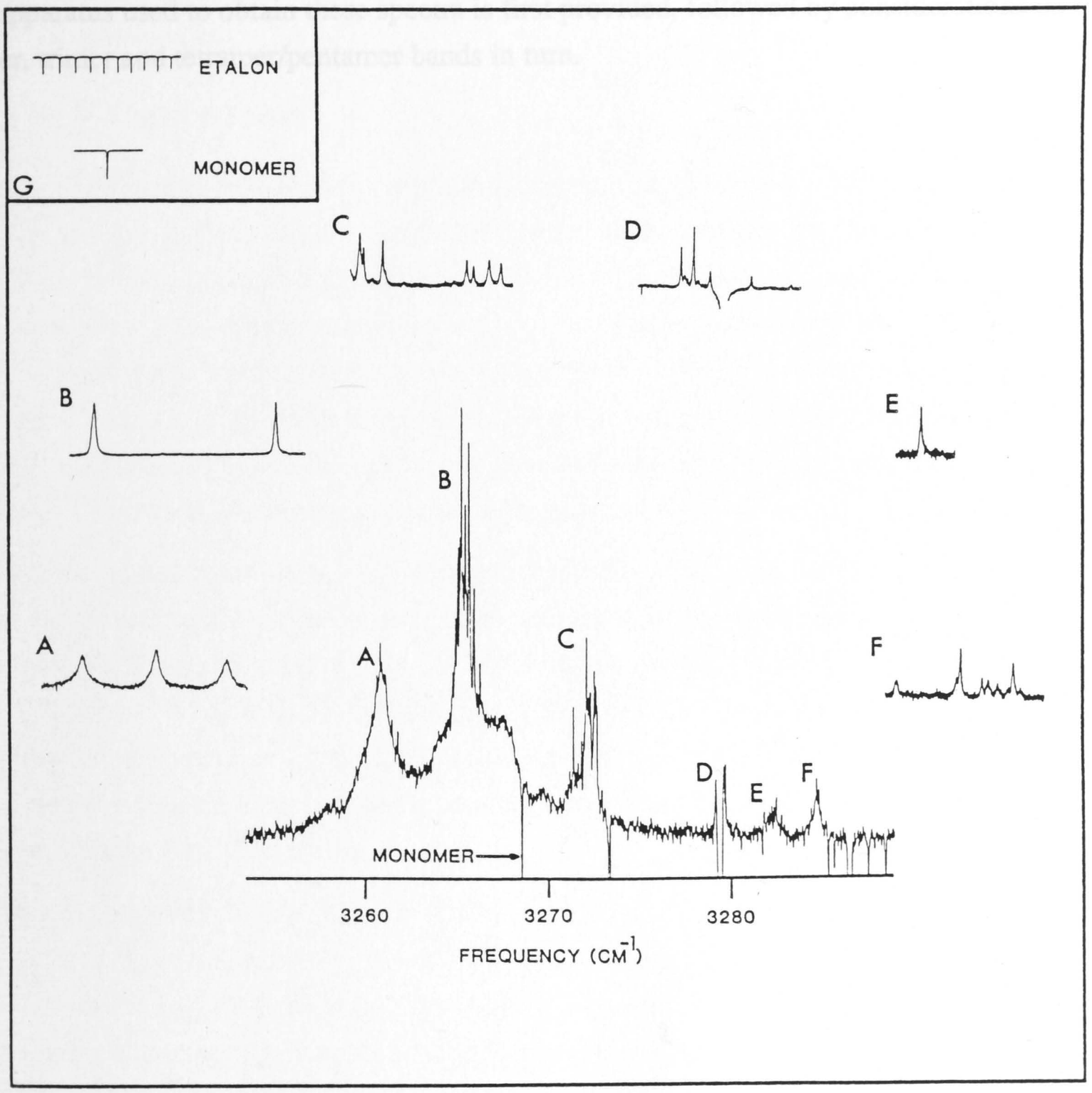


**Figure 1.3:** Dissociation spectrum of acetylene clusters obtained from a 1% mixture of acetylene in helium, at a source pressure of 1160kPa (Miller 1984b). A portion of each band, scanned single-mode, is shown as an insert, on a frequency scale expanded by 155. An etalon (FSR=150MHz) and monomer trace are shown as a calibration.

In this thesis single-mode scans through each of bands A-F, obtained by placing the tuning of the F-center laser under the control of a microcomputer are presented. Analysis of the rotational structure in each case has allowed the identification of the species responsible for each band, and the assignments of Fischer *et.al.* are found to be essentially correct. A discussion of the apparatus used to obtain these spectra is first provided, followed by considerations on the dimer, trimer and tetramer/pentamer bands in turn.

# Chapter 2: Experimental Details

In this chapter the experimental apparatus used to obtain the spectra presented in this thesis is described. It is divided into three broad sections : the laser system, the beam source and finally the combination of the two, including a discussion of bolometric detection and line-width considerations.

## 2.1 The F-Centre Laser

Colour- or F-centres are defects in insulating crystals that act as traps for electrons (or holes). The study of the spectroscopic properties of these centres over the last few decades, particularly those formed in alkali-halide crystals, has led to the creation of a class of solid-state laser operating in the near infrared region ($0.8 < \lambda < 4$ μm), known as the F-centre laser. Details of the physics behind these lasers, as well as their design, construction and applications have been given by Mollenauer (1985). The lasers are analogous to optically pumped tunable dye lasers, in which the dye jet has been replaced by a thin, cryogenically cooled (77K) slab of crystal containing the active centres.

The device used in these studies is a commercial laser - a Burleigh Instruments FCL-20, based on the most stable of the various laser-active colour centres in the alkali halides (the $F_A$(II) and $F_B$(II) type centres in KCl and RbCl). It is a cw high resolution laser with a short term linewidth < 2 MHz, and is tunable over the range 2.22 - 3.64 μm using appropriate crystal, pump wavelength and output coupling selections (German 1986). While a dye laser represents the most flexible choice of pump system, two of the crystals can be efficiently pumped with the output of a $Kr^+$ ion laser.

In these experiments the RbCl:Na crystal was used, being pumped with 1.3W of red light (615/647nm) from a Spectra Physics 171 $Kr^+$ laser in "light control" mode, which provided some degree of amplitude stability. Typical output powers at 3.00 μm were 10-20mW single mode, using a grating with an output coupling of about 10% (i.e. Burleigh's standard "B" grating ). The crystal chamber was kept at less than $10^{-6}$ Torr using an ion pump (Varian VacIon), and for the sake of cleanliness was roughed-out using a sorption pump (Varian Vac-sorb).

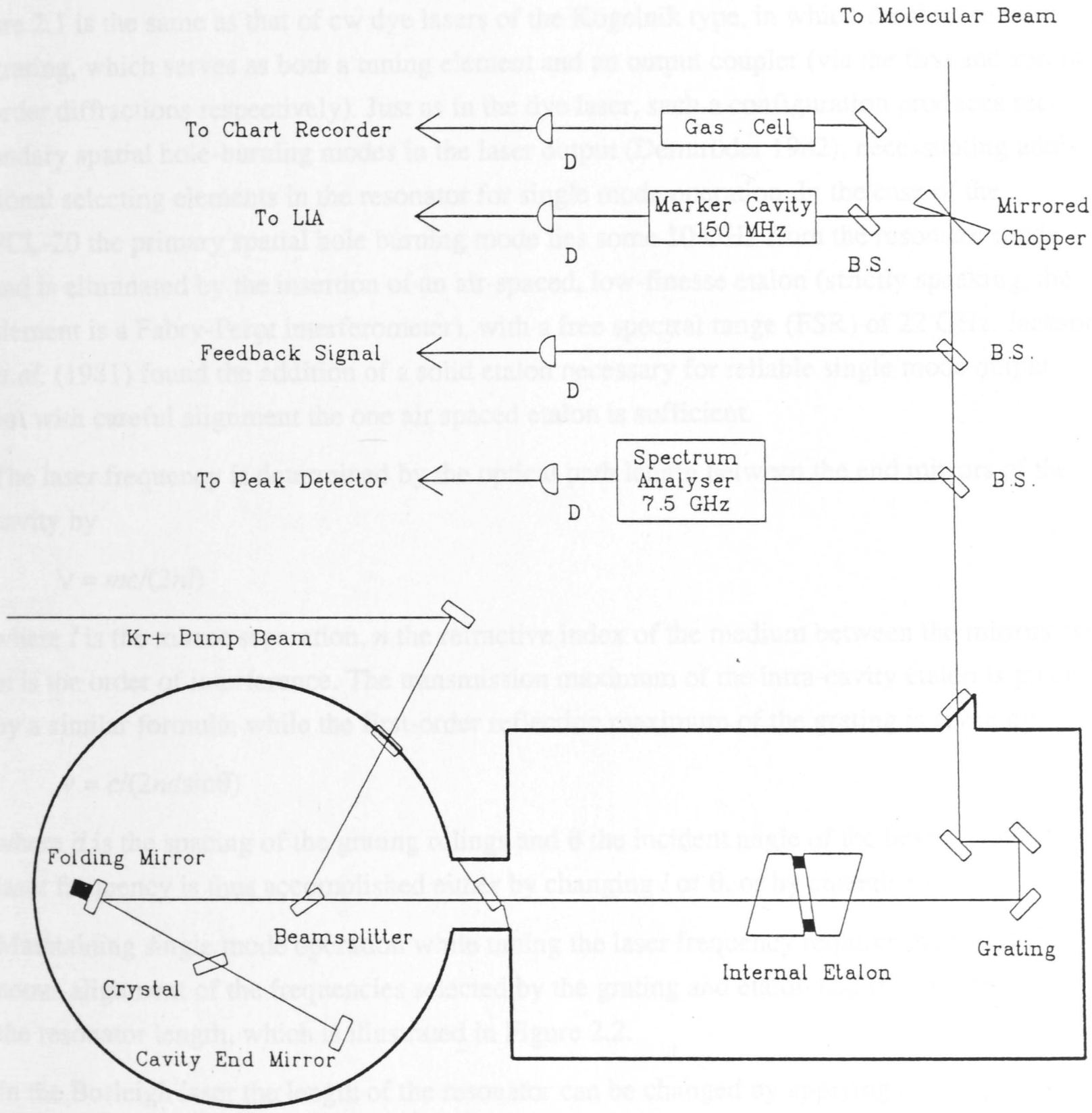


**Figure 2.1:** F-centre laser and associated optics. *D* is a photovoltaic detector, *B.S.* a pellicle beamsplitter.

### 2.1.1 Single Mode Operation

The folded astigmatically compensated 3-mirror cavity design of the FCL-20, shown in Figure 2.1 is the same as that of cw dye lasers of the Kogelnik type, in which the third mirror is a grating, which serves as both a tuning element and an output coupler (via the first and zeroth order diffractions respectively). Just as in the dye laser, such a configuration produces secondary spatial hole-burning modes in the laser output (Demtröder 1982), necessitating additional selecting elements in the resonator for single mode operation. In the case of the FCL-20 the primary spatial hole burning mode lies some 10 GHz from the resonator mode and is eliminated by the insertion of an air-spaced, low-finesse etalon (strictly speaking, the element is a Fabry-Perot interferometer), with a free spectral range (FSR) of 22 GHz. Jackson *et.al.* (1981) found the addition of a solid etalon necessary for reliable single mode output, but with careful alignment the one air spaced etalon is sufficient.

The laser frequency is determined by the optical path length between the end mirrors of the cavity by

$$\nu = mc/(2nl)$$

where $l$ is the mirror separation, $n$ the refractive index of the medium between the mirrors and $m$ is the order of interference. The transmission maximum of the intra-cavity etalon is given by a similar formula, while the first-order reflection maximum of the grating is given by

$$\nu = c/(2nd\sin\theta)$$

where $d$ is the spacing of the grating rulings and $\theta$ the incident angle of the beam. Tuning the laser frequency is thus accomplished either by changing $l$ or $\theta$, or by changing $n$.

Maintaining single mode operation while tuning the laser frequency requires the simultaneous alignment of the frequencies selected by the grating and etalon and that determined by the resonator length, which is illustrated in Figure 2.2.

In the Burleigh laser the length of the resonator can be changed by applying a voltage to a piezo-ceramic element (PZAT) on which the folding mirror is mounted. Similar stacks of such elements adjust the separation of the etalon mirrors (as well as their alignment). The angle of the grating is controlled with a "sine-bar" drive made up of a finely threaded screw, which can be attached to a stepper motor. There are several modes of operation of the laser:

**(a)** The grating is held fixed and the voltage on the folding mirror PZAT is ramped from 0 to the 1000 volt limit imposed by electrical breakdown of the ceramic. This causes the piezo-elements to contract and so the laser scans to the red. The same ramp drives the etalon

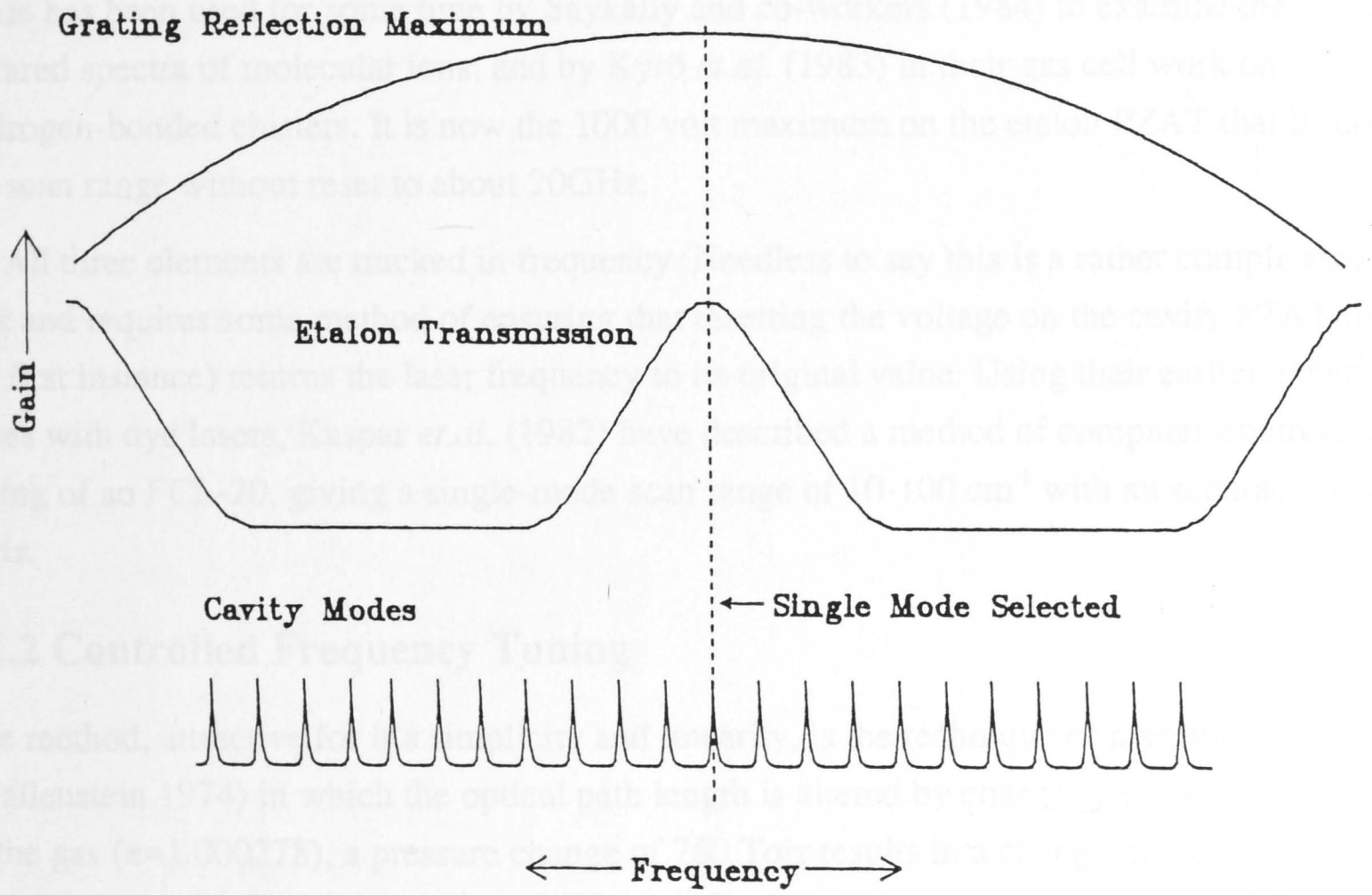


**Figure 2.2:** The use of 3 optical elements to produce single mode operation of the F-centre laser.

PZAT, but it's amplitude adjusted to about 100 V, since the different mirror spacing in the two elements and different PZAT responsivities (in μm movement/kV) result in a $\Delta\nu_{etalon}/\Delta\nu_{cavity}$ of about 10 or so for a given $\Delta V$.

(**b**) The frequencies selected by the etalon and grating are adjusted, keeping the cavity length fixed. This results in a discontinuous scan in which the laser frequency hops from one resonator mode to the next (i.e. different values of *m*). The effective resolution become one cavity FSR, or 300 MHz, which makes the method suitable for Doppler-limited spectroscopy, since this is of the same order as the Doppler width at these frequencies. Indeed, this scanning mode has been used for some time by Saykally and co-workers (1984) to examine the infrared spectra of molecular ions, and by Kyrö *et.al.* (1983) in their gas cell work on hydrogen-bonded clusters. It is now the 1000 volt maximum on the etalon PZAT that limits the scan range without reset to about 20GHz.

(**c**) All three elements are tracked in frequency. Needless to say this is a rather complicated task and requires some method of ensuring that resetting the voltage on the cavity PZAT (in the first instance) returns the laser frequency to its original value. Using their earlier experiences with dye lasers, Kaspar *et.al.* (1982) have described a method of computer-controlled tuning of an FCL-20, giving a single-mode scan range of 10-100 $cm^{-1}$ with an accuracy of 10 MHz.

### 2.1.2 Controlled Frequency Tuning

One method, attractive for it's simplicity and linearity, is the technique of pressure tuning (Wallenstein 1974) in which the optical path length is altered by changing *n*. Using nitrogen as the gas ($n$=1.000278), a pressure change of 760 Torr results in a change in the laser frequency of about 28GHz (0.9 $cm^{-1}$) at 3300 $cm^{-1}$. Back-filling the tuning arm of the FCL would result in the automatic synchronization of the tuning of the grating and intracavity etalon, but because part of the resonator length must remain in vacuum, the laser would hop between cavity modes. Thus for continuous single mode scanning this method would need to be supplemented by electronically controlling the resonator length, perhaps with a reference etalon linked to the same pressurizing circuit. Movement of the intracavity beam at the internal Brewster window, and probably of the optical elements themselves with changing pressure, made the method difficult to implement without modifying the laser.

Another technique providing good linearity and long-range tuning is that used by Pine and Coulombe (Coulombe 1979) to control a difference-frequency IR laser spectrometer, in which the laser frequency is monitored with respect to that of a stabilized HeNe using a scanning Fabry-Perot. The frequency stability of the HeNe is thus transferred to the IR laser

output, and tuning is accomplished by altering the offset at which the IR frequency is stabilised. Pine *et.al.* (Fraser 1987) have reported extending this control system to a Burleigh FCL-20, used to obtain the high resolution IR spectra of the $CO_2$ trimer.

Nesbitt and co-workers have developed a method of tuning an FCL-20 without the need for a control computer by introducing an angle-tuned Brewster plate into the tuning arm, in addition to the piezo-scanned etalon (Nelson 1988). Scans of up to 0.8 $cm^{-1}$ are made before the grating is stepped and the next segment started.

The method of Kaspar *et.al.* relies on the calibration of the response of each optical element to changes in their position, which in turn are related to changes in the voltages on the piezo-elements or to a number of steps of the grating stepper motor. The responses are stored as a 'look-up' table in the control computer memory so that whenever the laser is required to step in frequency the positions for each element are determined from the tables and they are moved accordingly. Drifts in the position of the etalon, caused principally by 'creep' of the piezo-crystals, created the need for a feedback loop to lock it's transmission maximum to the resonator mode. Miller *et.al.* have used this method in their molecular beam optothermal spectrometer (Huang 1986a).

The method adopted here, described in detail below, is similar to that of Kryö *et.al.* (1986) - a somewhat simplified version of the technique of Kaspar *et.al.*, which was also used in a molecular beam optothermal spectrometer.

### 2.1.3 Optics

A layout of the optical components is given in Figure 2.1; all components were mounted on the same vibration-isolated granite slab as the FCL and pump laser. About 1% of the laser output is first split off by a pellicle beamsplitter (NPC ST-LQ-UNC) and focussed with a $CaF_2$ lens ($f$=20mm) onto a photovoltaic detector (Judson J12A), whose output was used in the cavity-etalon feedback loop. A further portion of the beam was split into a spectrum analyser (Burleigh FCL-975) with a FSR of 7.5GHz, scanned using a high-voltage ramp generator (Burleigh RC-45). The transmitted light was monitored with another photovoltaic detector, whose output was directed to a low-noise amplifier and then to a CRO and a peak detector circuit.

A mirrored chopper (Valtec) directed the output of the laser into two arms. In the first, some of the chopped output was split off into a confocal etalon (Burleigh CFT-500P) with a FSR of 150 MHz; this device was temperature stabilized and hermetically sealed to minimize the effects of ambient pressure fluctuations, although it was not evacuated. The remainder of the output was directed through a 1m long gas cell filled with a few Torr (< 10) of water vapour, and the transmitted light monitored with yet another photovoltaic detector. The light in the

second arm was focussed by a $CaF_2$ lens ($f$=500mm) and directed into a multipass device producing some 50 or so slightly non-orthogonal crossings of the molecular beam (Gough 1981c).

A vacuum box was not used to contain the optics, and while this has generally been found necessary to eliminate the effects of atmospheric water absorptions, these did not cause major problems in the region of interest (3μm).

### 2.1.4 Electronics

The electronic components of the system are shown in Figure 2.3.

The control and data acquisition system was based on the STD buss. A single board microcomputer (Pulsar 'Little Big Board'), with 64K RAM and two 1.2Mbyte disk-drives was used to control the remaining devices on the buss. The output of the bolometer, the marker cavity and the error signal from the feedback loop were acquired via a 12 bit (8 channel) analog-to-digital converter (Robotrol RSD-7728) set for bipolar operation (-10 to +10V) since both the error and bolometer signals can be negative. The transmission through the gas-cell could also be recorded. The same card performed the digital-to-analog conversion to drive the high-voltage amplifiers (Burleigh) connected to the piezo elements on the FCL folding mirror and intracavity etalon. The stepper motor controller was driven by 2 lines of a 48 line parallel I/O card (STD 2300).

A peak detector was used to determine the position of the transmission maximum of the scanning FPI with respect to the start of the high voltage ramp. This is depicted in Figure 2.4.

The signal from the detector is amplified and filtered, and compared to an adjustable DC signal level, which results in a negative going TTL pulse at the peak position(s). This is used to reset a flip-flop, which has been previously set by the positive going edge of the (inverted) trigger pulse from the ramp generator. To avoid a 'collision' between the trace and retrace peaks a time delay was introduced, preventing a reset before time $\tau$. The output of the flip-flop is gate pulse that is fed into a counter-timer card on the STD buss (micro-sys SB8355) to determine the duration of the active level. The length of the gate pulse is a measure of the position of the first peak seen after $\tau$ secs. from the start of the ramp. The ramp amplitude and duration were selected to provide a suitable oscilloscope trace and the clock period chosen to provide about a resolution of 7.5 MHz/count.

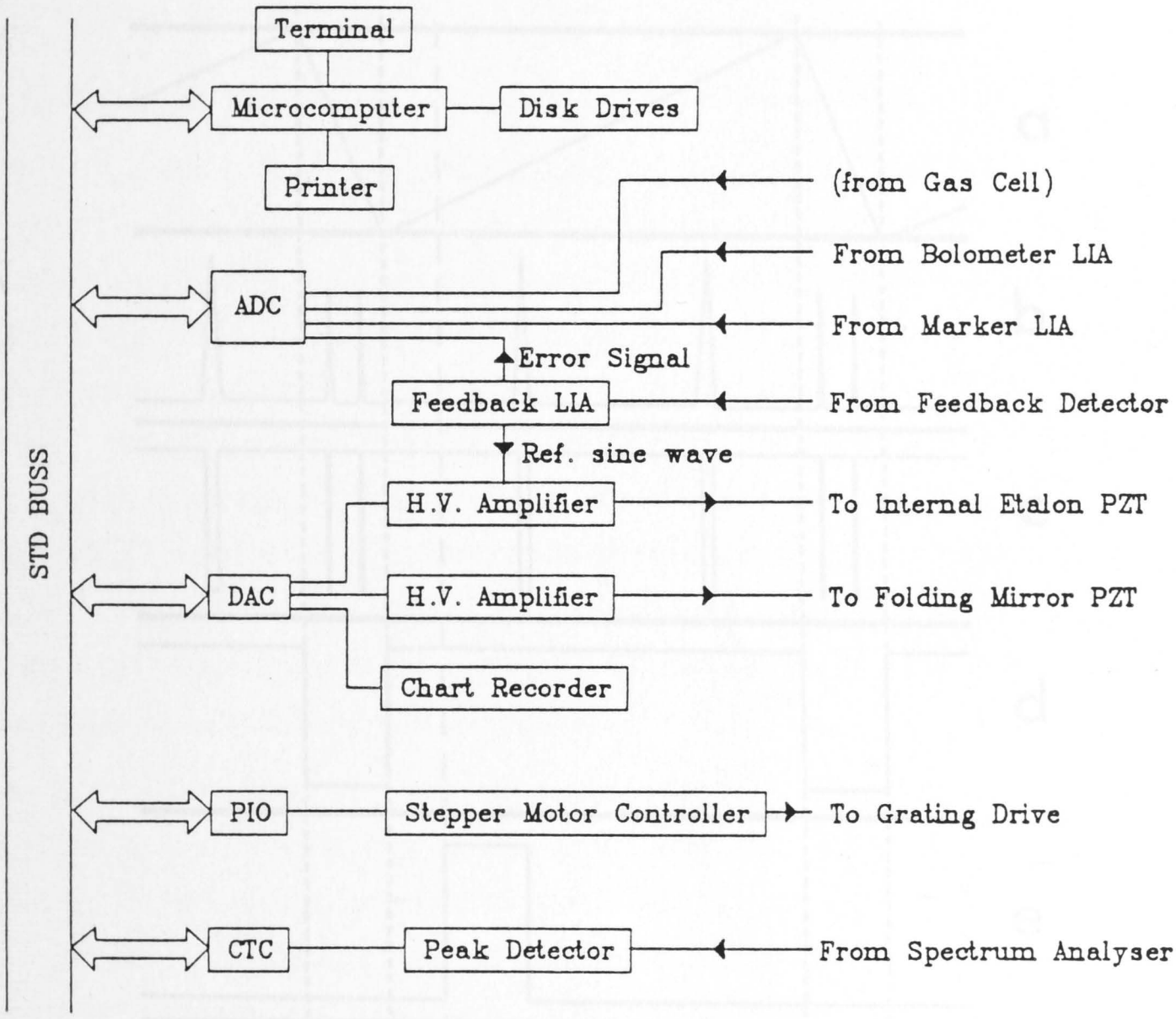


**Figure 2.3:** The control and data acquisition electronics for the F-centre laser. *ADC*: Analog-to-digital converter, *DAC*: Digital-to-analog converter, *PIO*: Parallel I/O card, *CTC*: counter-timer card, *LIA*: Lock-in amplifier.

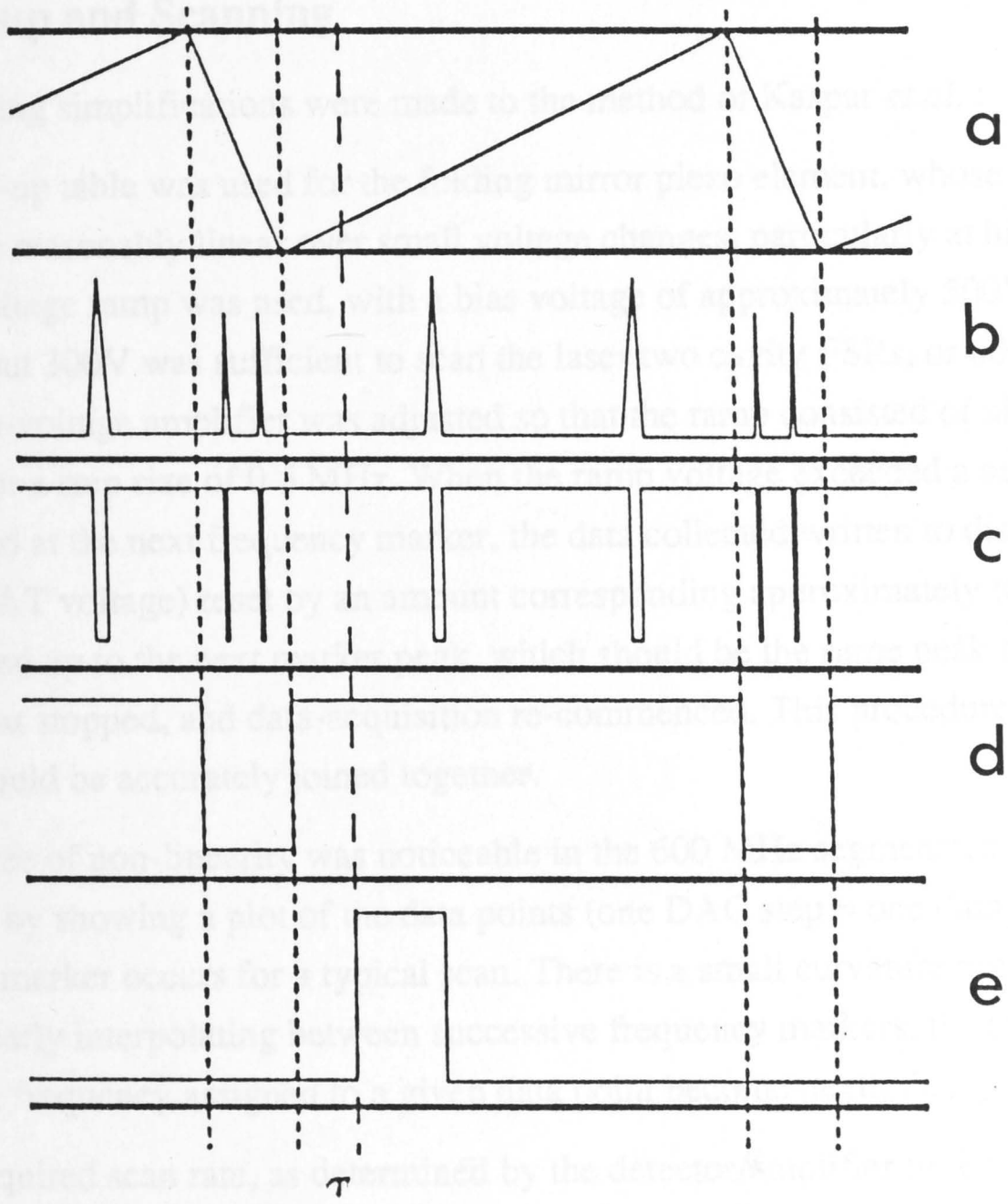


**Figure 2.4** A timing diagram for the peak detector circuit, showing the high voltage ramp applied to the spectrum analyser, **a** and the output from it's detector circuit, **b**. Negative going TTL pulses are generated at the peak positions by the comparator, **c**. A gate pulse, **e** is opened a time τ after the ramp trigger **d**, and closed by the first peak seen by the comparator.

The feedback loop between the resonator mode and the transmission maximum of the intracavity etalon (Kaspar 1982) was established using a PAR 128A lock-in amplifier. The sinusoidal output of the internal reference oscillator (50mV p-p) was fed into the 'DRIFT' input on the Burleigh ramp generator, producing a ± 2V modulation on the etalon piezo-element. A modulation frequency of 800Hz was selected, and the LIA operated with a bandpass input filter and a 300ms time constant (6dB/oct) on the output filter.

### 2.1.5 Set-up and Scanning

The following simplifications were made to the method of Kaspar *et.al.* :

**(i)** No look-up table was used for the folding mirror piezo element, whose response was found to be reasonably linear over small voltage changes, particularly at higher bias voltages. A linear voltage ramp was used, with a bias voltage of approximately 500V, and an amplitude of about 300V was sufficient to scan the laser two cavity FSRs, or 600 MHz. The gain on the high-voltage amplifier was adjusted so that the ramp consisted of about 1000 steps of the DAC, or a step size of 0.6 MHz. When the ramp voltage exceeded a set value, the scan was stopped at the next frequency marker, the data collected written to disk, and the cavity length (PZAT voltage) reset by an amount corresponding approximately to $\lambda$. The laser was then scanned up to the next marker peak, which should be the same peak at which the previous segment stopped, and data-acquisition re-commenced. This procedure ensured that each segment could be accurately joined together.

Some degree of non-linearity was noticeable in the 600 MHz segments, and Figure 2.5 illustrates this, by showing a plot of the data points (one DAC step = one data point) at which a frequency marker occurs for a typical scan. There is a small curvature noticeable in the plot, but by linearly interpolating between successive frequency markers, the effects of this curvature on the frequency assigned to a given data point become negligible.

**(ii)** The required scan rate, as determined by the detector/amplifier time constant, is relatively slow, and so no "feed forward" was used to scan the intracavity etalon. Instead the position of the etalon was determined solely by the integrated error signal from the feedback loop, and adjusted in step sizes of approximately 10 MHz (this step size was limited by the resolution of the DAC). The performance of this loop was found to depend rather critically on the alignment of the laser, the focussing of the beam onto the detector, atmospheric absorptions and the position (in frequency) of the grating with respect to the etalon. Such factors could ultimately result in a mode- hop during a scan.

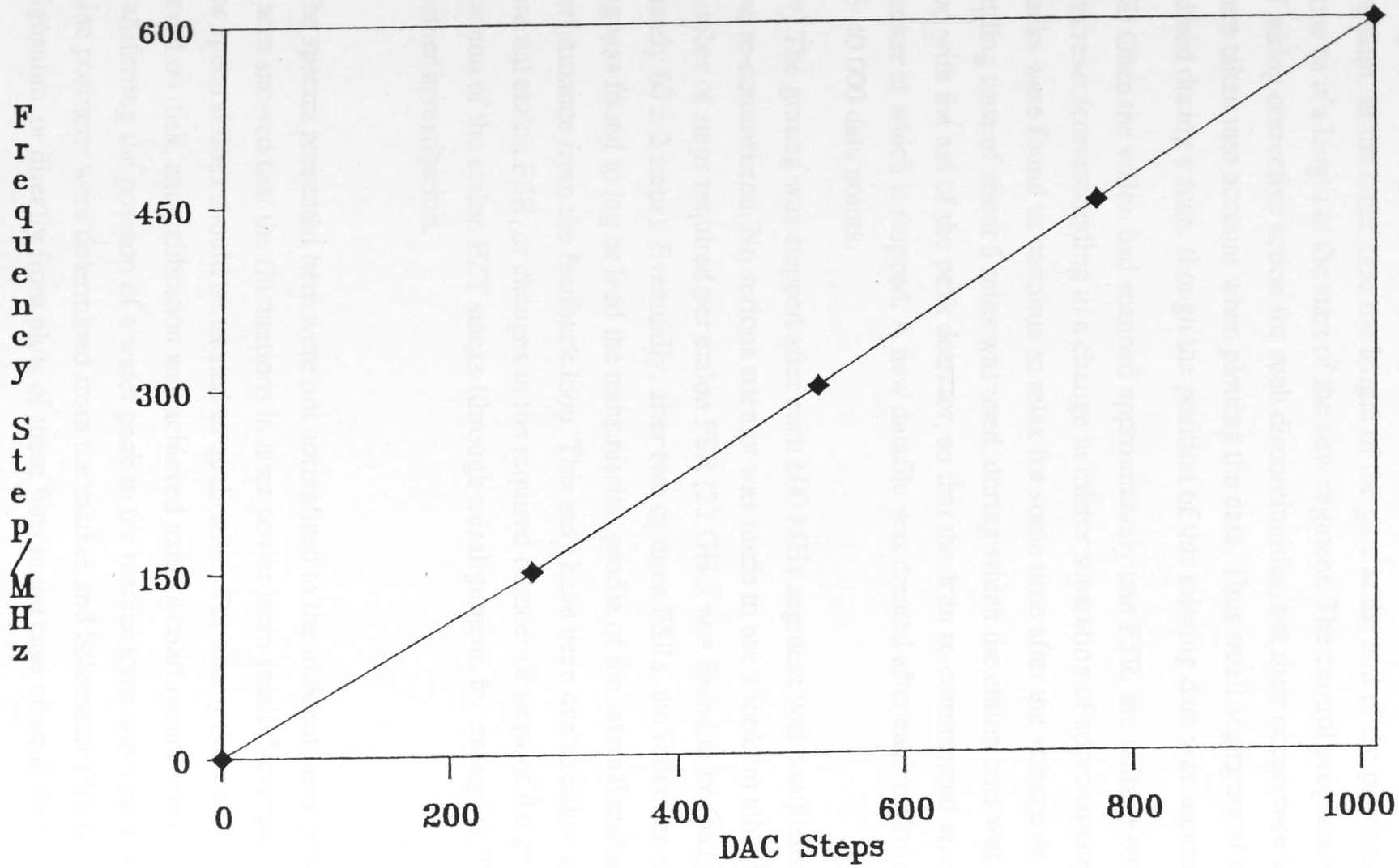


**Figure 2.5:** A plot of the voltage applied to the cavity PZAT, in steps of the DAC, vs. the relative frequency of the laser output.

Possible mode-hops or the restarting of a scan at the wrong frequency marker could be checked using the scanning FPI. In the former case deviations are noticed in the ratio of the change in the length of the peak detector gate to the number of DAC steps taken over a given segment. In the latter case the length of the gate at the end of the previous segment is not the same as it's length at the start of the new segment. The control program was not at the stage of taking corrective action for such discontinuities, but their occurrence was logged and they were taken into account when plotting the data. Thus small segments of the data could be missed during a scan, though the position of this missing data was accurately known.

**(iii)** Once the etalon had scanned approximately one FSR, the voltage on its piezo element was reset (corresponding to a change in mirror separation of approximately $\lambda/2$). The piezo stacks were found to continue to relax for some time after the voltage on them was reset. A settling time of about 5 mins was used, during which the etalon bias was adjusted manually and with the aid of the peak detector, so that the scan re-commenced at, or at least before, the marker at which it stopped. A new datafile was created after each etalon reset to take the next 35-40 000 data points.

**(iv)** The grating was stepped after each 600 MHz segment was completed and before the new one re-commenced. No serious attempt was made to use a look-up table for the grating, as the number of steps required per etalon FSR (22 GHz) was found to be fairly constant (approximately $60 \pm 2$ steps). Eventually, after two or three FSRs, the reflection maximum of the grating was found to lag or lead the transmission profile of the internal etalon, resulting in poor performance from the feedback loop. This may have been due to either a poor estimate of the internal etalon FSR, or changes in the required number of steps of the grating with the contraction of the etalon PZT stacks (through misalignment, for example). This matter requires further investigation.

The spectra presented here were not normalized to the incident laser power, although recorder traces showed that the fluctuations in laser power were small. Nevertheless the intensity of the spectral lines should be treated as qualitative. The absorptions of the gas cell were not saved on disk, and calibration was achieved using a chart recorder trace. The accuracy of transferring the position of a water peak to the marker trace was approximately $\pm 0.001$ $cm^{-1}$. Line positions were determined from the marker and bolometer files using a peak-locating algorithm, or directly from plots of these files in the case of weak lines.

## 2.2 The Molecular Beam

The molecular beam chamber has been described elsewhere (Boughton 1982, Vorhalik 1986), but a brief description of the relevant features will be given for completeness - refer

to Figure 2.6. A monel nozzle (diameter 40μm) is mounted on an *xyz*-translation stage inside the beam source chamber, which is kept at an operating pressure of $10^{-3}$-$10^{-4}$ Torr by an unbaffled 5300ls$^{-1}$ oil diffusion pump (Varian VHS-10, using Santovac 5). The central core of the expansion is sampled some 2-3 cm from the nozzle by a brass conical skimmer (26/30°) with a 200μm hole at it's apex. The resulting molecular beam then enters the main chamber, kept at less than $10^{-6}$ Torr by a 1600 ls$^{-1}$ oil diffusion pump (Varian VHS-6 with 'Mexican Hat'), where it passes through the multiple crossing device. Finally the beam impinges on a liquid helium cooled bolometer (Infrared Laboratories Inc.), whose operating characteristics are described in detail by Vorhalik (1986). The oil diffusion pumps are backed by a common two-stage 50ls$^{-1}$ rotary pump (Edwards E2M175).

The molecular beam source can be rotated inside the main chamber and directed into a commercial quadrupole mass spectrometer (UTI 100c), although this was not used in the present investigations.

Expansion conditions were identical to those used to obtain the spectra in Figure 1.3. A 1.1% mixture of acetylene in helium (CIG) was expanded from a source pressure of 1170 kPa. In some cases, spectra were collected using ≈ 1% mixtures made by diluting more concentrated mixtures based on partial pressures.

## 2.3 Linewidth Considerations

Given that the residual broadening of spectral lines due to lifetime effects is of some interest, a consideration of factors limiting the resolution of the experiment is warranted. The principle source of spectral broadening stems from the divergence of the molecular beam and the non-orthogonality of the laser crossings. For the orthogonal laser-molecular beam geometry, the residual Doppler broadening is given by

$$\Delta\nu = (v_s/c)\nu\sin\alpha$$

where $\alpha$ is the angle subtended by the bolometer (≈ 0.2°) and $v_s$ is the stream velocity (typically about 1700 ms$^{-1}$ for a dilute mixture in helium). At 3300 cm$^{-1}$ this width is 2 MHz, and is comparable to the free-running linewidth of the F-centre laser. When the laser-molecular beam crossing is non-orthogonal, as in the multipass device, a component of the molecular velocity in the direction of the radiation is introduced, and a shift in the transition frequency is seen, given by

$$\nu-\nu_0 = \nu_0(v_s/c)\sin\theta$$

where $\theta$ is the angular deviation from non-orthogonality. For $\theta \approx 10°$, as in the multipass device, this shift amounts to about 100 MHz (0.003 cm$^{-1}$). This is of the same order as the error with which absolute wavenumbers could be determined from water absorptions in the

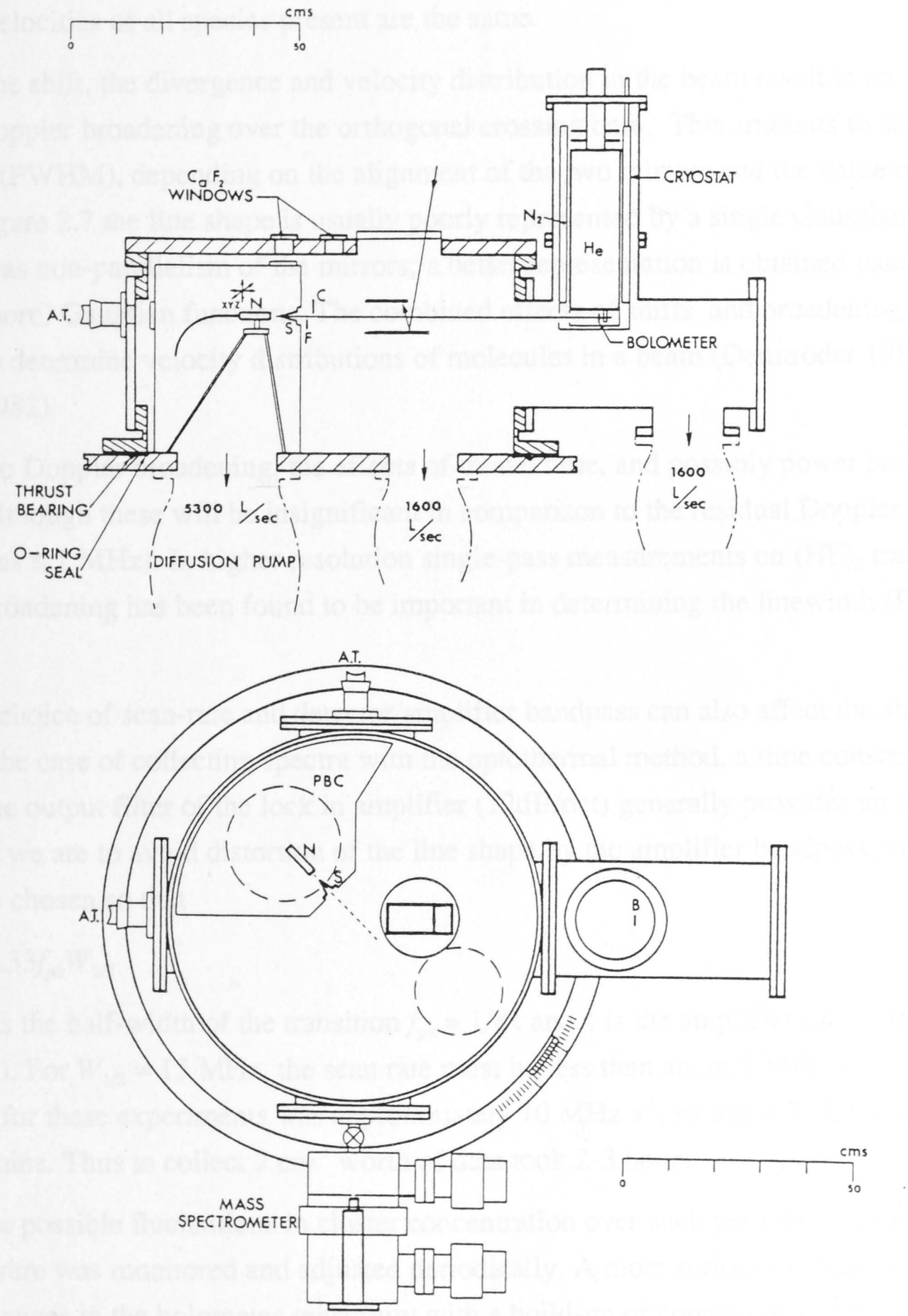


**Figure 2.6:** The molecular beam apparatus, showing the beam source chamber *PBC*, the multipass device and the bolometer cryostat.

gas cell (which are not be shifted), and was therefore not taken into account in doing so. Of course this shift does not affect calibration from monomer transitions in the beam, assuming the stream velocities of all species present are the same.

As well as the shift, the divergence and velocity distribution in the beam result in an increased Doppler broadening over the orthogonal crossing case. This amounts to some 15-20 MHz (FWHM), depending on the alignment of the two mirrors and the value of $\theta$. As shown in Figure 2.7 the line shape is usually poorly represented by a single Gaussian, due to effects such as non-parallelism of the mirrors; a better representation is obtained using a sum of two (or more) Gaussian functions. The combined effects of shifts and broadening has been used to determine velocity distributions of molecules in a beam (Demtröder 1982, Boughton 1982).

In addition to Doppler broadening, the effects of transit time, and possibly power broadening can occur, although these will be insignificant in comparison to the residual Doppler width (contributions $\leq$ 1 MHz). In higher resolution single-pass measurements on $(HF)_2$ transitions, saturation broadening has been found to be important in determining the linewidth (Pine 1988b).

Finally, the choice of scan-rate and detector/amplifier bandpass can also affect the shape of the line. In the case of collecting spectra with the optothermal method, a time constant of 300ms on the output filter of the lock in amplifier (12dB/oct) generally provides an adequate S/N ratio. If we are to avoid distortion of the line shape by the amplifier bandpass, the scan rate must be chosen so that

$$r_s \leq 1.33 f_{pb} W_{1/2}$$

where $W_{1/2}$ is the half-width of the transition $f_{pb} = 1/8\tau$ and $\tau$ is the amplifier time constant (Blass 1981). For $W_{1/2}$ = 15 MHz, the scan rate must be less than about 8 MHz $s^{-1}$. The scan rate chosen for these experiments was approximately 10 MHz $s^{-1}$, so that a 22 GHz scan took around 40 mins. Thus to collect 2 $cm^{-1}$ worth of data took 2-3 hours.

To minimize possible fluctuations in cluster concentration over such periods of time, the source pressure was monitored and adjusted periodically. A more serious problem arises from potential changes in the bolometer sensitivity with a build-up of condensed matter on it's surface. After several days running at cryogenic temperatures, even with a dilute beam, the sensitivity of the detector decreased (by a factor of 2-3); however, allowing the device to warm to room temperature before cooling it again returned the detectors sensitivity. Similarly the bolometer "spiking", thought to be caused by structural changes in the "frost" on it's surface, tends to get worse with exposure to the molecular beam, but is again curable by allowing the detector to warm up between liquid helium transfers.

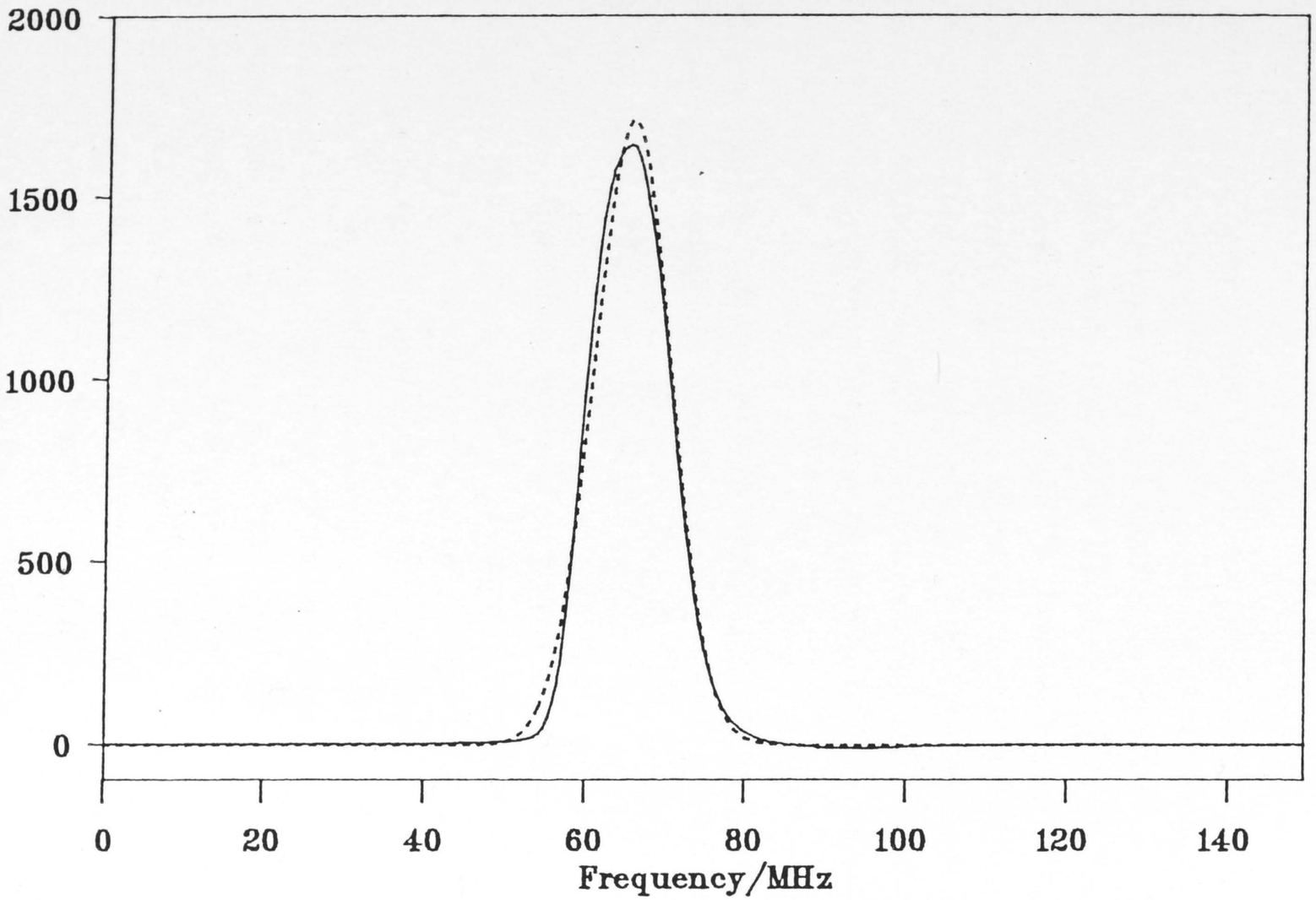


**Figure 2.7:** A scan through the $P(1)$ transition of the combination band of acetylene, using the multipass device (solid line), and an attempt to fit the line shape with a single Gaussian (dotted line). The FWHM of the Gaussian is 11.3 MHz.

Despite these drawbacks, this method offers both high sensitivity and high resolution, and is therefore ideal for cluster spectroscopy in molecular beams.

# Chapter 3: Bands C-F : The Acetylene Dimer

The study of the source pressure dependence of the acetylene cluster spectra by Fisher *et.al.* suggested that the four bands closest to the monomer vibrational origin, bands C-F, should be assigned to the dimer. Examination of the high-resolution spectra presented here has confirmed this assignment.

As in the case of the carbon dioxide dimer, the structure of the acetylene dimer has been the subject of debate for some time. Both staggered-parallel and T-shaped structures, of the type shown in Figure 3.1, have been proposed to explain experimental observations, and predicted with various theoretical models. High resolution infrared spectroscopy has shown that $(CO_2)_2$ adopts the non-polar parallel form (Jucks 1987a, Walsh 1988, Jucks 1988a), and a similar structural determination for $(HCCH)_2$ should be possible from an analysis of the spectra presented here. Through the work of a number of groups this has indeed been the case; the acetylene dimer has been found to have a T-shaped structure in which the roles of proton "donor" and "acceptor" molecules are exchanged through internal rotational tunnelling (Fraser 1988, Ohshima 1988).

The approach taken in this chapter will essentially be to describe a chronology of work on the dimer, including the presentation of single mode scans through bands C-F.

## 3.1 Early Work

In an examination of the infrared spectra of acetylene in nitrogen matrices at 20K (Bagdanskis 1972), two bands in the region of the C-H stretch $\nu_3$ were assigned to the dimer. These were red-shifted from the molecular absorption by 6 and 24 $cm^{-1}$. Similar behaviour is seen in the X-H stretching vibrations of matrix-isolated dimers of hydrogen bonding species such as $H_2O$ and HCN. This was interpreted in terms of structures that are open rather than cyclic. One molecule acts as a proton donor, and the consequent weakening of the X-H bond results in a lower stretching vibrational frequency. In the acceptor molecule the X-H stretch is essentially "free", and is only shifted slightly from that of the isolated molecule. This interpretation was alluded to Chapter 1 in connection with the infrared spectra of $(HF)_2$. This matrix isolation study therefore suggested that, at least in nitrogen matrices, the acetylene dimer was T-shaped, due to a weak hydrogen-bonding interaction.

The acetylene pair potential has been modelled using empirically determined parameters with terms for dispersion and quadrupolar forces, and a spindle-shaped core representing exchange repulsion derived from *ab initio* electron density calculations (Sakai 1977). The potential energy minimum was found to be the staggered-parallel structure. In contrast, low-level SCF calculations predicted the T-shaped form to have the lowest energy (Aoyama 1979).

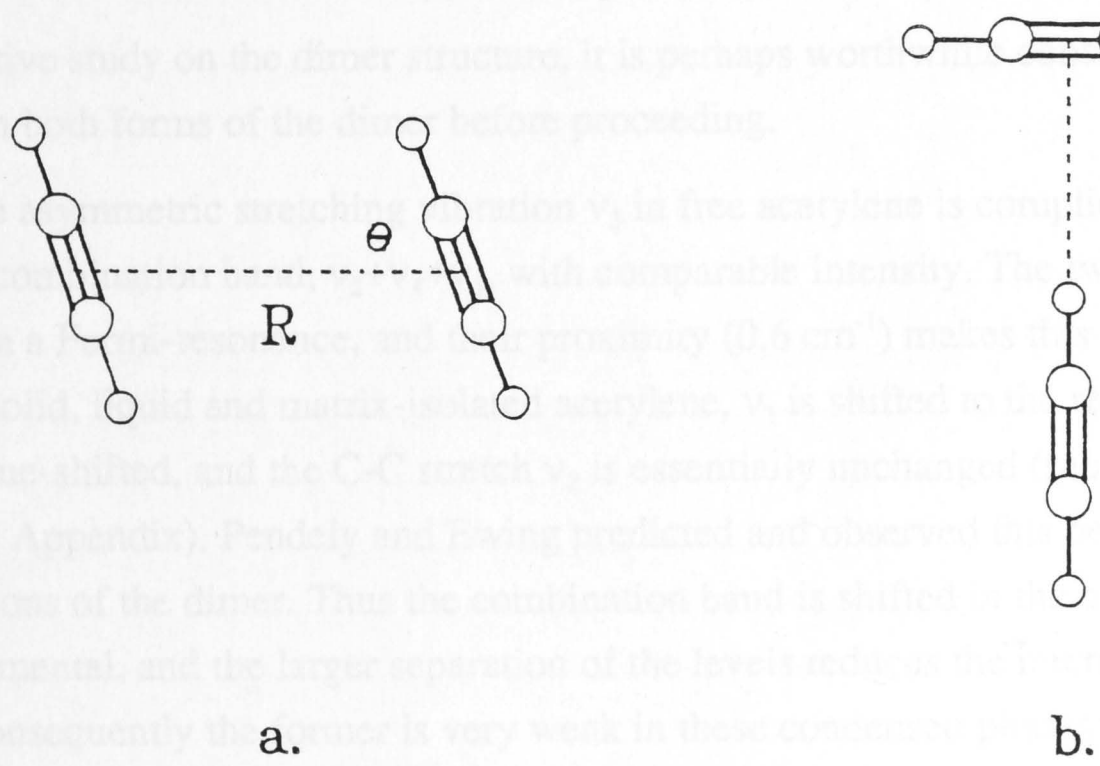


**Figure 3.1:** Two proposed structures for the acetylene dimer: **a.** the staggered-parallel, $C_{2h}$ form and **b.** the T-shaped, $C_{2v}$ form.

The absorptions of gaseous acetylene in a long-path White cell cooled to 215K have been studied with an FTIR spectrometer (Pendely 1983). Several weak absorptions in the regions of the non-IR active $\nu_4$, $\nu_2$ and $2\nu_5$ vibrations (the vibrations of acetylene are described in the Appendix), were assigned to the dimer on the basis of the pressure dependence of the peak intensities. The spectral resolution (0.8 $cm^{-1}$) was not high enough to observe individual ro-vibrational transitions, but by taking account of collision-induced and residual monomer absorptions the features remaining could be compared to simulations of the rotational contours of the dimer. Using the potential of Sakai *et.al.*, and the known acetylene force constants, predictions of the shifts of the monomer vibrational frequencies upon dimerization were made. The shape and position of the features were found to be consistent with the staggered parallel structure predicted by this potential.

## 3.2 Preliminary Discussion

Without a definitive study on the dimer structure, it is perhaps worthwhile considering the C-H vibrations in both forms of the dimer before proceeding.

The region of the asymmetric stretching vibration $\nu_3$ in free acetylene is complicated by the appearance of a combination band, $\nu_2+\nu_4+\nu_5$, with comparable intensity. The two vibrational levels interact via a Fermi-resonance, and their proximity (0.6 $cm^{-1}$) makes this interaction quite strong. In solid, liquid and matrix-isolated acetylene, $\nu_3$ is shifted to the red, the bending vibration $\nu_5$ is blue-shifted, and the C-C stretch $\nu_2$ is essentially unchanged (see the work referred to in the Appendix). Pendely and Ewing predicted and observed this behaviour in the latter two vibrations of the dimer. Thus the combination band is shifted in the opposite direction to the fundamental, and the larger separation of the levels reduces the interaction strength considerably. Consequently the former is very weak in these condensed phases. The "dimer" bands C-F are red-shifted by 6-16 $cm^{-1}$ from the unperturbed $\nu_3$ origin in the monomer, and are likely to arise out of this vibration, rather than the combination. No bands were observed at higher frequencies where the latter is expected to appear, suggesting that it is very weak in the dimer as well.

In the staggered parallel $C_{2h}$ structure, $\nu_3$ correlates with vibrations type $A_g + B_u$. The latter is IR active, and so only one band is expected, with hybrid *a*/*b*-type selection rules. In the $C_{2v}$ T-shaped dimer, $\nu_3$ gives rise to two IR active vibrations, of symmetry $A_1$ and $B_1$. The $A_1$ vibration corresponds to an *a*-type band, and is the C-H vibration of the proton "donor". It would thus be shifted more to the red than the $B_1$, *b*-type band, which is the C-H vibration in the proton "acceptor".

There are also differences in the statistical weights of the rotational levels in the two structures, which can be seen from Table 3.1. In the $C_{2h}$ dimer, with the $C_2$-axis parallel to the $c$-inertial axis, a 6:10 intensity alternation is expected for $J$ even:odd in the $K_a$=1 sub-band $P$- and $R$-branches (in a totally symmetric ground state). This alternation is reversed in the $Q$-branch. No alternation would occur with $J$ in the $C_{2v}$ dimer, but a 3:1 alternation would be observed for $K_a$ odd:even.

| Structure | $K_aK_c$ | | | |
|---|---|---|---|---|
| | ee | eo | oe | oo |
| $C_{2h}$, parallel | 6 | 10 | 6 | 10 |
| $C_{2v}$, T-shape | 1 | 1 | 3 | 3 |

**Table 3.1:** Spin statistical weights for two proposed forms of the acetylene dimer. e:even, o:odd.

## 3.3 Description and Assignment

Scans through bands D-F are given in Figures 3.2-3.4, plotted on the same vertical scale. Absolute positions were obtained using water absorptions at 3280.07382 and 3279.09602 $cm^{-1}$ for band D, 3283.06163 $cm^{-1}$ for band E, and 3284.22429 $cm^{-1}$ for band F (Camy-Peyret 1973). As discussed in the previous chapter, no allowance was made for the Doppler shifting of transitions of species in the molecular beam resulting from non-orthogonal laser-molecular beam crossings. This shift is some 0.004-0.005 $cm^{-1}$ to the red. (refer to the Appendix for more detail).

Both proposed structures are prolate, near-symmetric tops, with asymmetry parameters ($\kappa$) close to -1, and have C-H vibrations that can lead to perpendicular bands with the selection rule $\Delta K=\pm 1$. This type of band is composed of a series of $K$ sub-bands, spaced by $2(A-B)$ (Herzberg 1945). For reasonable choices of geometry, this quantity is about 2 $cm^{-1}$ in both cases, which is the same as the spacing between bands D,E and F. This suggests the following assignments:

Band D : $K_a$=0-1

Band F : $K_a$=2-1

Band E : $K_a$=1-0

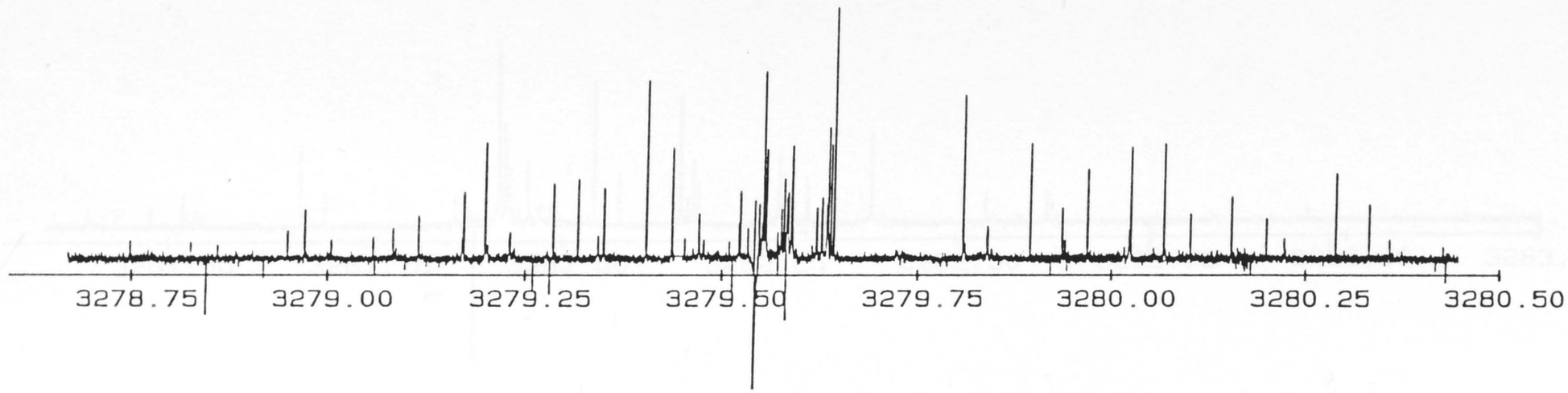


**Figure 3.2:** Single-mode scan through band D.

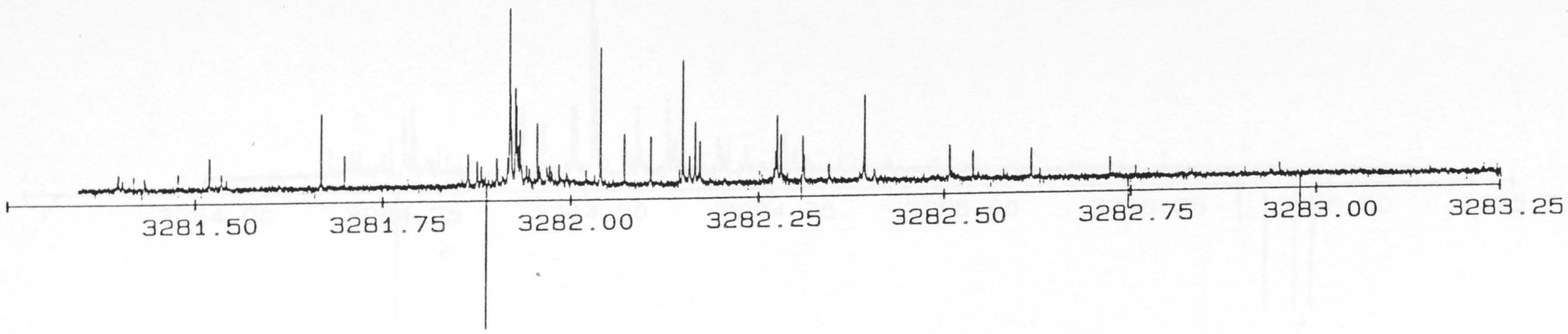


**Figure 3.3:** Single-mode scan through band E.

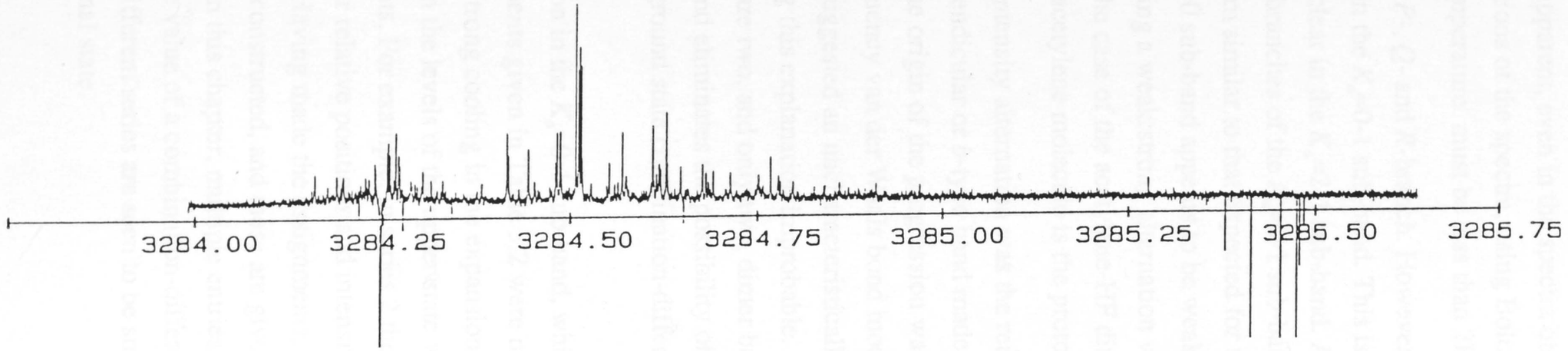


**Figure 3.4:** Single-mode scan through band F.

Additional $K$ sub-bands were not apparent, even in the spectra obtained under less severe conditions (Fischer 1985). Simulations of the spectra, using Boltzman population weights, indicate that the final rotational temperature must be less than 2K for this to be the case.

Each sub-band should consist of a $P$-, $Q$- and $R$-branch. However a progression of three series of such branches is evident in the $K_a$=0-1 sub-band. This is not as easily seen in the $K_a$=1-0 sub-band, and is not at all clear in the $K_a$=2-1 sub-band. An intensity alternation with $J$ even:odd is discernible in the $Q$-branches of the $K_a$=0-1 sub-band, the one nearest the monomer transition having a pattern similar to that expected for the $C_{2h}$ dimer in the ground state. On the other hand, the $K_a$=1-0 sub-band appears to be weaker than that expected on the basis of Boltzman factors, suggesting a weak:strong alternation with $K$ even:odd, as in the $C_{2v}$ dimer. This was also observed in the case of the acetylene-HF dimer (Huang 1987), which has a T-shaped from in which the acetylene molecule is the proton acceptor.

The existence of the $J$-dependent intensity alternation was the reason for an earlier assignment of this band (that is, the perpendicular or $b$-type band made up of three sub-bands) to the $C_{2h}$ structure (Bryant 1988). The origin of the progression was unclear; a hot-band sequence arising out of a low-frequency van der Waals bond mode was considered, but the small spacing between the series suggested an uncharacteristically small degree of anharmonicity for this vibration, making this explanation improbable. Assigning bands D-F to the one vibrational band means there are two, and only two, dimer bands, which is more consistent with the $C_{2v}$ structure, and eliminates the possibility of both forms being present in the beam. If this is the case, then ground state combination-differences should be the same in both bands.

For each member of the progression in the $K_a$=0-1 sub-band, which have been numbered from 1 to 3, the rotational assignments given in Table 3.2 were made. A maximum $J$-value of 5 was observed, again indicating strong cooling in the expansion. In making these assignments a number of perturbations in the levels of the upper state were noticed from the splitting of lines into several components. For example, in series 2 the $R(2)$ and $P(4)$ transitions have components with very similar relative positions and intensities, implying a perturbation to the $3_{03}$ level in the upper state. Having made the assignments, a number of ground state combination differences could be constructed, and these are given in Table 3.3. In all of the tables of line positions presented in this chapter, multiple entries indicate that more than one pair of transitions having the same value of a combination-difference was observed. Variations in the $\Delta F$ values between different series are seen to be small, which suggests that all three arise from the same vibrational state.

| | | | | | | Series | | |
|---|---|---|---|---|---|---|---|---|
| $J'$ | $K_a'$ | $K_c'$ | $J''$ | $K_a''$ | $K_c''$ | 1 | 2 | 3 |
| 6 | 0 | 6 | 5 | 1 | 5 | - | 3280.3313 | 3280.3579 |
| 5 | 0 | 5 | 4 | 1 | 4 | 3280.2879 | 3280.1985 | 3280.2215 |
| 4 | 0 | 4 | 3 | 1 | 3 | 3280.1539 | 3280.0666 | 3280.1010 |
| 3 | 0 | 3 | 2 | 1 | 2 | 3280.0244 | 3279.9393 | 3279.9678 |
| | | | | | | 3280.0227 | 3279.9353 | |
| 2 | 0 | 2 | 1 | 1 | 1 | 3279.8947 | 3279.8079 | 3279.8400 |
| | | | | | | | | 3279.8390 |
| 1 | 0 | 1 | 1 | 1 | 0 | 3279.6434 | 3279.5568 | 3279.5898 |
| 2 | 0 | 2 | 2 | 1 | 1 | 3279.6395 | 3279.5530 | 3279.5850 |
| | | | | | | | | 3279.5839 |
| 3 | 0 | 3 | 3 | 1 | 2 | 3279.6362 | 3279.5515 | 3279.5798 |
| | | | | | | 3279.6345 | 3279.5476 | |
| 4 | 0 | 4 | 4 | 1 | 3 | 3279.6284 | 3279.5419 | 3279.5763 |
| 5 | 0 | 5 | 5 | 1 | 4 | 3279.6217 | 3279.5333 | 3279.5558 |
| 6 | 0 | 6 | 6 | 1 | 5 | 3279.6157 | 3279.5218 | 3279.5476 |
| 0 | 0 | 0 | 1 | 1 | 1 | 3279.5234 | 3279.4369 | 3279.4707 |
| 1 | 0 | 1 | 2 | 1 | 2 | 3279.4048 | 3279.3172 | 3279.3502 |
| 2 | 0 | 2 | 3 | 1 | 3 | 3279.2861 | 3279.1994 | 3279.2314 |
| | | | | | | | | 3279.2301 |
| 3 | 0 | 3 | 4 | 1 | 4 | 3279.1724 | 3279.0836 | 3279.1159 |
| | | | | | | 3279.1709 | - | - |
| 4 | 0 | 4 | 5 | 1 | 5 | 3279.0586 | 3278.9715 | 3279.0057 |
| 5 | 0 | 5 | 6 | 1 | 6 | 3278.9494 | - | - |
| 6 | 0 | 6 | 7 | 1 | 7 | - | 3278.7498 | - |

**Table 3.2:** Assignments in the $K_a$ = 0-1 sub-band in the perpendicular band of the acetylene dimer

| Combination | Series | | |
|---|---|---|---|
| -difference | 1 | 2 | 3 |
| $2_{12}$-$1_{10}$ | 0.2396 | 0.2396 | 0.2396 |
| $2_{11}$-$1_{11}$ | 0.2552 | 0.2549 | 0.2550 |
| | | | 0.2552 |
| $3_{13}$-$2_{11}$ | 0.3535 | 0.3536 | 0.3536 |
| $3_{12}$-$2_{12}$ | 0.3882 | 0.3878 | 0.3880 |
| | 0.3882 | 0.3877 | |
| $4_{14}$-$3_{12}$ | 0.4638 | 0.4640 | 0.4638 |
| | 0.4637 | | |
| $4_{13}$-$3_{13}$ | 0.5254 | - | 0.5247 |
| $5_{15}$-$4_{13}$ | 0.5699 | 0.5704 | 0.5706 |
| $3_{13}$-$1_{11}$ | 0.6086 | 0.6085 | 0.6086 |
| $4_{14}$-$2_{12}$ | 0.8520 | 0.8519 | 0.8518 |
| | 0.8519 | | |
| $5_{15}$-$3_{13}$ | 1.0953 | 1.0951 | 1.0953 |
| $6_{16}$-$4_{14}$ | 1.3385 | | |
| $7_{17}$-$5_{15}$ | | 1.5815 | |

**Table 3.3:** Ground state combination-differences (in $cm^{-1}$) derived from the assignments in the $K_a$ = 0-1 sub-band of the perpendicular band.

In the $K_a$=1-0 sub-band, one member of the progression was easily identified. Transitions in the other two series were located using the assumption that, as in the $K_a$=0-1 sub-band, the ground state combination-differences were similar in each member of the progression. From the assignments listed in Table 3.4 it is clear that in series 1 the levels with $J''$ odd are missing. In series 2 only three transitions were identified, with $J'$=2, suggesting that the $J''$ even levels are absent in this series. Three ground-state combination differences could be constructed, and these are listed in Table 3.5. No assignments were made in the $Q$-branches.

| | | | | | | Series | | |
|---|---|---|---|---|---|---|---|---|
| $J'$ | $K_a'$ | $K_c'$ | $J''$ | $K_a''$ | $K_c''$ | 1 | 2 | 3 |
| 7 | 1 | 7 | 6 | 0 | 6 | | | 3282.7298 |
| 6 | 1 | 6 | 5 | 0 | 5 | | | 3282.6204 |
| 5 | 1 | 5 | 4 | 0 | 4 | 3282.5425 | | 3282.5114 |
| 4 | 1 | 4 | 3 | 0 | 3 | | 3282.3491 | 3282.3970 |
| 3 | 1 | 3 | 2 | 0 | 2 | 3282.3138 | | 3282.2845 |
| | | | | | | | | 3282.2793 |
| 2 | 1 | 2 | 1 | 0 | 1 | | 3282.1107 | 3282.1688 |
| | | | | | | | | 3282.1529 |
| 1 | 1 | 1 | 0 | 0 | 0 | 3282.0754 | | 3282.0441 |
| 1 | 1 | 1 | 2 | 0 | 2 | 3281.7039 | | 3281.6728 |
| 2 | 1 | 2 | 3 | 0 | 3 | | 3281.4921 | 3281.5499 |
| | | | | | | | | 3281.5341 |
| 3 | 1 | 3 | 4 | 0 | 4 | 3281.4477 | | 3281.4184 |
| | | | | | | | | 3281.4131 |

**Table 3.4:** Line positions (in $cm^{-1}$) and assignments in the $K_a$ = 1-0 sub-band of the perpendicular band of the acetylene dimer.

| Combination | Series | | |
|---|---|---|---|
| -difference | 1 | 2 | 3 |
| $2_{02}$-$0_{00}$ | 0.3715 | | 0.3712 |
| $3_{03}$-$1_{01}$ | | 0.6186 | 0.6188 |
| $4_{04}$-$2_{02}$ | 0.8661 | | 0.8661 |
| | | | 0.8662 |

**Table 3.5:** Ground-state combination differences derived from the assignments in the $K_a$ = 1-0 sub-band.

The $K_a$=2-1 sub-band only displayed $Q$- and $R$-branch transitions, and appears to have a large number of perturbations. Assignments were made by searching for combination-differences derived from the $K_a$=0-1 sub-band, and the results are listed in Table 3.6. In this sub-band only transitions up to $J''$=4 could be assigned, but the asymmetry doubling of the transitions was observed.

A scan through band C is presented in Figure 3.5. The vertical scale in this plot is approximately twice that in Figures 3.2-3.4. Absolute line positions were determined using water absorptions at 3273.77400, 3273.42697 and 3271.89070 $cm^{-1}$. A small part of the central region was missed due to a laser mode hop during this scan and a second scan is given in

| | | | | | | Series | | |
|---|---|---|---|---|---|---|---|---|
| $J'$ | $K_a'$ | $K_c'$ | $J''$ | $K_a''$ | $K_c''$ | 1 | 2 | 3 |
| 2 | 2 | 0 | 1 | 1 | 1 | 3284.5063<br>3284.5084 | 3284.4087 | 3284.4762 |
| 2 | 2 | 1 | 1 | 1 | 0 | 3284.6014 | 3284.5047<br>3284.5009 | 3284.5630 |
| 3 | 2 | 2 | 2 | 1 | 1 | 3284.6405 | 3284.5459 | 3284.6088<br>3284.6037 |
| 3 | 2 | 1 | 2 | 1 | 2 | | 3284.6217<br>3284.6142 | 3284.6841 |
| 4 | 2 | 3 | 3 | 1 | 2 | 3284.7719 | 3284.6743 | 3284.7073 |
| 4 | 2 | 2 | 3 | 1 | 3 | 3284.8527 | 3284.7610 | 3284.7911 |
| 2 | 2 | 0 | 2 | 1 | 1 | 3284.2514<br>3284.2535 | 3284.1538 | 3284.2212 |
| 2 | 2 | 1 | 2 | 1 | 2 | | 3284.2650<br>3284.2613 | 3284.3235 |
| 3 | 2 | 2 | 3 | 1 | 3 | 3284.2869 | 3284.1920 | 3284.2551<br>3284.2500 |
| 3 | 2 | 1 | 3 | 1 | 2 | | 3284.2335<br>3284.2260 | 3284.2958 |
| 4 | 2 | 3 | 4 | 1 | 4 | 3284.3082 | | |
| 5 | 2 | 4 | 5 | 1 | 5 | | | 3284.2212 |

**Table 3.6:** Line positions (in $cm^{-1}$) and assignments for the $K_a$ = 2-1 sub-band of the perpendicular band of the acetylene dimer.

Figure 3.6, from which it can be seen that only one transition was missed. The only difference between the conditions under which the two scans were collected is a slight decrease in the concentration of acetylene seeded in helium in the second case. It is clear from the reduced intensity of the higher $J$ lines and the lower S/N that a lower final temperature has been achieved as a result.

This band has $a$-type, or parallel-band structure, with distinct $P$-,$Q$- and $R$-branch regions. Searches were made for combination differences matching those found in the perpendicular band, and indeed a number of pairs of lines could be identified in this way. Using $a$-type selection rules, $\Delta K_a=0$, $\Delta K_c=\pm 1$, the assignments listed in Table 3.7 were made. Both $K_a=0$ and $K_a=1$ sub-bands were identified, and again a progression with three members was found. As in the perpendicular band, a number of perturbations were evident in the upper state rotational levels, and two of the series had missing transitions in the $K_a=0$ sub-band. These assignments account for the majority of stronger lines, but a number of weaker, unidentified transitions are present.

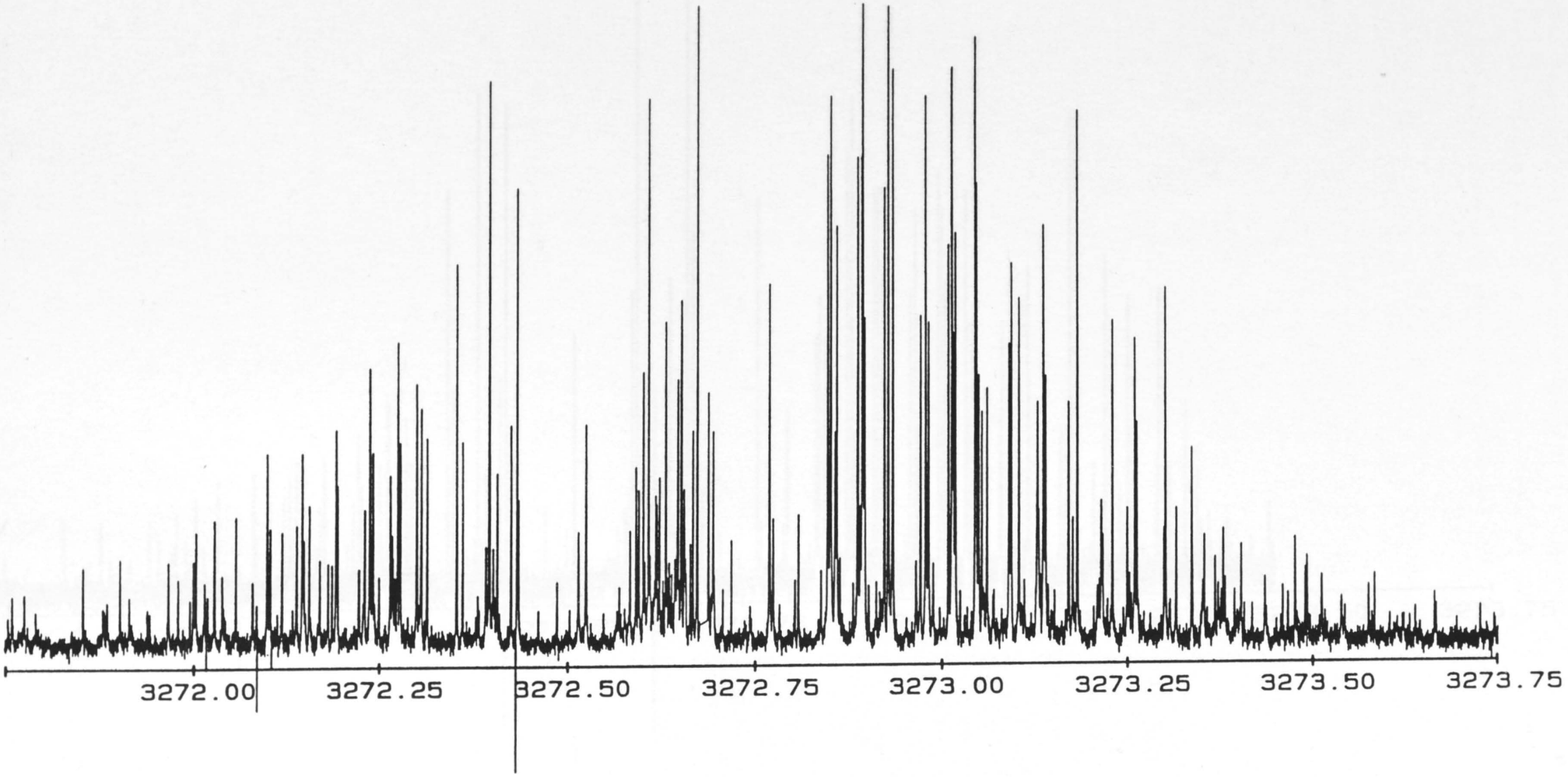


**Figure 3.5:** Single-mode scan through band C.

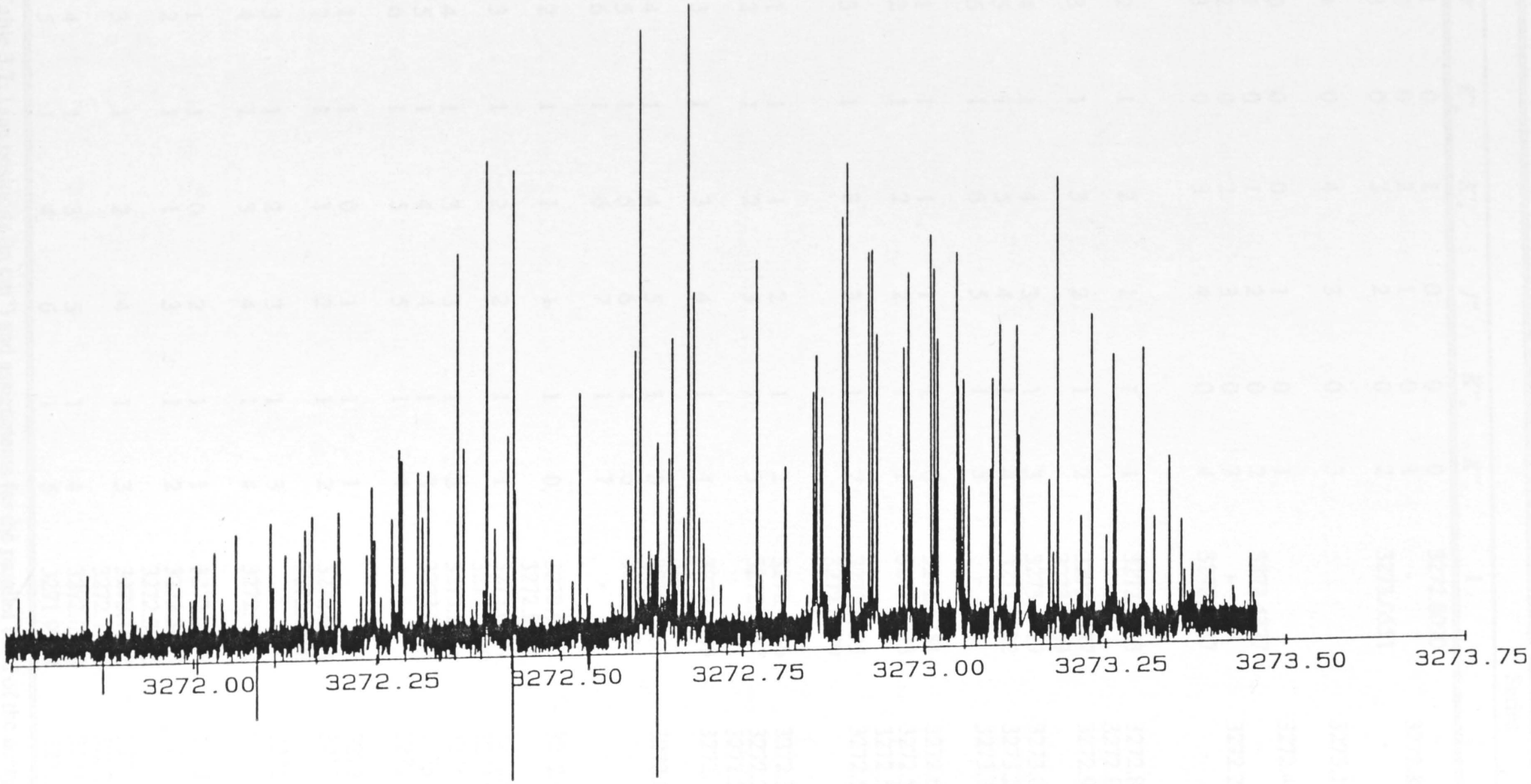


**Figure 3.6:** Single-mode scan through band C at a lower rotational temperature than Figure 3.5.

| | | | | | | Series | | |
|---|---|---|---|---|---|---|---|---|
| $J'$ | $K'_a$ | $K'_c$ | $J''$ | $K''_a$ | $K''_c$ | 1 | 2 | 3 |
| 1 | 0 | 1 | 0 | 0 | 0 | 3272.8090 | - | 3272.7704 |
| 2 | 0 | 2 | 1 | 0 | 1 | - | 3272.8574 | 3272.8951 |
| 3 | 0 | 3 | 2 | 0 | 2 | 3273.0551 | - | 3273.0145 |
| | | | | | | | | 3273.0169 |
| 4 | 0 | 4 | 3 | 0 | 3 | | 3273.1056 | 3273.1383 |
| 0 | 0 | 0 | 1 | 0 | 1 | | 3272.4879 | 3272.5262 |
| 1 | 0 | 1 | 2 | 0 | 2 | 3272.4377 | - | 3272.3991 |
| 2 | 0 | 2 | 3 | 0 | 3 | - | 3272.2391 | 3272.2765 |
| 3 | 0 | 3 | 4 | 0 | 4 | 3272.1887 | - | 3272.1508 |
| | | | | | | | | 3272.1483 |
| 2 | 1 | 2 | 1 | 1 | 1 | 3272.9243 | 3272.8476 | 3272.8886 |
| | | | | | | | 3272.8519 | |
| 3 | 1 | 3 | 2 | 1 | 2 | 3273.0477 | 3272.9729 | 3273.0097 |
| | | | | | | 3273.0459 | | |
| 4 | 1 | 4 | 3 | 1 | 3 | 3273.1719 | 3273.0953 | 3273.1306 |
| 5 | 1 | 5 | 4 | 1 | 4 | 3273.3022 | 3273.2158 | 3273.2508 |
| 6 | 1 | 6 | 5 | 1 | 5 | - | 3273.3378 | 3273.3692 |
| 1 | 1 | 1 | 1 | 1 | 0 | 3272.6751 | 3272.6030 | 3272.6493 |
| 2 | 1 | 2 | 2 | 1 | 1 | 3272.6693 | 3272.5970 | 3272.6337 |
| | | | | | | | 3272.5930 | |
| 3 | 1 | 3 | 3 | 1 | 2 | 3272.6595 | 3272.5850 | 3272.6217 |
| | | | | | | 3272.6579 | | |
| 1 | 1 | 1 | 2 | 1 | 2 | 3272.4356 | 3272.3635 | 3272.4097 |
| 2 | 1 | 2 | 3 | 1 | 3 | 3272.3157 | 3272.2435 | 3272.2799 |
| | | | | | | | 3272.2391 | |
| 3 | 1 | 3 | 4 | 1 | 4 | 3272.1959 | 3272.1212 | 3272.1579 |
| | | | | | | 3272.1941 | | |
| 4 | 1 | 4 | 5 | 1 | 5 | 3272.0766 | 3272.0002 | 3272.0354 |
| 5 | 1 | 5 | 6 | 1 | 6 | 3272.9634 | - | 3271.9124 |
| 6 | 1 | 6 | 7 | 1 | 7 | - | - | 3271.7564 |
| 2 | 1 | 1 | 1 | 1 | 0 | 3272.9357 | 3272.8600 | 3272.8951 |
| | | | | | | 3272.9294 | | 3272.8941 |
| 3 | 1 | 2 | 2 | 1 | 1 | 3273.0624 | 3272.9836 | 3273.0193 |
| | | | | | | 3273.0510 | 3272.9794 | 3273.0097 |
| 4 | 1 | 3 | 3 | 1 | 2 | 3273.1838 | 3273.1056 | 3273.1415 |
| 5 | 1 | 4 | 4 | 1 | 3 | 3273.3167 | 3273.2308 | 3273.2637 |
| 6 | 1 | 5 | 5 | 1 | 4 | | 3273.3546 | |
| 1 | 1 | 0 | 1 | 1 | 1 | | 3272.6102 | |
| 2 | 1 | 1 | 2 | 1 | 2 | 3272.6961 | 3272.6202 | |
| | | | | | | 3272.6898 | | |
| 3 | 1 | 2 | 3 | 1 | 3 | | 3272.6257 | 3272.6657 |
| 4 | 1 | 3 | 4 | 1 | 4 | 3272.7201 | | |
| 1 | 1 | 0 | 2 | 1 | 1 | 3272.4278 | 3272.3552 | 3272.3983 |
| 2 | 1 | 1 | 3 | 1 | 2 | 3272.3079 | 3272.2325 | 3272.2664 |
| | | | | | | 3272.3016 | | |
| 3 | 1 | 2 | 4 | 1 | 3 | 3272.1833 | 3272.1012 | |
| | | | | | | 3272.1722 | 3272.1053 | |
| 4 | 1 | 3 | 5 | 1 | 4 | 3272.0538 | 3271.9765 | 3272.0119 |
| 5 | 1 | 4 | 6 | 1 | 5 | 3271.9358 | 3271.8508 | |

**Table 3.7:** Line positions (in $cm^{-1}$) and assignments for the parallel band of the acetylene dimer.

## 3.4 Discussion

Clearly both the perpendicular and parallel bands arise from the same species, and since it is hard to reconcile the appearance of two relatively widely spaced bands with the $C_{2h}$ dimer structure, the $C_{2v}$ T-shaped form is a more likely candidate, as already indicated. However the origin of the progression, and the intensity alternations and missing levels remains unknown at this stage.

Despite being able to assign a number of transitions in both bands, the analysis of the spectra to obtain rotational constants, particularly those of the two upper states, is complicated by the large number of perturbations observed. It is possible to obtain approximate values for two of the ground state constants from the combination differences. Neglecting centrifugal distortion, the differences $F''(2_{12}\text{-}1_{10})$ and $F''(2_{11}\text{-}1_{11})$ are equal to $4C''$ and $4B''$ respectively (Herzberg, 1945). The estimates of $B''$ and $C''$ based on the average value for each $\Delta F''$ can be found in Table 3.8. Obtaining similar estimates for the upper states was hampered by the perturbations noted earlier. These rotational constants are seen to be very similar in each of the series, providing further evidence against the suggestion that the progression is a hot-band sequence.

| Series | 1 | 2 | 3 |
|---|---|---|---|
| $C''$[a] | 0.05990 | 0.05990 | 0.05990 |
| $B''$[b] | 0.06375 | 0.06370 | 0.06375 |

a: $F(2_{12}\text{-}1_{10})/4$ cm$^{-1}$

b: $F(2_{11}\text{-}1_{11})/4$ cm$^{-1}$

**Table 3.8:** Estimates of the ground state rotational constants for the acetylene dimer

If the $C_{2v}$ structure is assumed, then the only parameter that can be derived from these rotational constants is the intermolecular separation R. If the intramolecular bond distances and angles are assumed not to change upon complexation, then the moments of inertia of this dimer are given by:

$$I_{aa}=I_{HCCH}$$

$$I_{bb}=MR^2/2 + I_{HCCH}$$

$$I_{cc}=MR^2/2 + 2I_{HCCH}$$

where $I_{HCCH}$ is the moment of inertia (14.3267 amu Å$^2$), and M is the mass (26 amu) of an acetylene molecule. The estimates of R become 4.385 Å if $B''$ is used, and 4.410 Å if $C''$ is used. Both of these are larger than the 4.34 Å found in the low-temperature phase of crystalline acetylene (Koski 1975).

The absence of sub-bands with $K_a \geq 2$ makes the task of obtaining a reasonable estimate for a value of the $A$ rotational constant difficult. If a zero inertial defect, $\Delta=I_c-I_b-I_a$, is assumed for this planar structure, a value for $A''$ of 0.982 cm$^{-1}$ can be derived. This is considerably smaller than the 1.1766 cm$^{-1}$ expected (the value of the rotational constant $B_0$ for HCCH), which may indicate a large inertial defect exists. This is likely to be the result of large amplitude motions of the monomer units, and may also explain the discrepancy between the two values of R calculated using $B''$ and $C''$ (see the article by Muenter in (Weber 1987)).

An estimate of the excited state value for A in the perpendicular band can be obtained from the difference $F'(2_{21}-1_{01}) = 4A'$. For the three members of the progression, these estimates are 1.236, 1.240 and 1.243 cm$^{-1}$. Because the transitions used to obtain these values are in different sub-bands, absolute errors of ±0.001 cm$^{-1}$ are applicable, since each sub-band was calibrated separately. However, this will not affect the relatives differences between the values. These values of $A'$ are larger than expected for the $C_{2v}$ structure, and Coriolis interactions between the two dimer vibrations, and/or large amplitude motions may be implicated.

Perturbations in molecular spectra result from the interactions of two or more near-degenerate vibrational states, and are divided into two categories. A Fermi-resonance occurs between levels of the same vibronic species, and is independent of angular momentum ($J$). A Coriolis resonance is $J$-dependent, and disappears for $J$=0. A necessary (but not sufficient) condition for two levels to undergo such an interaction is given by Jahn's rule (Wollrab 1987): the product of the irreducible representations of the two vibronic species must contain that of a rotation in the molecular point group.

The rotational structure of the infrared spectra of dimers have been found to display perturbations in a number of cases (Bender 1987, Jucks 1988a, Jucks 1987b). In these cases there are potentially many perturbing states present, thanks to the low-frequency vibrations of the van der Waals bond. In only one example in HCH-HF has it been possible to identify the perturbing state, due partly to the extensive spectroscopic study of this species (Bender 1987). In all cases, combination vibrations involving intra- and intermolecular vibrations have been implicated. Interestingly, in both the HCN-HF and OC-HF (Jucks 1987b) examples, the mixing of these "dark" levels with the IR active vibration, as well as producing extraneous lines in the spectra, also reduces the width of the perturbed lines relative to the unperturbed ones. The lifetime of the perturbing state is apparently longer than that of the intramolecular fundamental in both cases.

The two acetylene dimer vibrations are separated by some 10 $cm^{-1}$ and an *x,y*-Coriolis resonance between them is allowed by Jahn's rule. However, the vibrations can be thought of as being on either the bound or the free acetylene, and their coupling would be very small. Additionally, since both carry oscillator strength, such an interaction does not explain the extra lines observed.

As mentioned in section 3.2, the combination vibration $\nu_2+\nu_4+\nu_5$ is likely to be shifted to frequencies higher than that found in the monomer. In the $C_{2v}$ dimer this combination would give rise to 32 vibrations, including states in which the three quanta are shared between the two molecules. With symmetries $8(A_1+B_1+A_2+B_2)$ a myriad of interactions of both types is possible, the strengths of which depend on the level separation and coupling coefficients. Another possible perturbing state is the level $\nu_2+2\nu_4$ in combination with one or more van der Waals bond modes.

As an illustration of the effects these perturbations have on the spectra, Figure 3.7 shows an expanded plot of the parallel band of the dimer in the region of $R(2)$. Similar splittings are seen in the $P(4)$ lines, indicating perturbations to various $J'$=3 levels. Transitions in each of the three series are shown, and it is evident that the splittings are different in each case. No dramatic changes in the linewidths are evident, suggesting that the state or states responsible have much the same lifetime as the C-H vibration.

The parallel and perpendicular bands observed here should be compared to the infrared spectra of the HF and HCN dimers. In both cases two bands are observed - the "free" and "bound" HF (H-C) stretches (Pine 1984, Jucks 1988b). The linewidth of the transitions in the bound stretching bands are larger than those in the "free" molecule, particularly in the HF case (as seen in Chapter 1).

This difference in the widths of the transitions in the two bands is not obvious in the case of the acetylene dimer. Transitions in the parallel (bound C-H) band had a FWHM of the order of 20-30 MHz, as did those in the $K_a$=2-1 and 1-0 sub-bands, while those in the $K_a$=0-1 sub-band were generally narrower, being of much the same width as the monomer transitions observed. This is consistent with the results of Miller *et.al.* given in Table 1.1, in which higher resolution was achieved. However, both increases and decreases in the linewidths within sub-bands are seen in perturbed transitions. For example, the strong $2_{20}$-$1_{11}$ (Series 1) and $2_{21}$-$1_{10}$ (Series 2) transitions are some 10 MHz narrower than the majority of $K_a$=2-1 (perpendicular band) lines, while the $2_{12}$-$3_{13}$ and $2_{02}$-$3_{03}$ (Series 2) are 10 MHz wider than most of the parallel band lines.

For $K'$=0 then there is a lifetime (linewidth) effect similar to that seen in the HF and HCN dimers, albeit a small one. With increasing angular momentum about the top axis, however, this effect disappears.

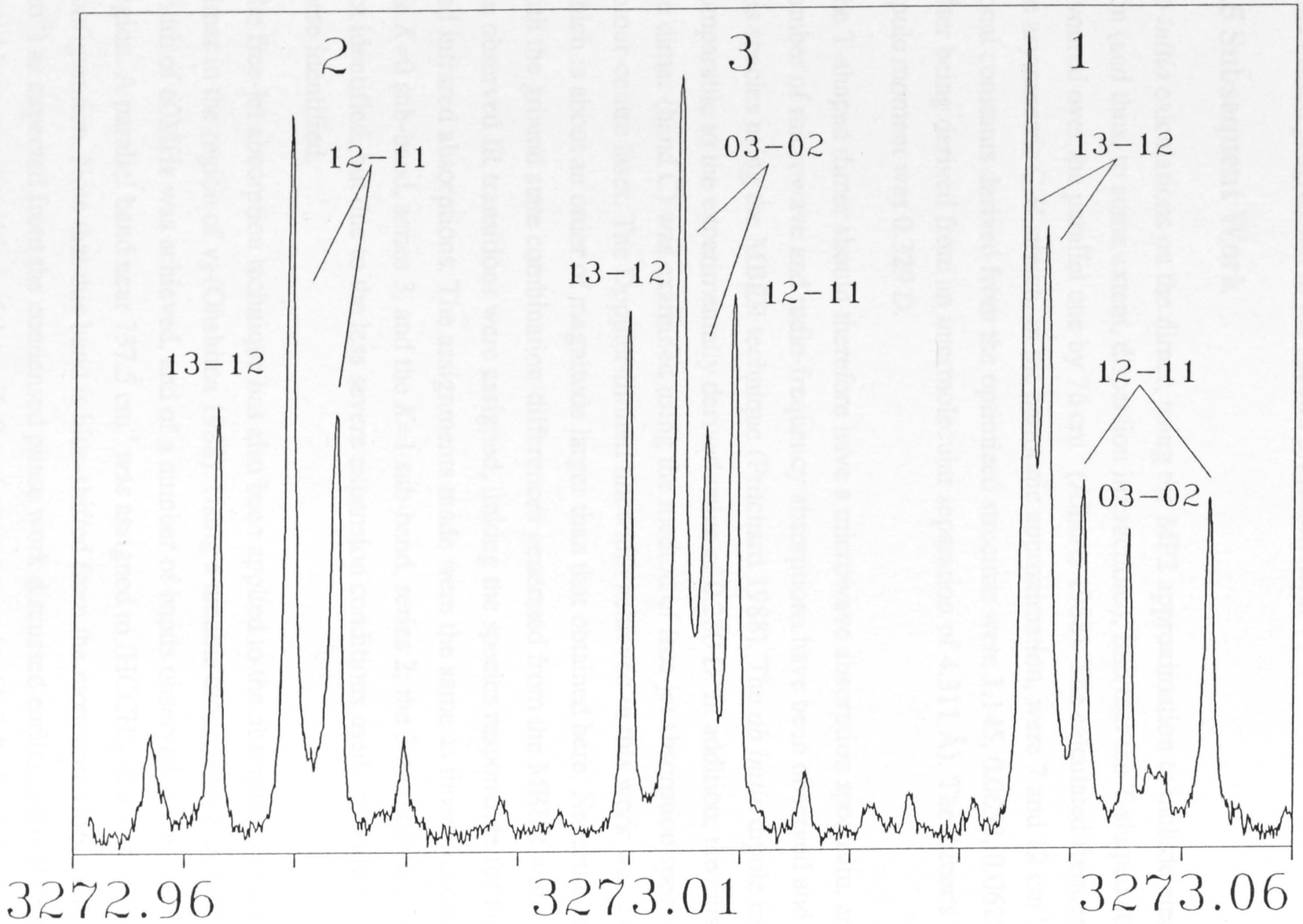


**Figure 3.7:** Expanded plot of the $R(2)$ transitions in the dimer parallel band, showing the effects of perturbations on the lines.

The HF dimer has been found to undergo interconversion via an internal rotational tunnelling motion (Dyke 1972), which manifests itself as a doubling of the ro-vibrational lines observed in the infrared bands. As will be discussed in the next section, a similar motion has been suggested in the acetylene dimer case (Ohshima 1988, Fraser 1988), which explains the hitherto unidentified progression in the spectra presented here.

## 3.5 Subsequent Work

*Ab initio* calculations on the dimer, using the MP2 approximation to include electron correlation (and thus, to some extent, dispersion interactions), find that the T-shaped structure is favoured over the parallel one by 76 $cm^{-1}$ (Alberts 1988). The calculated frequency shifts of the asymmetric C-H stretch, in the harmonic approximation, were 7 and 12 $cm^{-1}$, and the rotational constants derived from the optimized structure were 1.145, 0.0658, 0.0622 $cm^{-1}$ (the latter being derived from an intermolecular separation of 4.311 Å). The dimer's predicted dipole moment was 0.329 D.

The T-shaped dimer should therefore have a microwave absorption spectrum, and indeed, a number of microwave and radio-frequency absorptions have been observed and assigned to this species using the MBER technique (Pritchard 1988). The *ab initio* dipole moment is comparable to the experimentally derived value of 0.280 D. In addition, the parallel band of the dimer (band C) was examined using the method of free-jet absorption spectroscopy with a colour-centre laser. The Doppler-limited linewidth achieved in this work was 240MHz, which is about an order of magnitude larger than that obtained here. Nevertheless, armed with the ground state combination-differences generated from the MBER work, about 50% of the observed IR transitions were assigned, linking the species responsible for the microwave and infrared absorptions. The assignments made were the same as those presented here for the $K$=0 sub-band, series 3, and the $K$=1 sub-band, series 2; the 3 membered progression was not identified, but due to the less severe expansion conditions used, transitions up to $J$=12 were identified.

The free-jet absorption technique has also been applied to the absorptions of the acetylene dimer in the region of $\nu_5$ (Ohshima 1988). Using a tunable diode laser a Doppler-limited linewidth of 60MHz was achieved, and of a number of bands observed in the 730-745 $cm^{-1}$ region. A parallel band near 737.5 $cm^{-1}$ was assigned to $(HCCH)_2$ in a T-shaped configuration. Note that this band is blue-shifted from the monomer vibrational origin (729 $cm^{-1}$) as expected from the condensed phase work discussed earlier. As in the spectra presented here, a progression of three $K$=0 and asymmetry doubled $K$=1 sub-bands were observed and interpreted as a splitting of the rotational levels by interconversion tunnelling of the type shown in Figure 3.7. This represents and in-plane, geared interconversion of the two acetylene sub-units, with the staggered-parallel form as a transition state.

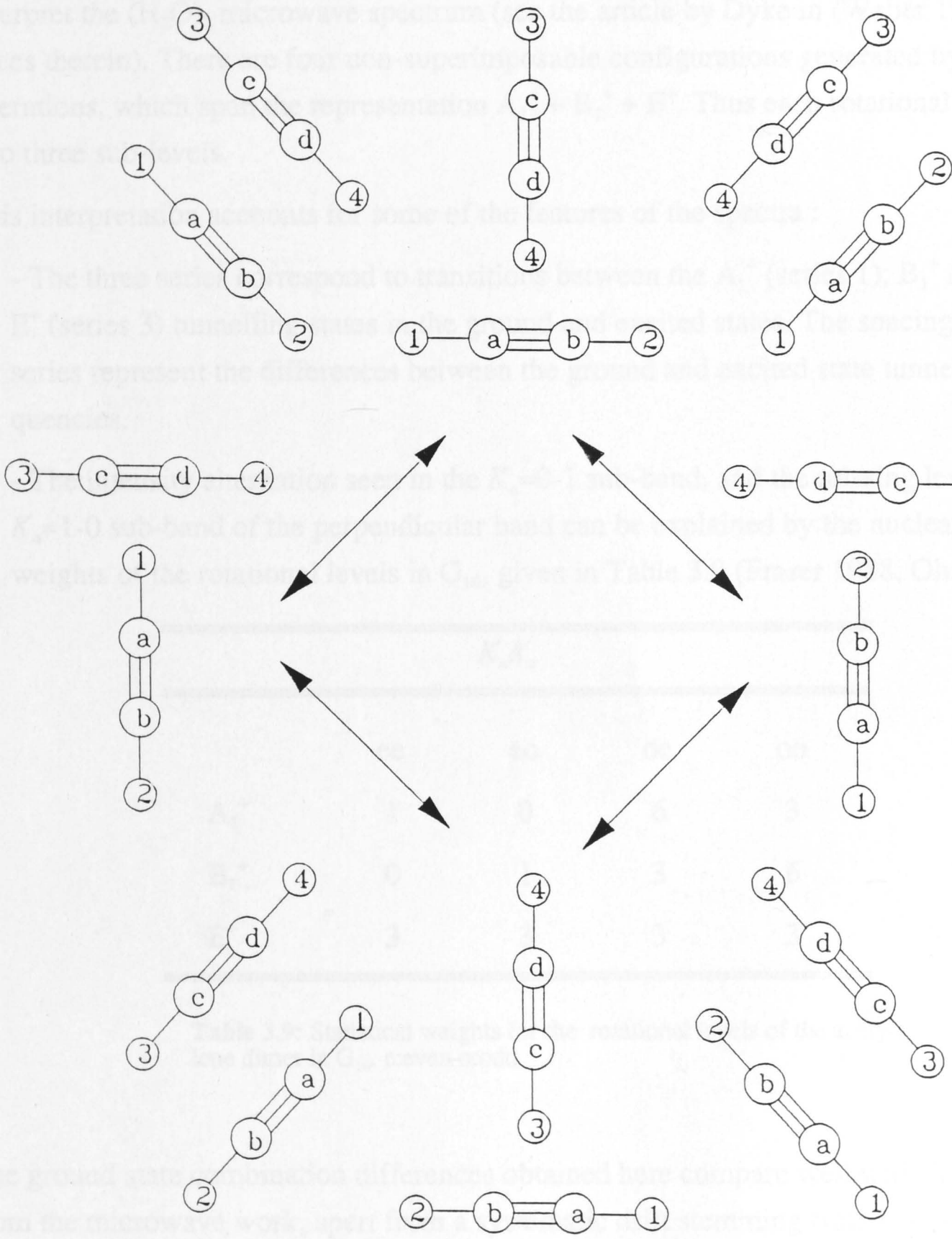


**Figure 3.8:** Interconversion tunnelling in the acetylene dimer (Fraser 1988, Ohshima 1988).

In an independent study, Fraser *et.al.* (1988) extended the microwave measurements on the dimer using the pulsed molecular beam FT-microwave method, and also scanned bands C-F with an arrangement similar to that used here. An interpretation of the spectra was presented in terms of the $G_{16}$ permutation-inversion (PI) group, the same group used by Dyke to interpret the $(H_2O)_2$ microwave spectrum (see the article by Dyke in (Weber 1987) and references therein). There are four non-superimposable configurations generated by the group operations, which span the representation $A_1^+ + B_1^+ + E^+$. Thus each rotational level is split into three sub-levels.

This interpretation accounts for some of the features of the spectra :

- The three series correspond to transitions between the $A_1^+$ (series 1), $B_1^+$ (series 2) and $E^+$ (series 3) tunnelling states in the ground and excited states. The spacing between the series represent the differences between the ground and excited state tunnelling frequencies.

- The intensity alternation seen in the $K_a$=0-1 sub-band, and the missing levels in the $K_a$=1-0 sub-band of the perpendicular band can be explained by the nuclear spin statistical weights of the rotational levels in $G_{16}$, given in Table 3.9 (Fraser 1988, Ohshima 1988).

| | $K_aK_c$ | | | |
|---|---|---|---|---|
| | ee | eo | oe | oo |
| $A_1^+$ | 1 | 0 | 6 | 3 |
| $B_1^+$ | 0 | 1 | 3 | 6 |
| $E^+$ | 3 | 3 | 3 | 3 |

**Table 3.9:** Statistical weights for the rotational levels of the acetylene dimer in $G_{16}$. e:even o:odd

The ground state combination differences obtained here compare well with those derived from the microwave work, apart from a systematic drift stemming from the assumption that the marker etalon used here had a free spectral range of 150.00 MHz; a value of 150.055 MHz is more appropriate from a comparison of the two sets of data (Figure 3.9). This result is carried over to a comparison of the two sets of infrared data (once the Doppler-shift is taken into consideration).

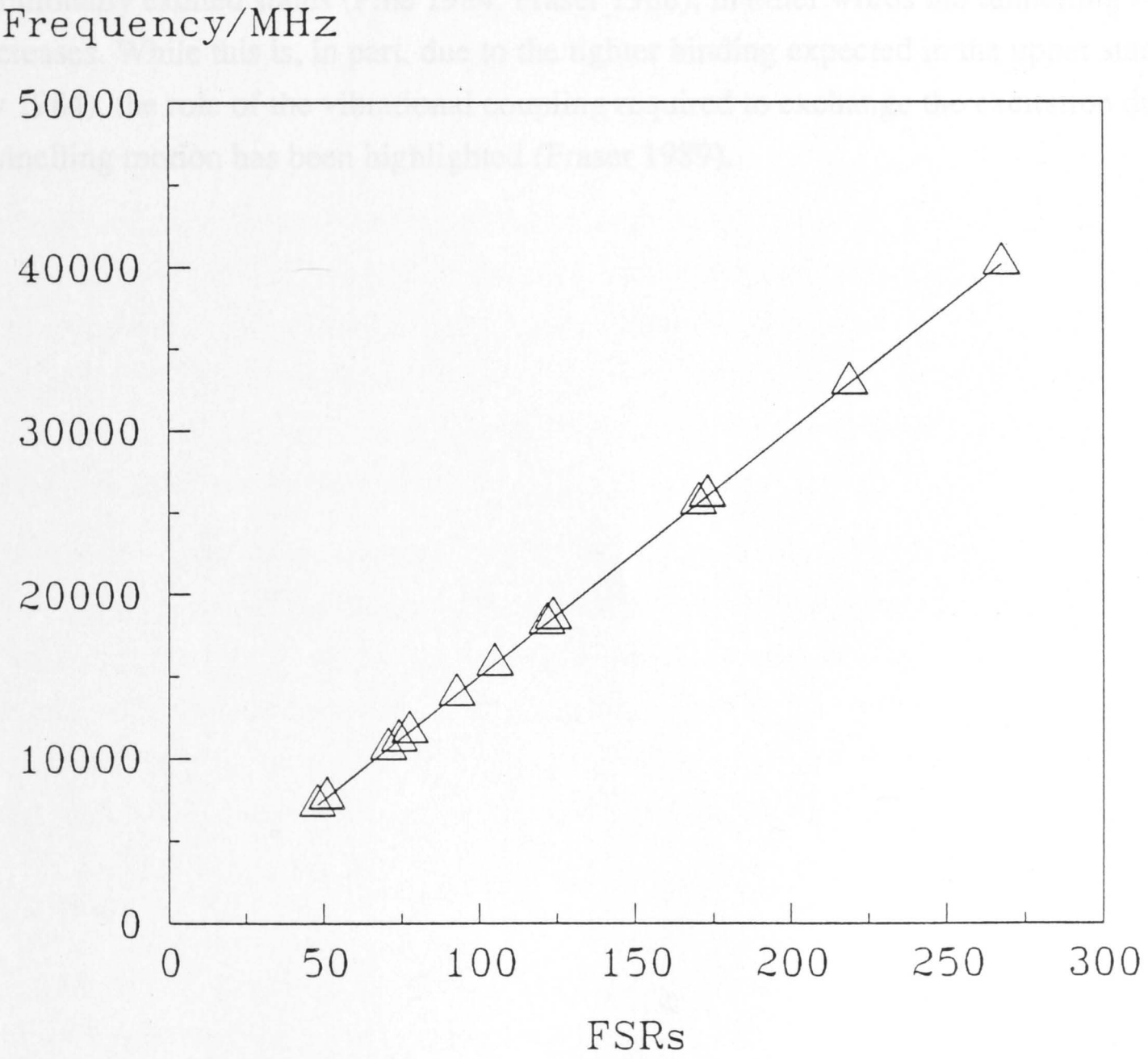


**Figure 3.9:** Comparison of the ground state combination differences obtained in this work, and the microwave data of Fraser *et.al.* (1988). The infrared values in terms of marker etalon free spectral ranges (FSRs) are plotted against the microwave values (in MHz). Linear regression indicates a value of 150.055(8) MHz for the etalon FSR.

All of the spectra presented in this work been calibrated assuming an etalon FSR of 150.00 MHz, and the effect of doing this can be easily corrected by appropriately scaling the rotational constants obtained in this and subsequent chapters. Given this, the estimates of the ground state rotational constants for the dimer in Table 3.8 are in good agreement with the microwave values of Fraser *et.al.*. In the infrared work they were able to observe transitions with higher values of $J''$, and their assignments are consequential more extensive.

In both the HF and the acetylene dimers, the tunnel splitting is found to decrease dramatically in the vibrationally excited states (Pine 1984, Fraser 1988); in other words the tunnelling barrier increases. While this is, in part, due to the tighter binding expected in the upper state (Sandorfy 1984), the role of the vibrational coupling required to exchange the excitation during the tunnelling motion has been highlighted (Fraser 1989).

# Chapter 4: Band B : The Acetylene Trimer

In this chapter the spectrum identified as band B by Miller, Vorhalik and Watts is discussed, the analysis of which has been reported by Pritchard, Muenter and Howard (1987). However, the resolution achieved here with a collimated beam is an order of magnitude better than that obtained in their free-jet absorption spectra.

## 4.1 Description

A single mode scan through the region of band B is shown in Figure 4.1. The vertical scale on this plot is approximately twice that of the plot of band C (Figure 3.5). Absolute line positions were determined with respect to the water absorption at 3267.09189 $cm^{-1}$ (Camy-Peyret 1973). Note that the $P(7)$ line of the $\nu_{245}$ band of acetylene does not appear in the bolometer trace, indicating strong rotational cooling of the monomer during the expansion. Pritchard *et.al.* used this absorption (in a gas cell) to calibrate their spectrum, taking it's absolute position from the work of Lafferty and Thibault (1964). However as pointed out by Scott and Rao (1966), and indicated by the subsequent work of Lafferty (1988), this value is shifted by 0.02-0.03 $cm^{-1}$ from the currently accepted one, leading to a similar difference between their line positions and those presented here.

The most striking features of the spectrum are it's regularity and apparent simplicity : there is no $Q$-branch, nor a "zero gap" between what might be $P$- and $R$-branches. Furthermore, while some of the lines in the middle of the band seem to be well represented by a Voigt profile, the majority display shoulders and even splitting, indicating that they are not isolated ro-vibrational transitions. There is an obvious splitting of the lines at the high frequency end of the spectrum, as well as some weaker, apparently unrelated structure of unknown origin.

## 4.2 Assignment

These observations can be reconciled if we assume that the spectral features are a series of $Q$-branches in a perpendicular band of a symmetric top, for which the selection rules are (Herzberg 1945) :

$$\Delta J = 0,\pm 1 \qquad \Delta K = \pm 1$$

When these are combined with the expression for the energy levels of an oblate top, the transition frequencies in the $K$ sub-bands are given by :

$$\nu_{sub}^{K} = \nu_0 + (C'-B') \pm 2(C'-B')K + [(C'-B')-(C''-B'')]K^2$$

$$\nu_{Q}^{K} = \nu_{sub}^{K} + (B'-B'')J(J+1)$$

$$\nu_{P,R}^{K} = \nu_{sub}^{K} + (B'+B'')m + (B'-B'')m^2$$

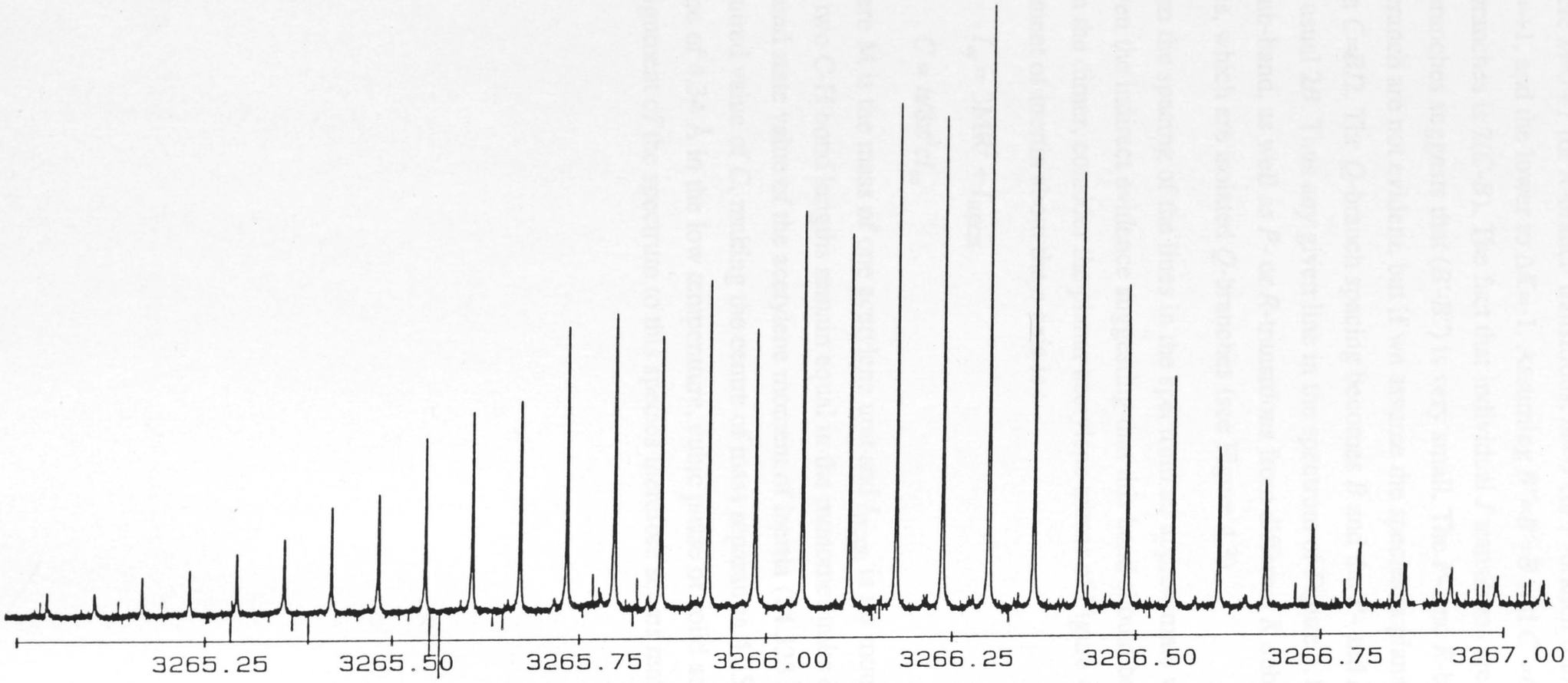


**Figure 4.1:** Single-mode scan through band B.

where $m=J+1$ for $R$-branch transitions, $m=-J$ for $P$-branch transitions, the upper sign refers to $\Delta K=+1$, and the lower to $\Delta K=-1$. Assuming $B''=B'=B$ and $C''=C'=C$, the spacing of the $Q$-branches is $2(C-B)$. The fact that individual $J$ transitions are not resolved in these $Q$-branches suggests that $(B'-B'')$ is very small. The $P$- and $R$-branches associated with each $Q$-branch are not evident, but if we assume the species is planar and the inertial defect is zero, then $C=B/2$. The $Q$-branch spacing becomes $B$ and the $P$- and $R$-branch lines are spaced by the usual $2B$. Thus any given line in the spectrum of Figure 4.1 can consist of a $Q$-branch of a $K$ sub-band, as well as $P$- or $R$-transitions from different $K$ sub-bands, except the ${}^{R}Q_0$ and ${}^{P}Q_1$ lines, which are isolated $Q$-branches (see Figure 4.3).

From the spacing of the lines in the spectrum an approximate value for $B$ is 0.0629 $cm^{-1}$. Given the indirect evidence suggesting that this band should be assigned to a species larger than the dimer, consider the planar acetylene trimer of Figure 4.2. For this species the moment of inertia about the $c$-axis is :

$$I_{cc} = 3MR^2 + I_{HCCH}$$

$$C = h/8\pi^2 c I_{cc}$$

where M is the mass of one acetylene unit and $I_{HCCH}$ is it's moment of inertia (again, assuming the two C-H bond lengths remain equal in the monomer units of the complex). Using the ground state value of the acetylene moment of inertia (14.323 amu Å$^2$), R = 2.5 Å gives the required value of $C$, making the centre of mass separation 4.35 Å. This should be compared a value of 4.34 Å in the low temperature, cubic phase of solid acetylene (Figure A.2). The assignment of the spectrum to this species therefore seems reasonable.

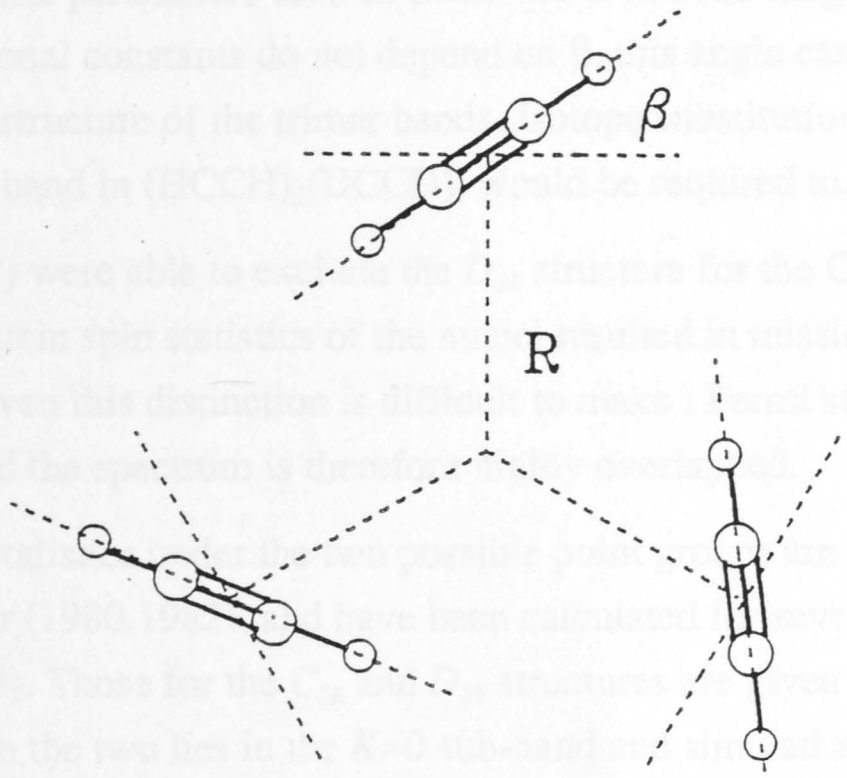


**Figure 4.2:** Proposed planar structure of the acetylene trimer.

## 4.3 Analysis

The planar trimer can have $C_{3h}$ or $D_{3h}$ symmetry, depending on the value of the angle β in Figure 4.2. The former is likely to be favoured for reasons similar to those which determine the dimer structure : reduced H-H repulsive interaction, the angular dependence of the quadrupolar interaction and a weak H-bonding interaction with the triple bond π-cloud. While an accurate value of R is readily obtained from the spectrum, much less can be said about other structural parameters such as β and the C-H bond lengths in the monomer units. Because the rotational constants do not depend on β, this angle cannot be determined from the ro-vibrational structure of the trimer bands. Isotope substitution experiments, such as a study of the same band in $(HCCH)_2(DCCD)$, would be required to obtain this parameter.

Fraser *et.al.* (1987) were able to exclude the $D_{3h}$ structure for the $CO_2$ trimer from the fact that the Bose-Einstein spin statistics of the nuclei resulted in missing rotational levels. For the acetylene trimer even this distinction is difficult to make : Fermi statistics do not lead to missing levels, and the spectrum is therefore highly overlapped.

The nuclear spin statistics under the two possible point groups are easily determined from the work of Weber (1980,1982), and have been calculated for several possible trimer structures (Weber 1988). Those for the $C_{3h}$ and $D_{3h}$ structures are given in Table 4.1. The only difference between the two lies in the $K$=0 sub-band and simulations of the trimer spectrum using both sets of weights are very similar.

| | | $D_{3h}$ | $C_{3h}$ |
|---|---|---|---|
| K=0 | $J$ even | 8 | 12 |
| | $J$ odd | 16 | 12 |
| K=3$n$ | | 24 | 24 |
| K=3$n$±1 | | 20 | 20 |

**Table 4.1:** Spin-statistical weights for two possible symmetries of the acetylene trimer.

The shift from the unperturbed monomer vibrational frequency is about 22 $cm^{-1}$, which will affect the resonance interaction between the $\nu_{245}$ combination band and the asymmetric stretch $\nu_3$, to the extent that the former is likely to be weak in the trimer. The $\Sigma_u^+$ vibrations of the monomer correlate with A'+E' in the $C_{3h}$ point group, and the E' vibration is IR active, so

the perpendicular band involves a transition to a degenerate excited state. In such cases there are a number of effects than can complicate the spectrum. One of these is the first order Coriolis interaction, which changes the spacing of the sub-bands to (Herzberg 1945):

$$\nu_{sub}^{K} = \nu_0 + [C'(1-2\zeta_i)-B'] \pm 2[C'(1-\zeta_i)-B']K + [(C'-B')-(C''-B'')]K^2$$

where $\zeta_i$ is the Coriolis zeta parameter, $|\zeta_i| \leq 1$, which is a measure of the vibrational angular momentum about the top axis for the degenerate vibration $\nu_i$. The fact that the *P*- and *R*-branch lines lie on top of the *Q*-branches indicates that the latter are spaced by some multiple of *B*. This means that $\zeta_i$ must be very close to 0 or ±1. For $\zeta_i = -1$ the *Q*-branch spacing becomes zero and the band would resemble a parallel band, which is clearly not the case. For $\zeta_i = +1$ the *Q*-branches are spaced by 2*B* instead of *B*, and tend to dominate the shape of the spectrum. The $\zeta$ parameter is therefore likely to be close to zero, and such a value is consistent with the discussions on degenerate vibrations found in (Herzberg 1945). In the case of the trimer only small changes in the nature of the C-H stretching vibrations from those in the monomer are expected, so that in both components of the degenerate vibration arising from $\nu_3$ the nuclei will move on approximately the same line, namely the monomer bond directions. No superposition of the two will result in vibrational angular momentum about the top axis, meaning $\zeta_i$ must be very close to zero for the vibration being considered here, if our assignment of the band to the trimer is correct. Confirmation of this could be obtained from studies on the other E" vibration of the trimer and the application of the $\zeta$-sum rules (Nemes 1981).

There is also the possibility of *l*-doubling occurring (Mills 1972) which splits the $k=l=\pm 1$ levels (note that $K=|k|$), and produces a different effective *B'* in the *Q*- and *P*- and *R*-branches of the *K*=1-0 sub-band ($K=0, \Delta K=+1$):

$B'_{eff} = B'+q/2$ for the *P*- and *R*-branch

$B'_{eff} = B'-q/2$ for the *Q*-branch

where *q* is the *l*-doubling constant. The nature of the spectrum means we cannot determine a precise value for this parameter. However, all of the lines appear to have about the same width, which indicates that $(B'_{eff} - B'')$ in the ${}^{R}Q_0$ branch is little different from $(B'-B'')$ i.e. $q \approx 0$.

In analysing the trimer spectrum one is faced with the task of choosing the position of the band origin. While the ${}^{R}Q_0$ "line" is usually the most intense of the *Q*-branches, this does not mean the most intense line of the observed spectrum should be assigned to it, since the *P*- and *R*-branch transitions enhance the intensity of other *Q*-branches with which they coincide. In Figure 4.3 a simulation of the trimer spectrum is given, in which a temperature of 1K has been assumed, and we have set $B'=B''=B$ and $C'=C''=C$; the transitions contributing to each

line are also shown in the Figure. The comparison between simulated and observed intensities is rather poor, but the position of the ${}^{R}Q_0$ line appears to be either at 3265.9224, 3265.9853 or 3265.0477 $cm^{-1}$ from the overall shapes of the two bands. It is possible that drifts in the source conditions, bolometer sensitivity or laser power might affect the relative intensities of lines at opposite ends of the observed spectrum, although such changes are expected to be small.

Figure 4.4 shows another scan through the trimer band, which was taken under similar source conditions, except for a slightly lower concentration of $C_2H_2$ in the gas mixture (as discussed in the previous chapter with regard to the band C spectra). While neither spectrum was normalised to the incident laser power, the intensities seen in Figure 4.4 were reproduced in another scan, similar expansion conditions. It would seem then, that the differences between the relative line intensities of the two scans are due to different rotational temperatures in the trimer.

In fact it is not only the intensities that differ: the lines in the spectrum of Figure 4.1 are about a factor of two broader than those of Figure 4.4. This increase in the linewidth suggests that the trimer is at a higher temperature in Figure 4.1 and that there is a substantial inhomogeneous contribution to the lineshape. In some cases lines that show splitting in the lower temperature spectrum disappear in the higher temperature one, which we have shown in Figure 4.5. These lines are in the same region in which the band origin is assumed to lie, and because the ${}^{R}Q_0$ and ${}^{R}Q_1$ lines contain no *P*- or *R*-branch transitions neither of these are expected to show such splitting. For this reason, a likely assignment would ${}^{R}Q_0$ : 3265.9224 $cm^{-1}$ and ${}^{P}Q_1$ : 3265.9853 $cm^{-1}$. The ${}^{R}Q_1$ branch is then at 3265.8591 $cm^{-1}$, and contains the ${}^{P}P_1(1)$ transition, which may be shifted slightly due either to a small Coriolis constant $\zeta_i$ or a non-zero inertial defect in the upper state. These assignments would place the band origin at about 3265.95 $cm^{-1}$, which, while not definitive, is perhaps a better estimate than the 3265.6 $cm^{-1}$ of Pritchard *et.al.*. The latter would require the unlikely situation of *P*-branch transitions of the low *K* sub-bands with practically no intensity, despite strong *R*-branch transitions. One objection to these assignments is the fact that the relative intensities of the ${}^{R}Q_1$ and ${}^{P}Q_1$ branches are different in the two spectra, although we should expect them to be the about the same, unless the *J* states of the $K$=1 state are strongly cooled (the first transition of the $\Delta K$=+1 *Q*-branch is for $J$=2, while the first for the $\Delta K$=-1 *Q*-branch is for $J$=1).

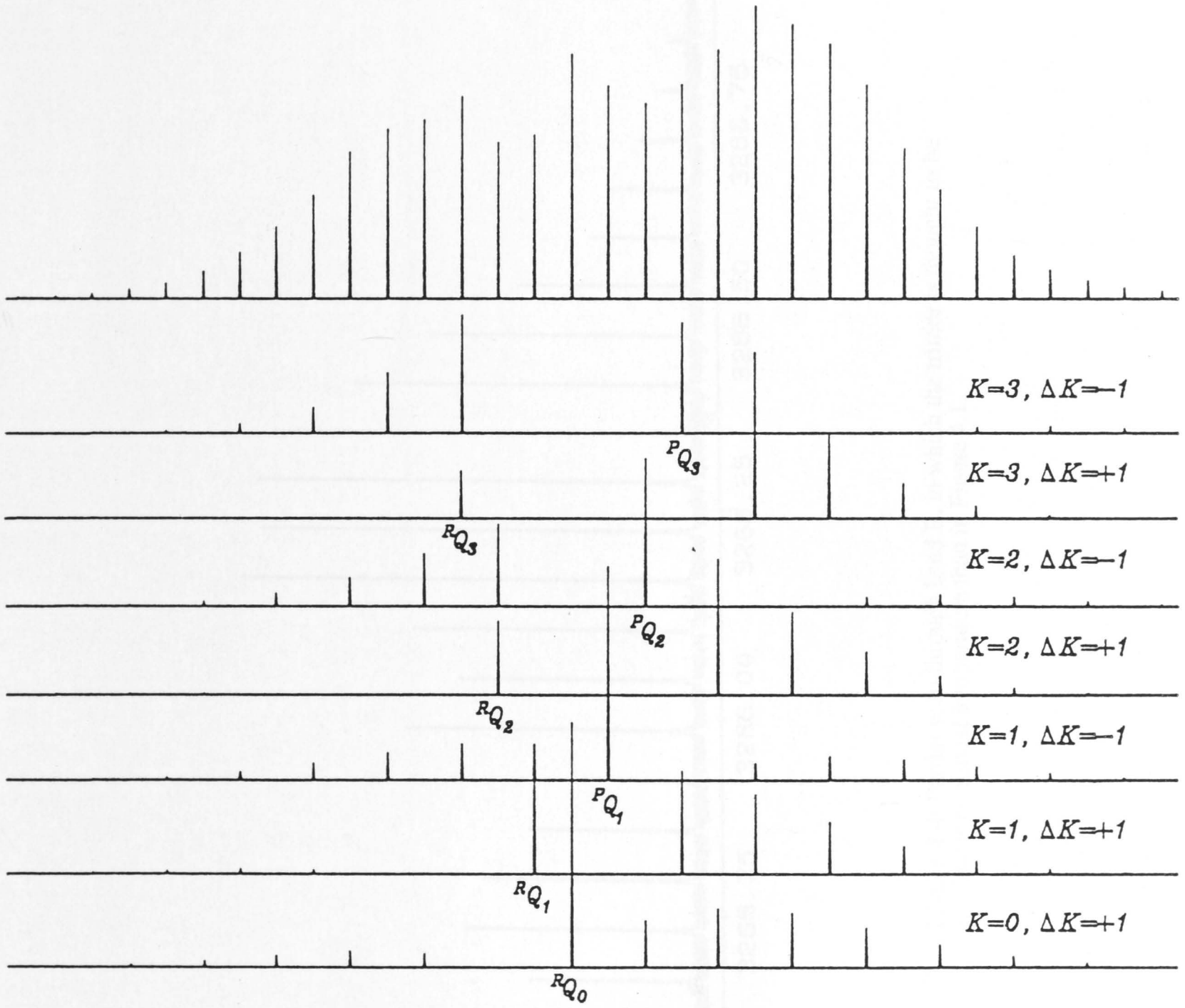


**Figure 4.3:** Simulation of the acetylene trimer spectrum at 1K, assuming $B'=B''=B$, $C=B/2$, and $\zeta_{ti}=0$. The $C_{3h}$ spin statistical have been used in calculating the line intensities. In addition, the low-$K$ sub-bands are shown to illustrate the manner in which they overlap.

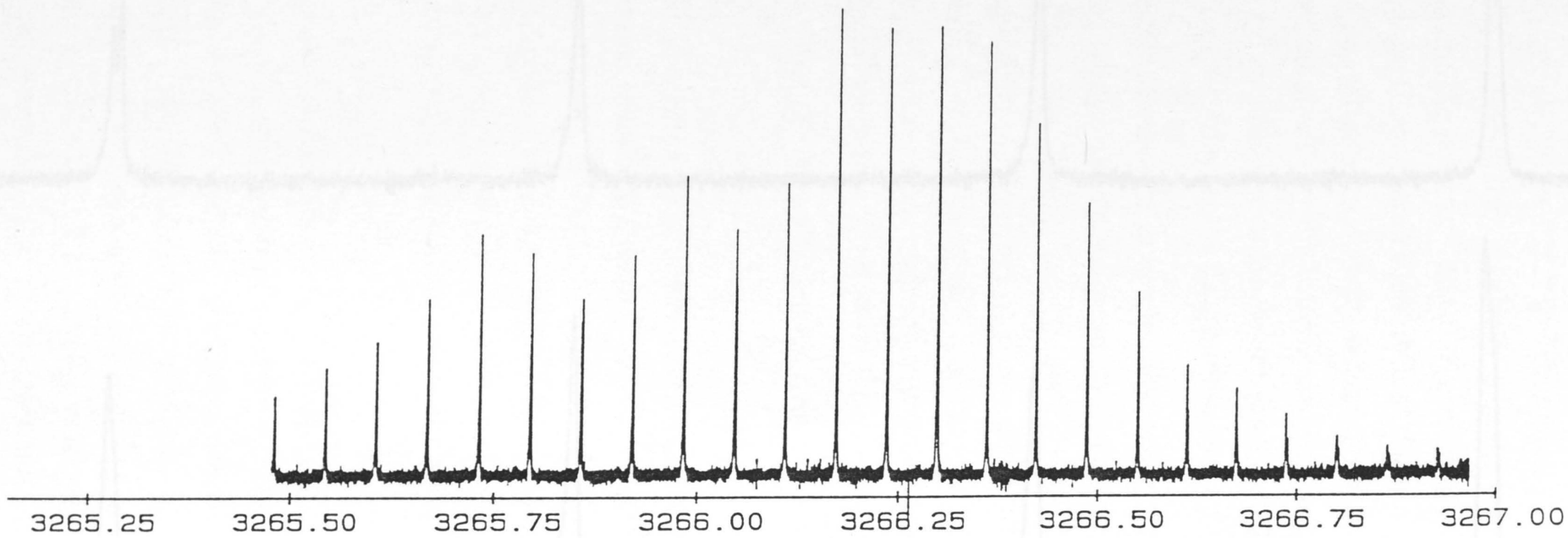


**Figure 4.4:** Partial scan through band B, in which the trimer is thought to be at a lower rotational temperature than in Figure 4.1.

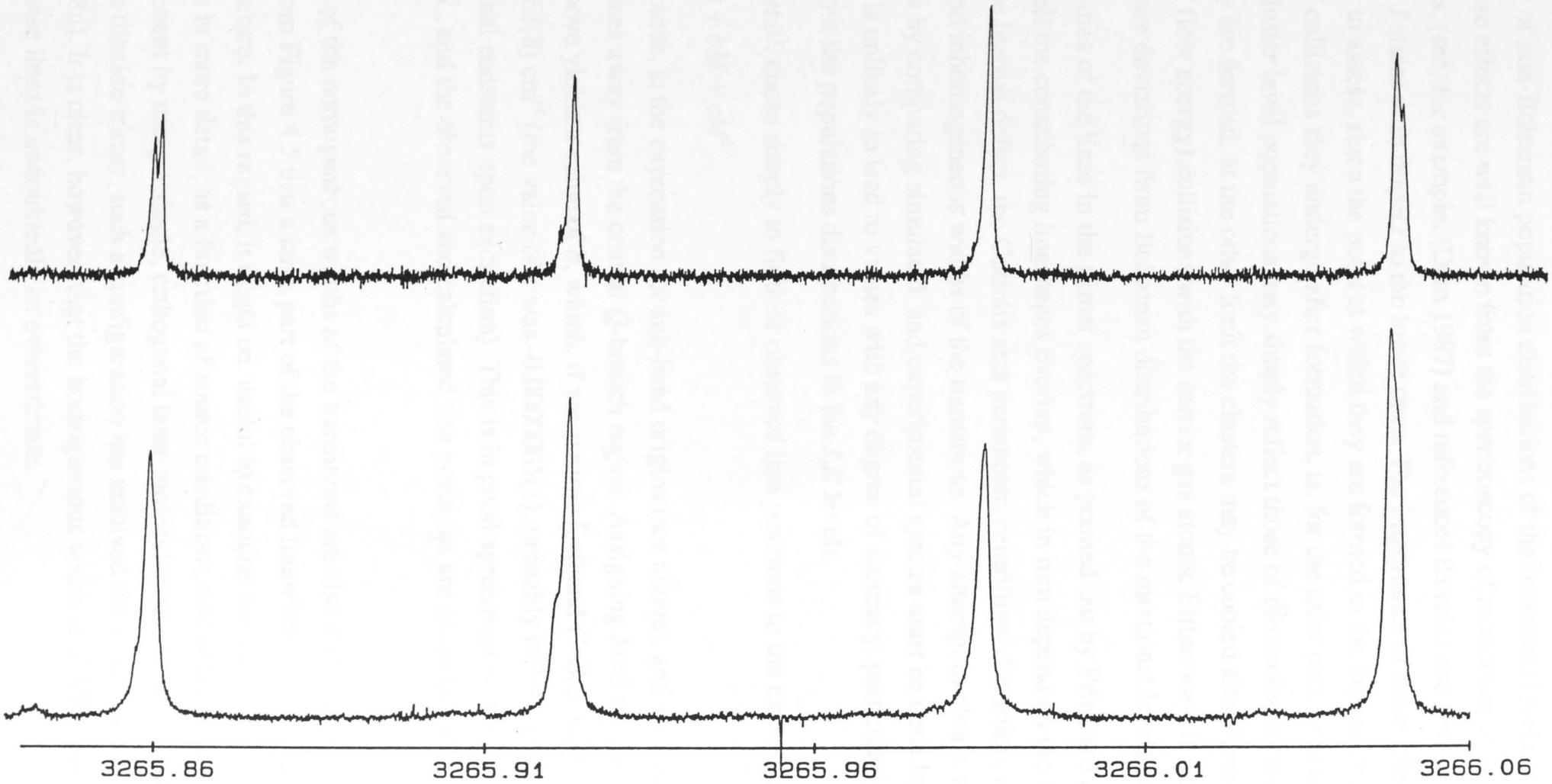


**Figure 4.5:** Expansions of Figures 4.1 and 4.4 in the region where the band origin is most likely to be found.

A comparison between simulated and experimental intensities can be complicated by the possibility of non-Boltzman population distributions of the rotational levels of species in the beam. These effects are well known from the spectroscopy of monomers in supersonic expansions, (see, for example, (Dam 1987) and references therein) and tend to over-populate the higher $J$ states with respect to the lower ones. The importance of these effects in clusters is difficult to assess, since the point at which they are formed in the expansion, and hence the number of collisions they undergo after formation, is, for the most part, undetermined. At one limit the cluster level populations may simply reflect those of the cooled monomers from which they are formed; at the other limit the clusters may be cooled after formation by a number of (low energy) collisions with the carrier gas atoms. Either way, it would not be surprising to see deviations from Boltzman distributions of the rotational levels in the trimer.

The intensities of the lines in the trimer spectrum, as pointed out by Pritchard *et.al.*, depend on how well the contributing lineshapes overlap, which in turn depend on the values of $(B'\text{-}B'')$, the inertial defect, the Coriolis zeta parameter, centrifugal distortion, and the homogeneous and inhomogeneous widths of the transitions. Any attempt to obtain values for these parameters by comparing simulated and experimental spectra must be done by trial and error, and is unlikely to lead to values with any degree of accuracy, particularly if little is known about the populations distributions in the $J,K$ levels.

Pritchard *et.al.* chose simply to fit their observed line positions to the expression

$$\nu = a + bM + cM^2$$

This, of course, is the expression for sub-band origins (see above), and so is only approximate for lines away from the central $Q$-branch region. Assigning $M$=0 on the basis of the discussion above yields a value of $b$, which, if we assume $\zeta_i$=0 and $C$=$B$/2, suggests $B$=0.062865(8) $cm^{-1}$ (the value of $c$ was -0.0000005(1), probably reflecting a small change in the rotational constants upon excitation). This is in good agreement with the value of Pritchard *et.al.*, and the observed and calculated line positions are given in Table 4.2.

Estimates of the homogeneous widths of the transitions are also difficult to obtain, but it can be seen from Figure 4.5 that a large part of the observed linewidth is due to overlapping rotational structure. In this regard, it might be useful to examine the width and shape of each of these lines in more detail, as a function of source conditions, and to increase the resolution of the experiment by using a single, orthogonal laser-molecular beam crossing. In the case of the carbon dioxide trimer, such a configuration has resolved the $J$-structure in the $Q$-branches (Pine 1988a). It is clear, however, that the homogeneous width of 30MHz assigned by Miller *et.al.* to these lines is undoubtedly an overestimate.

| M | Observed | Calculated | Difference |
|---|---|---|---|
| 19 | 3267.1154 | - | |
| | 3267.1143 | | |
| | 3267.1111 | | |
| 18 | 3267.0538 | - | |
| | 3267.0526 | | |
| | 3267.0500 | | |
| 17 | 3266.9903 | - | |
| | 3266.9868 | | |
| 16 | 3266.9275 | - | |
| | 3266.9261 | | |
| 15 | 3266.8621 | - | |
| | 3266.8644 | | |
| | 3266.8652 | | |
| 14 | 3266.8022 | - | |
| | 3266.8007 | | |
| 13 | 3266.7390 | 3266.7390 | 0.0000 |
| | 3266.7374 | | |
| 12 | 3266.6768 | 3266.6762 | 0.0006 |
| | 3266.6750 | | |
| 11 | 3266.6137 | 3266.6135 | 0.0002 |
| | 3266.6124 | | |
| 10 | 3266.5502 | 3266.5507 | -0.0005 |
| 9 | 3266.4881 | 3266.4879 | 0.0002 |
| | 3266.4872 | | |
| 8 | 3266.4248 | 3266.4251 | -0.0003 |
| 7 | 3266.3620 | 3266.3623 | -0.0003 |
| 6 | 3266.2994 | 3266.2995 | -0.0001 |
| 5 | 3266.2367 | 3266.2367 | 0.0000 |
| 4 | 3266.1740 | 3266.1739 | 0.0001 |
| 3 | 3266.1111 | 3266.1111 | 0.0000 |
| 2 | 3266.0477 | 3266.0482 | -0.0005 |
| 1 | 3265.9853 | 3265.9854 | -0.0001 |
| 0 | 3265.9224 | 3265.9225 | -0.0001 |
| -1 | 3265.8591 | 3265.8596 | -0.0005 |
| -2 | 3265.7972 | 3265.7968 | 0.0004 |
| -3 | 3265.7342 | 3265.7339 | 0.0003 |
| | 3265.7340 | | |
| -4 | 3265.6714 | 3265.6710 | 0.0004 |
| -5 | 3265.6083 | 3265.6081 | 0.0002 |
| -6 | 3265.5453 | 3265.5452 | 0.0001 |
| -7 | 3265.4825 | 3265.4822 | 0.0003 |
| -8 | 3265.4194 | 3265.4193 | 0.0001 |
| -9 | 3265.3563 | 3265.3563 | 0.0000 |
| -10 | 3265.2934 | 3265.2934 | 0.0000 |
| -11 | 3265.2304 | 3265.2304 | 0.0000 |
| -12 | 3265.1672 | 3265.1675 | -0.0003 |
| -13 | 3265.1042 | 3265.1045 | -0.0003 |

**Table 4.2:** Observed and calculated line positions (in $cm^{-1}$) for the acetylene trimer band. Split transitions at the high frequency end of the band were not included in the fit.

## 4.4 Discussion

There have been a number of spectroscopic studies of polyatomic trimers to date, and in most cases structural information has been obtained. The majority of studies have been on hydrogen-bonded systems, since in these systems a general trend in the red shifts of the X-H stretching vibrations to increase with cluster size separates the bands associated with the smaller clusters from each other.

The HF trimer dissociation spectrum has been studied at relatively low resolution (0.06 $cm^{-1}$) by Lisy *et.al.* (Michael 1986), who assigned a band at 3712 $cm^{-1}$, some 250 $cm^{-1}$ to the red of the free HF stretching frequency, to the trimeric species. This shift should be compared to 30 and 100 $cm^{-1}$ for the two dimer vibrations. They were unable to resolve individual rotational transitions, but from the number of vibrational bands that appear on isotopic substitution ($(HF)_2DF$, $(DF)_2HF$), they concluded that $(HF)_3$ is cyclic, in agreement with *ab initio* calculations (Liu 1986a). Given the results for $(C_2H_2)_3$, it would be interesting to examine the HF trimer at similar resolution since the rotational structure of the band should be much the same. Unfortunately, as in the somewhat lower resolution work of Lisy and Michael, no *J,K* structure was evident in the H-F stretching band of the trimer at 3714 $cm^{-1}$.

In Figure 4.6a a low resolution scan (laser multimode, as in Figure 1.2) through this band is given. While it's shape is likely to be distorted by the laser linewidth, there is some broad structure evident corresponding to the *P*- and *R*-branch regions of the spectrum, and a weaker, local maximum near 3718 $cm^{-1}$. These features were not seen in the 0.8 $cm^{-1}$ resolution spectrum of Lisy, particularly the 'dip' in the band centre.

There are several differences between the two experiments :

- the optothermal method is not mass selective. This, however, would make features of a given species less rather than more discernible.

- the trimer rotational temperature(s) would be lower in the optothermal experiment, due to the higher source pressure used. If the inhomogeneous contribution to the linewidth is sufficiently large, this would reduce the width of the feature. In addition, further experimental and theoretical work by Lisy *et.al.* (Kolenbrander 1988) has demonstrated the significance of low frequency torsional vibrations in the trimer. Any role these have to play in this H-F stretching band will also be affected by temperature.

While the HF and acetylene trimer spectra would be expected to be similar in shape, this is apparently not the case: the dip in the band centre is unexpected. As demonstrated by the simulations of the trimer spectrum (Eggers 1986) in Figure 4.6, this inconsistency could be removed by adjusting $\zeta$ to spread the *Q*-branch intensity away from the centre, but as in the acetylene case, the value of this parameter is unlikely to be much different from zero (a value

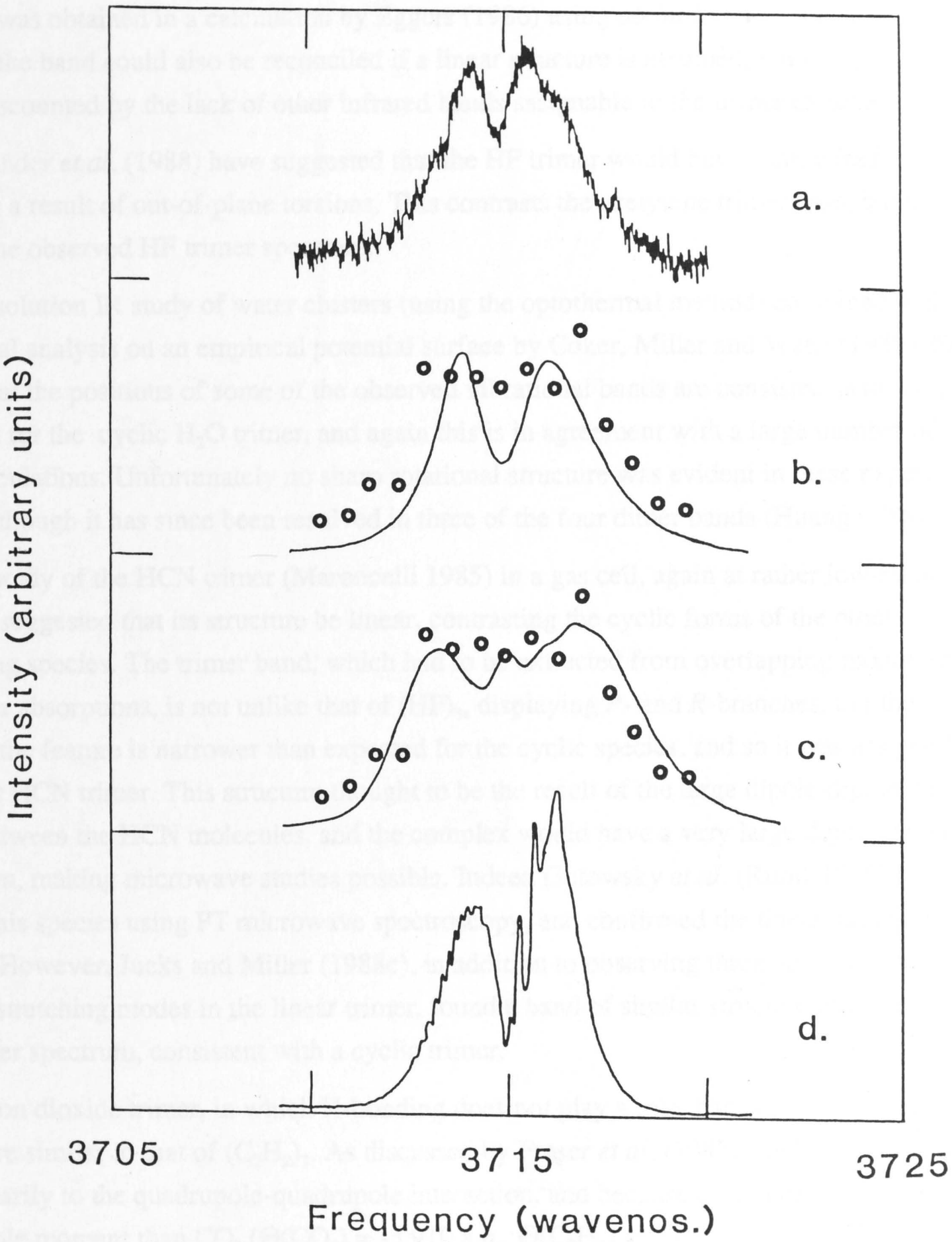


**Figure 4.6:** Low-resolution scan through the band assigned to the HF trimer. A 2% HF in He mixture was expanded from a source pressure of 600kPa to obtain this spectrum. **a:** Experiment. **b:** Simulation with $\zeta$=0.5 and a line-width of 0.5 $cm^{-1}$. **c:** Simulation with $\zeta$=0.002. **d:** Simulation of the linear HF trimer. The simulations were carried out by Eggers (1986) using *ab initio* structures, and a rotational temperature of 10K. The dots represent the results of Michael and Lisy (1986).

of 0.002 was obtained in a calculation by Eggers (1986) using *ab initio* force constants). The shape of the band could also be reconciled if a linear structure is assumed, but this possibility can be discounted by the lack of other infrared bands assignable to the trimer (Michael 1986).

Kolenbrander *et.al.* (1988) have suggested that the HF trimer would have a large inertial defect, as a result of out-of-plane torsions. This contrasts the acetylene trimer case, but may explain the observed HF trimer spectrum.

A low resolution IR study of water clusters (using the optothermal method) combined with a vibrational analysis on an empirical potential surface by Coker, Miller and Watts (1985), has shown that the positions of some of the observed vibrational bands are consistent with those predicted for the cyclic $H_2O$ trimer, and again this is in agreement with a large number of *ab initio* calculations. Unfortunately no sharp rotational structure was evident in these experiments, although it has since been resolved in three of the four dimer bands (Huang 1988).

A FTIR study of the HCN trimer (Maroncelli 1985) in a gas cell, again at rather low-resolution, has suggested that its structure be linear, contrasting the cyclic forms of the other H-bonding species. The trimer band, which had to be extracted from overlapping monomer and dimer absorptions, is not unlike that of $(HF)_3$, displaying *P*- and *R*-branches, but the width of the feature is narrower than expected for the cyclic species, and so it was assigned to the linear HCN trimer. This structure thought to be the result of the large dipole-dipole interaction between the HCN molecules, and the complex would have a very large dipole moment of it's own, making microwave studies possible. Indeed Gutowsky *et.al.* (Ruoff 1986) have studied this species using FT microwave spectroscopy, and confirmed the linear structure of $(HCN)_3$. However, Jucks and Miller (1988c), in addition to observing three bands assigned to the C-H stretching modes in the linear trimer, found a band of similar structure to the acetylene trimer spectrum, consistent with a cyclic trimer.

The carbon dioxide trimer, in which H-bonding does not play a role, has been shown to adopt a structure similar to that of $(C_2H_2)_3$. As discussed by Fraser *et.al.* (1987), such a structure is due primarily to the quadrupole-quadrupole interaction, and because acetylene has a larger quadrupole moment than $CO_2$ ($\Theta(CO_2)$ = -3.910 a.u., $\Theta(C_2H_2)$ = 5.45 a.u.), this interaction is likely to be prominent in determining this trimer's structure, so that the role of any weak H-bonding interaction is unclear. However, in the acetylene case a large red shift (22 $cm^{-1}$) of the C-H stretching vibration accompanies the formation of the trimer. This is not the case for the $CO_2$ trimer in the region of $2\nu_2^0+\nu_3$, nor the $C_2H_4$ trimer (Huisken 1987) in the region of $\nu_7$, where the observed vibrational frequency shifts are very small. Large shifts are typical in H-bonded systems (Liu 1986b), and for this reason such interactions seem to play a role in condensed acetylene.

*Ab initio* calculations have been performed on the acetylene trimer at the SCF level (Alberts 1988). The $C_{3h}$ structure is predicted, although the calculated values of the (harmonic) frequency shift and rotational constant $B$ (12 $cm^{-1}$ and 0.0564 $cm^{-1}$) only approximate the experimental values.

# Chapter 5: Band A : The Acetylene Tetramer and Pentamer

Miller *et.al.* proposed that band A might arise from either the acetylene tetramer or pentamer formed in the expansion. In this chapter a single mode scan through this band is examined, and we find that it has contributions from both species, which have a cyclic structure similar to the trimer. This represents the first example of rotationally resolved spectra for a van der Waals cluster larger than a trimer (Bryant 1988).

## 5.1 Description

A scan through band A is given in Figure 5.1. The vertical scale is the same as that for the plots of bands D-F. This was calibrated with the water absorption at 3260.42740 $cm^{-1}$ (Camy-Peyret 1973), and it is possible that this fairly strong absorption may affect the intensity of the transitions in the beam near this wavenumber, due to atmospheric absorption of the laser radiation.

There are at least 3 bands evident in this scan, all shifted to the red of the unperturbed monomer vibrational frequency by some 26-28 $cm^{-1}$ (and again the combination band is unlikely to be as important as the fundamental vibration in the species absorbing in this region.) Two resemble parallel bands of a symmetric, or at least nearly symmetric, rotor, with separate *P*- *Q*- and *R*-branches. The central portion of the scan bears some resemblance to the perpendicular band of the trimer, dominated by a set of *Q*-branches in the middle. The spacing in the *P*- and *R*- branches of the parallel bands indicates B rotational constants of approximately 0.018 and 0.032 $cm^{-1}$, and the spacing between the lines of the central portion of the scan is about 0.025 $cm^{-1}$. The ro-vibrational features are rather broad, and lie atop a continuous dissociation signal which presumably is due to overlap between adjacent features, and/or a continuum from the contributions of larger clusters, as observed in the $CO_2$ dimer spectrum (Jucks 1987a)

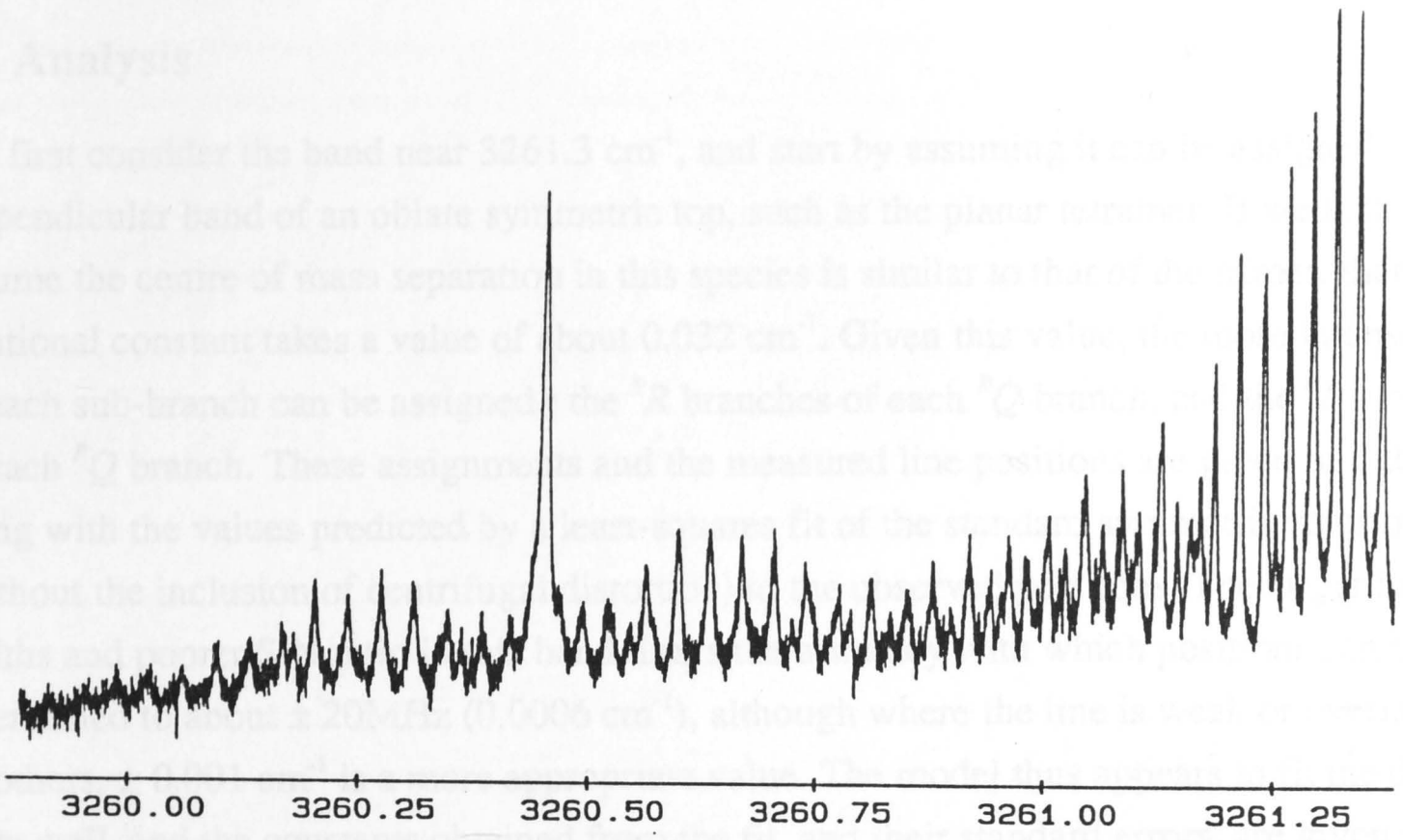


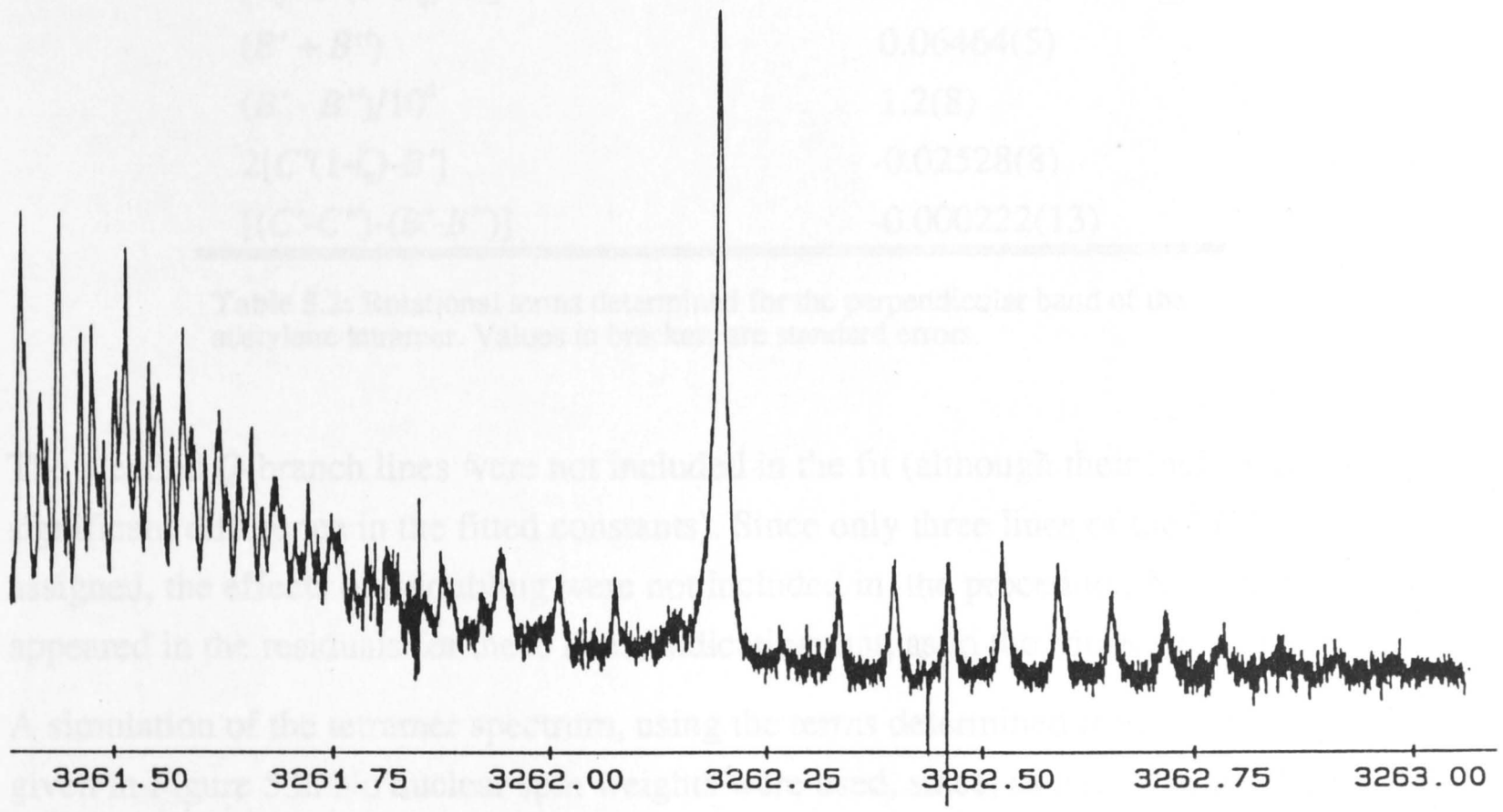


**Figure 5.1:** Scan through the region of band A

## 5.2 Analysis

We first consider the band near 3261.3 $cm^{-1}$, and start by assuming it can be assigned to the perpendicular band of an oblate symmetric top, such as the planar tetramer. If we further assume the centre of mass separation in this species is similar to that of the trimer, then the B rotational constant takes a value of about 0.032 $cm^{-1}$. Given this value, the more intense lines of each sub-branch can be assigned : the ${}^{R}R$ branches of each ${}^{R}Q$ branch, and the ${}^{P}P$ branches of each ${}^{P}Q$ branch. These assignments and the measured line positions are given in Table 5.1, along with the values predicted by a least-squares fit of the standard symmetric rotor model (without the inclusion of centrifugal distortion) to the observed positions. The larger line-widths and poorer S/N ratio in this band limits the accuracy with which positions can be determined to about ± 20MHz (0.0006 $cm^{-1}$), although where the line is weak or overlapped by others, ± 0.001 $cm^{-1}$ is a more appropriate value. The model thus appears to fit the data quite well, and the constants obtained from the fit, and their standard errors, are given in Table 5.2.

| | |
|---|---|
| $[\nu_0+C'(1-2\zeta)-B']$ | 3261.29317(16) |
| $(B' + B'')$ | 0.06464(5) |
| $(B' - B'')/10^4$ | 1.2(8) |
| $2[C'(1-\zeta)-B']$ | -0.02528(8) |
| $[(C'-C'')-(B'-B'')]$ | -0.000222(13) |

**Table 5.2:** Rotational terms determined for the perpendicular band of the acetylene tetramer. Values in brackets are standard errors.

The blended $Q$-branch lines were not included in the fit (although their inclusion made no significant difference in the fitted constants). Since only three lines of the ${}^{R}R_1$ branch were assigned, the effects of $l$-doubling were not included in the procedure. No abnormalities appeared in the residuals for these lines, indicating that, as in the trimer, $q$ is very small.

A simulation of the tetramer spectrum, using the terms determined from the above fit, is given in Figure 5.2. No nuclear spin weights were used, since, as indicated in (Weber 1988) the effects on intensities will be small. Each line was convolved with a Lorentzian function with a half-width of 100MHz, which is the linewidth determined by Miller *et.al.* (1984b). A rotational temperature of 1K was assumed. As in the trimer, the intensities of the experimental and simulated spectra are only in qualitative agreement, and reasons for this have been discussed.

| $J'$ | $K'$ | $J''$ | $K''$ | Observed | Calculated | Difference |
|---|---|---|---|---|---|---|
| 8 | 6 | 9 | 7 | 3260.8796 | 3260.8784 | 0.0012 |
| 7 | 5 | 8 | 6 | 3260.9195 | 3260.9205 | -0.0010 |
| 7 | 6 | 8 | 7 | 3260.9435 | 3260.9429 | 0.0006 |
| 6 | 5 | 7 | 6 | 3260.9837 | 3260.9849 | -0.0012 |
| 4 | 0 | 5 | 1 | 3260.9953 | 3260.9953 | 0.0000 |
| 5 | 3 | 6 | 4 | 3261.0036 | 3261.0033 | 0.0003 |
| 6 | 6 | 7 | 7 | 3261.0078 | 3261.0073 | 0.0005 |
| 4 | 1 | 5 | 2 | 3261.0195 | 3261.0199 | -0.0004 |
| 5 | 4 | 6 | 5 | 3261.0260 | 3261.0266 | -0.0006 |
| 4 | 2 | 5 | 3 | 3261.0448 | 3261.0441 | 0.0007 |
| 5 | 5 | 6 | 6 | 3261.0485 | 3261.0494 | -0.0009 |
| 3 | 0 | 4 | 1 | 3261.0597 | 3261.0598 | -0.0001 |
| 4 | 3 | 5 | 4 | 3261.0681 | 3261.0678 | 0.0003 |
| 3 | 1 | 4 | 2 | 3261.0845 | 3261.0845 | 0.0000 |
| 4 | 4 | 5 | 5 | 3261.0903 | 3261.0911 | -0.0008 |
| 3 | 2 | 4 | 3 | 3261.1088 | 3261.1086 | 0.0002 |
| 2 | 0 | 3 | 1 | 3261.1245 | 3261.1244 | 0.0001 |
| 3 | 3 | 4 | 4 | 3261.1332 | 3261.1324 | 0.0008 |
| 2 | 1 | 3 | 2 | 3261.1490 | 3261.1490 | 0.0000 |
| *J* | 6 | *J* | 5 | 3261.1630 | - | |
| 2 | 2 | 3 | 3 | 3261.1736 | 3261.1732 | 0.0004 |
| 1 | 0 | 2 | 1 | 3261.1891 | 3261.1890 | 0.0001 |
| *J* | 4 | *J* | 3 | 3261.2150 | - | |
| *J* | 3 | *J* | 2 | 3261.2408 | - | |
| 0 | 0 | 1 | 1 | 3261.2536 | 3261.2536 | 0.0000 |
| *J* | 2 | *J* | 1 | 3261.2682 | - | |
| *J* | 1 | *J* | 0 | 3261.2935 | - | |
| *J* | 0 | *J* | 1 | 3261.3184 | - | |
| *J* | 1 | *J* | 2 | 3261.3432 | - | |
| *J* | 2 | *J* | 3 | 3261.3676 | - | |
| *J* | 3 | *J* | 4 | 3261.3922 | - | |
| 2 | 2 | 1 | 1 | 3261.3973 | 3261.3970 | 0.0003 |
| *J* | 4 | *J* | 5 | 3261.4151 | - | |
| 2 | 1 | 1 | 0 | 3261.4230 | 3261.4225 | 0.0005 |
| 3 | 3 | 2 | 2 | 3261.4345 | 3261.4357 | -0.0012 |
| *J* | 5 | *J* | 6 | 3261.4366 | - | |
| 2 | 0 | 1 | 1 | 3261.4474 | 3261.4476 | -0.0002 |
| 3 | 2 | 2 | 1 | 3261.4613 | 3261.4617 | -0.0004 |
| 4 | 4 | 3 | 3 | 3261.4737 | 3261.4741 | -0.0004 |
| 3 | 1 | 2 | 0 | 3261.4877 | 3261.3872 | |
| 4 | 3 | 3 | 2 | 3261.5013 | 3261.5005 | 0.0008 |
| 5 | 5 | 4 | 4 | 3261.5125 | 3261.5120 | 0.0005 |
| 4 | 2 | 3 | 1 | 3261.5268 | 3261.5264 | 0.0004 |
| 5 | 4 | 4 | 3 | 3261.5387 | 3261.5388 | -0.0001 |
| 6 | 6 | 5 | 5 | 3261.5496 | 3261.5495 | 0.0001 |
| 5 | 3 | 4 | 2 | 3261.5646 | 3261.5652 | -0.0006 |
| 6 | 5 | 5 | 4 | 3261.5772 | 3261.5768 | 0.0004 |
| 6 | 4 | 5 | 3 | 3261.6033 | 3261.6036 | -0.0003 |
| 5 | 1 | 4 | 0 | 3261.6169 | 3261.6167 | 0.0002 |
| 6 | 3 | 5 | 2 | 3261.6288 | 3261.6300 | -0.0012 |
| 7 | 5 | 6 | 4 | 3261.6418 | 3261.6416 | 0.0002 |
| 6 | 2 | 5 | 1 | 3261.6561 | 3261.6559 | 0.0002 |
| 7 | 4 | 6 | 3 | 3261.6680 | 3261.6684 | -0.0004 |
| 8 | 5 | 7 | 4 | 3261.7065 | 3261.7064 | 0.0001 |
| 7 | 2 | 6 | 1 | 3261.7211 | 3261.7207 | 0.0004 |

**Table 5.1:** Observed and calculated line positions (in $cm^{-1}$) in the perpendicular band of the acetylene tetramer

Four parameters cannot be determined from the fit: the band origin, $\nu_0$, $C'$, $C''$, and the Coriolis constant $\zeta$. Without the aid of other spectroscopic information on the tetramer, it remains to examine the possible constraints to obtain further insight into the interpretation of the

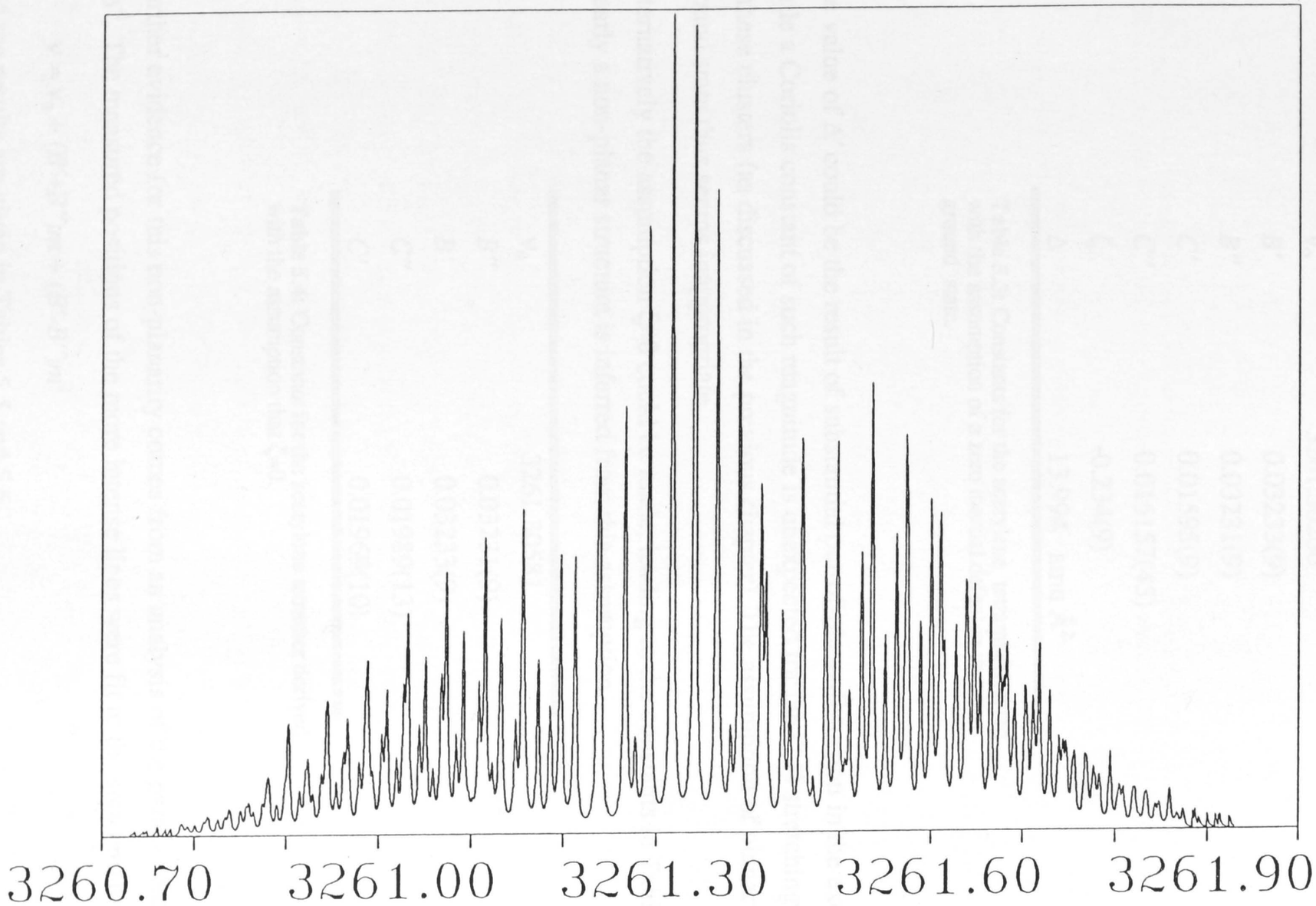


**Figure 5.2:** Simulation of the tetramer spectrum using a rotational temperature of 1K and a Lorentzian lineshape of 100MHz FWHM.

spectrum. If the tetramer is assumed to be planar in the ground state with a zero inertial defect ($B''= 2C''$), then the molecular constants that can be derived from the rotational terms become those in Table 5.3

| | |
|---|---|
| $\nu_0$ | 3261.30206 |
| $B'$ | 0.03233(9) |
| $B''$ | 0.03231(9) |
| $C'$ | 0.01595(9) |
| $C''$ | 0.016157(45) |
| $\zeta$ | -0.234(9) |
| $\Delta$ | 13.994 amu Å$^2$ |

**Table 5.3:** Constants for the acetylene tetramer derived with the assumption of a zero inertial defect in the ground state.

The value of $\Delta'$ could be the result of substantial out-of-plane distortion in the excited state, while a Coriolis constant of such magnitude is unexpected for the C-H stretching vibrations in these clusters (as discussed in the previous chapter). The assumption of planarity in the ground state thus seems inappropriate.

Alternatively the assumption $\zeta$=0 could be made, leading to the constants in Table 5.4. Clearly a non-planar structure is inferred from this assumption.

| | |
|---|---|
| $\nu_0$ | 3261.30581 |
| $B''$ | 0.03231(9) |
| $B'$ | 0.03233(9) |
| $C''$ | 0.01989(13) |
| $C'$ | 0.01969(10) |

**Table 5.4:** Constants for the acetylene tetramer derived with the assumption that $\zeta$=0.

Further evidence for this non-planarity comes from an analysis of the parallel band at 3262.2 cm$^{-1}$. The measured positions of the more intense lines were fit to the standard expression

$$\nu = \nu_0 + (B'+B'')m + (B'-B'')m^2$$

and the results are given in Tables 5.5 and 5.6

| $J'$ | $J''$ | Observed | Calculated | Residual |
|---|---|---|---|---|
| 3 | 4 | 3261.9420 | 3261.9425 | -0.0005 |
| 2 | 3 | 3262.0080 | 3262.0077 | 0.0003 |
| 1 | 2 | 3262.0729 | 3262.0727 | 0.0002 |
| 3 | 2 | 3262.3313 | 3262.3308 | 0.0005 |
| 4 | 3 | 3262.3955 | 3262.3950 | 0.0005 |
| 5 | 4 | 3262.4583 | 3262.4589 | -0.0006 |
| 6 | 5 | 3262.5214 | 3262.5227 | -0.0013 |
| 7 | 6 | 3262.5864 | 3262.5863 | 0.0001 |
| 8 | 7 | 3262.6504 | 3262.6497 | 0.0007 |

**Table 5.5:** Observed and calculated line positions (in $cm^{-1}$) for the parallel band of the acetylene tetramer

| | |
|---|---|
| $\nu_0$ | 3262.2021(4) |
| $(B'+B'')$ | 0.06455(9) |
| $(B'-B'')$ | -0.000086(24) |
| $B'$ | 0.03223(5) |
| $B''$ | 0.03232(5) |

**Table 5.6:** Rotational constants from the parallel band of the acetylene tetramer.

Despite the small number of lines used in the fit, it is apparent that the ground state value of $B$ is the same for this band as for the perpendicular band, indicating that the two bands should be assigned to the same species. In the planar tetramer the $\nu_3$ vibration in the acetylene monomer correlates with vibrations of symmetry $A_g+B_g+E_u$, and only one IR active vibration is expected ($E_u$). Reducing the symmetry of the cluster to $C_4$ by allowing for out-of-plane twisting of the monomer sub-units results in vibrations of symmetry A+B+E from this monomer mode. This leads to two bands: a parallel and a perpendicular band, of symmetries A and E respectively. Possible tetramer structures will be considered in the next section.

The parallel band at 3260.5$cm^{-1}$ can be analysed in the same way as the tetramer parallel band. The results are given in Tables 5.7 and 5.8.

| $J'$ | $J''$ | Observed | Calculated | Residual |
|---|---|---|---|---|
| 7 | 6 | 3260.7054 | 3260.7054 | 0.0000 |
| 6 | 5 | 3260.6702 | 3260.6701 | 0.0001 |
| 5 | 4 | 3260.6345 | 3260.6346 | -0.0001 |
| 4 | 3 | 3260.5991 | 3260.5991 | 0.0000 |
| 3 | 4 | 3260.3130 | 3260.3131 | -0.0001 |
| 4 | 5 | 3260.2772 | 3260.2771 | 0.0001 |
| 5 | 6 | 3260.2411 | 3260.2410 | 0.0001 |
| 6 | 7 | 3260.2047 | 3260.2048 | -0.0001 |

**Table 5.7:** Observed and calculated line positions (in $cm^{-1}$) for the parallel band of the pentamer.

| | |
|---|---|
| $\nu_0$ | 3260.45658(4) |
| $(B'+B'')$ | 0.035756(9) |
| $(B'-B'')$ | -0.000030(4) |
| $B'$ | 0.01789(1) |
| $B''$ | 0.01786(1) |

**Table 5.8:** Rotational constants from the parallel band of the acetylene pentamer.

The $B$ rotational constant is consistent with a cyclic pentamer in which the centre of mass spacing is similar to that found in the tetramer. However, in $C_{5h}$ symmetry, the $\nu_3$ vibration correlates with $A'+E'_1+E'_2$, and only one IR active vibration ($E'_1$) is expected. Again, this perpendicular band could take on the appearance of a parallel band if $\zeta$ is near -1, but as in the other clusters, it is more likely to be close to zero. Removing the constraint of a horizontal plane of symmetry leads to two IR active vibrations from $\nu_3$ : $A+ E_1$. It seems reasonable to assign this band to the A vibration of a cyclic pentamer, but there remains the question of the location of the $E_1$ perpendicular band of the same species.

## 5.3 Discussion

As in the acetylene dimer, two bands have been connected by identical ground state rotational constants, and in this case have been assigned to the acetylene tetramer. Unlike the dimer bands, these are very close together ($\approx 1$ $cm^{-1}$ separation), indicating that the monomer units in this cluster must be in very similar positions, and it therefore seems reasonable to retain the four-fold axis of symmetry suggested above. The question remains as to which point group, amongst the likely candidates $C_{4h}$, $C_4$ and $S_4$, is compatible with the observations. The set of rotational constants obtained for the tetramer are in marked contrast with those of the trimer. While no significant change in $B$ is seen, the change in $C$ is relatively large.

For the $C_{4h}$ tetramer,

$$I_{cc} = 4MR^2 + 4I_{HCCH}$$

using the notation of previous chapters. From the value of $C''$ derived with the assumption of planarity in the ground state, R=3.11 Å is obtained, which in turn means an intermolecular separation of 4.41 Å. This is consistent with values of the latter in the dimer, trimer and solid (4.35-4.4 Å).

Large changes in the $C$ rotational constant may result from Coriolis coupling between the vibrational modes arising from $\nu_3$ (Wollrab 1967). Such an interaction between the E and the A or B vibrations would be symmetry-allowed for the point-groups mentioned, and could be expected to be strong, given the likely proximity of these levels. It is interesting to speculate on the possibility that the cluster has $C_{4h}$ symmetry, and that parallel band stems from an intensity borrowing through an interaction between the $E_u$ and $A_g$ vibrations. However, as for the $\zeta$ constant for the E vibration, the nature of the vibrations, namely that they are principally "monomeric", means the coupling constant will be very small. In addition, no such effects are seen in the trimer spectrum.

In $C_4$ symmetry the values of the rotational constants are still primarily determined by R, and if we accept that the set obtained using the assumption $\zeta$=0 are more realistic, $C''$ suggests a value of R of only 2.8 Å, and therefore an intermolecular separation of ≈ 4 Å. This point group thus appears inappropriate.

The derived constants can be reproduced by staggering the acetylene monomers above and below a horizontal plane, in a manner similar to the stacking of the molecules in the unit cell of the solid phase(s) (Figure A.2). Note that this staggering affects the $B$ constant, but not $C$, and that the cluster needs to have higher than two-fold symmetry in order that only two vibrational bands are observed. For this structure,

$$I_{bb} = 4Md^2 + 2MR^2 + 2I_{HCCH}(1+\sin^2\varphi)$$

$$I_{cc} = 4MR^2 + 4I_{HCCH}\cos^2\varphi$$

where $\varphi$ is the out-of-plane twisting angle, and $d$ is the spacing of the pairs of molecules above and below the plane. This structure is depicted in Figure 5.3. As in the trimer, the angle $\beta$ cannot be determined from this work. Assuming R=2.8 Å, one set of parameters consistent with the rotational constants is $d$=0.89 Å and $\varphi$=27°. Although this set is probably not unique, the intermolecular separation in this structure is 4.34 Å, in good agreement with other cluster values.

The assumption that the intermolecular separation should be similar in all of the cluster geometries is supported by *ab initio* calculations on the dimer (Alberts 1988). For both staggered-parallel and T-shaped forms essentially the same monomer centre-of-mass separation is predicted.

It is interesting to note that in the work in (Bryant 1988), estimates of the ratio of the parallel/perpendicular band intensities by Eggers predict a similar value of φ by assuming that the transition dipole moments of these bands are simply the vector components of the molecular moment.

Accepting the $S_4$ structure, the decrease in $C$ on going from the ground to excited state, suggests either a decrease in φ and/or an increase in R. For no change in $B$ to occur an increase in the height of the monomer units above and below the plane upon excitation is required. While this rearrangement of the cluster upon vibrational excitation may be a consequence of the "Sheppard effect" (Sandorfy 1984), i.e. the tighter binding of hydrogen bonded complexes when the X-H donor is vibrationally excited, the cancellation of the effects of these changes on $B$ does seem rather fortuitous. Although Coriolis effects cannot be dismissed entirely, the $S_4$ structure does appear to be the most consistent option.

In the case of the pentamer band, only two point groups, $C_5$ and $C_{5h}$, are likely. The fact that only one band has been observed makes choosing between the two difficult. It is possible that, as in the tetramer, the other band that is expected is shifted to the red of the parallel band, into regions not investigated in this work. This shift is not likely to be very large, given the small difference observed between the tetramer band origins. Another possibility is that the band is diffuse, being broadened due to a short excited state lifetime. This would imply a mode-dependent dissociation lifetime, which is also not seen in the tetramer, and this explanation is therefore doubtful. Once again, the values of $B$ change very little between ground and excited states, and are consitent with the intermolecular distances mentioned above.

The inference of structural parameters from observed rotational constants (and changes in them) in the preceding discussion should be tempered by the fact that large amplitude motions can be expected for the monomer units of these clusters (Kolenbrander 1988), which can have profound effects on terms such as the inertial defect.

In their study of the infrared spectra of HCN clusters, Jucks and Miller (1988c) observed two bands in the C-H stretching region which they assigned to the HCN tetramer. No sharp rotational structure was observed, and they could not distinguish between linear or cyclic structures. While the cyclic structures have been indicated in the acetylene case, even with an analysis of the rotational structure, the determination of cluster geometry cannot be unequivocal.

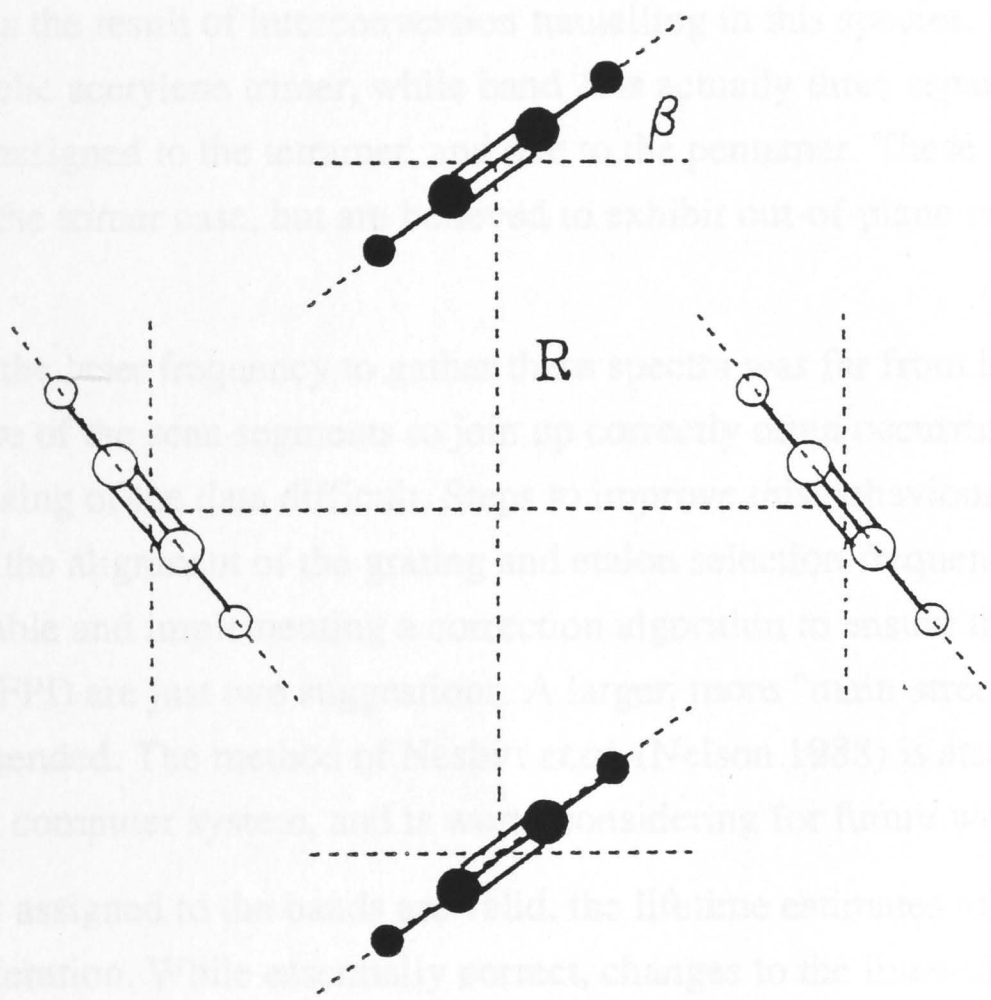


**Figure 5.3:** Possible structure for the acetylene tetramer. Solid monomers are below the plane of the page a distance $d$, while open monomers are above it. In addition, each monomer is twisted out of the horizontal plane, about its centre-of-mass, by an angle $\varphi$.

# Chapter 6: Conclusion

The high-resolution scans of the acetylene cluster bands presented in this work have shown that the assignments of cluster species to each by Fischer *et.al.* are essentially correct.

Bands C-F belong to the acetylene dimer, and constitute two bands, parallel (C) and perpendicular (D-F) bands of a T-shaped structure. While not identified in this work, it has been shown in work elsewhere (Fraser 1988, Ohshima 1988) that the splitting of ro-vibrational transitions in this bands is the result of interconversion tunnelling in this species. Band B belongs to the planar, cyclic acetylene trimer, while band A is actually three separate bands, two of which have been assigned to the tetramer, and one to the pentamer. These larger clusters are cyclic, as in the trimer case, but are believed to exhibit out-of-plane twisting of the monomer units.

The method of scanning the laser frequency to gather these spectra was far from ideal. Mode-hopping and failure of the scan segments to join up correctly often occurring, making the collection and processing of the data difficult. Steps to improve this behaviour would be well advised. Improving the alignment of the grating and etalon selection frequencies with, for example, a look-up table and implementing a correction algorithm to ensure the segments join (using the scanning FPI) are just two suggestions. A larger, more "main-stream" microcomputer is also recommended. The method of Nesbitt *et.al.* (Nelson 1988) is attractive for it's independence from a computer system, and is worth considering for future work.

While the cluster species assigned to the bands are valid, the lifetime estimates of Fischer *et.al.* need further consideration. While essentially correct, changes to the linewidths in perturbed transitions are noticeable. There appears to be a dependence of the dissociation lifetime on the value of $K$ in the state with the "free" monomer excited - the lifetime decreases with increasing $K$. This is not the case in the state in which the "bound" monomer is vibrationally excited, where the linewidths do not depend on $K$. The trimer lines are actually highly overlapped, and their width has been found to depend on the trimer rotational temperature. The tetramer bands contain both isolated and overlapped transitions, but the former indicate that the estimate of 100 MHz for the transition linewidth to be correct. This value also applies to the pentamer parallel band. There is a general trend for theses linewidths to increase with cluster size and so with the density of vibrational states imbedded in the continuum. Whether this increase represents shorter dissociation lifetimes, or faster vibrational relaxation through coupling with other states, has been the subject of debate since work on the spectroscopy of van der Waals systems began.

The relatively high density of states occurring in such species at these vibrational frequencies can have pronounced effects on the observed rotational structure. In the dimer spectra, a large number of perturbations in the upper states have been observed, but the states responsible, and so the type of interaction (Fermi or Coriolis), remain unidentified. Coriolis interactions may play a role in determining the large inertial defects and changes in axial rotational constants observed in the dimer and tetramer. Against this stands the trimer spectrum, apparently free from such effects.

The intermolecular potential function of acetylene has been the investigated on several occasions (Marchi 1985, LeSar 1987), and the failure of a number of models to predict the stability of the orthorhombic phase over the cubic at low temperature is notable in these studies. The proposed cluster geometries presented here may be of some relevance to the search for a suitable potential model. They all indicate that a weak hydrogen-bonding interaction is important, which is not surprising since acetylene has been found to behave both as a proton donor and acceptor in various heterogeneous dimers (Peterson 1985) and while the effects are not as dramatic, one feature typical to hydrogen bonded clusters is present, separating the acetylene clusters from classical van der Waals species like $(CO_2)_n$. This is the shifting of the X-H vibrational frequencies to the red of the unbound value, and the tendency for this shift to increase with cluster size. This shift is due to the weakening of the X-H bond, and increasing the number of interactions in which each molecule participates enhances this effect.

Accompanying the weakening of this bond is an increase in the X-H distance. However, in all of the examinations of cluster geometry presented here, the intramolecular distances have been fixed at the monomer values. *Ab initio* calculations on the dimer and trimer (Alberts 1988) have shown that the C-H bond of the proton "donor" does increase, but the change is very small (0.001-0.002 ). In other theoretical work on large clusters (simulating the solid state), the trend for the C-H length to increase with cluster size has also been established (Popelier 1988). Unfortunately no experimental verification of this exists, or can come from the work in this thesis.

Further spectroscopic studies of the acetylene clusters would be useful. Isotope substitution experiments could help determine parameters such as the angle $\beta$ in the trimer structure (Figure 4.2) and the extent of out-of-plane twisting in the tetramer and pentamer, although in these larger species the many, possibly overlapping, bands would be observed, unless pure isotopes were used. Note that the approximately 5-10% of tetramers and pentamers will contain one $^{13}C$ atom (in one of two isomers, depending on whether the H atom to which it is bonded is "bound" or "free"), based on this isotopes natural abundance. The rotational features of these species are probably buried under the three main bands in the 3261 $cm^{-1}$ region. Searches for further bands assignable to the pentamer should be carried out, since at

least one other band is predicted. The spectra of the clusters in the regions of other vibrations would also bring useful information, and is in fact already under way (Takami 1988). One band accessible to the F-centre laser is $\nu_1$, the symmetric C-H stretch. In addition, measurements using a single, orthogonal laser crossing, such as those performed on $CO_2$ clusters (Pine 1988a), could be useful in confirming the vibrational origin of the trimer band assigned here, and in studying the role of state mixing on lifetimes in the case of the dimer.

Reduction of the final state rotational temperatures obtained here (1-2K) by reducing the source pressure and/or increasing the concentration of acetylene seeded in helium would provide a greater number of transitions in the cluster bands, from which further refinement of the derived rotational constants could be possible (such as accounting centrifugal distortion).

A great deal of information can be obtained from high-resolution studies of clusters, as is evidenced by the number of groups undertaking such studies, principally on dimeric systems. As well as structural parameters, information on the dynamics of these weakly bound species is becoming available. Extending these measurements to larger and larger clusters is confounded by the ever increasing density of vibrational states, and as a result studies at low frequency may prove more successful. Efforts to do so can only help strengthen the links between solid-state and molecular physics.

# Appendix A: The Infrared Spectrum of Acetylene in the 3μm Region

In this appendix information available in the literature on the IR absorption spectrum of gaseous and solid acetylene in the region of the IR active C-H stretching vibration is gathered together, and a discussion on the ro-vibrational transitions of the monomer observed in the molecular beam is included.

## A.1 Gas Phase Acetylene

The five normal modes of acetylene are shown in Figure A.1, along with their respective symmetry species. The asymmetric stretching vibration $\nu_3$, and the doubly degenerate bend $\nu_5$ are IR active, and the remainder are Raman active (the rule of exclusion applies).

The absorptions of acetylene in the 3μm region have been studied by a several workers (Lafferty 1964, Scott 1966, Palmer 1972, Ghersetti 1975), who have identified a number of bands in the room-temperature spectrum. These bands have been examined at elevated temperatures (Rinsland 1982), leading to a revision of some of the ro-vibrational assignments of the hot-bands. Most prominent in the region are the two close lying bands originating from the ground state of $^{12}C_2H_2$ (natural abundance ≈ 98%), assigned to $\nu_3$ and a combination band $\nu_2 + \nu_4 + \nu_5$ (subsequently abbreviated $\nu_{245}$) that gains intensity through a Fermi resonance interaction with $\nu_3$ (interaction strength : 6.46 $cm^{-1}$ (Lafferty 1964)). In addition to these, a number of hot bands originating from the $\nu_4$ and $\nu_5$ levels have been identified, as well as similarly assigned bands for the $H^{13}C^{12}CH$ species using both enriched and naturally occuring samples (natural abundance ≈ 2%).

Under the expansion conditions used to obtain the acetylene cluster spectra one can expect a strong cooling of the rotational degrees of freedom of the monomer, limiting the observed transitions to those with low $J$-values ($J \leq 5$-10). Vibrational degrees of freedom are far less efficiently cooled, and it would not be surprising to see some of the hot band transitions in the beam. At room temperature the two closely spaced $\nu_4$ and $\nu_5$ levels have significant populations - about 13.8% of all $^{12}C_2H_2$ molecules are in these levels.

A number of absorptions in which the excitation was carried to the bolometer were observed in the cluster spectra, and most of these can be assigned to known monomer transitions. The remainder are rather weak and of unknown origin.

Three transitions in the $\nu_{245}$ band and two in the $\nu_3$ band of $^{12}C_2H_2$ were observed in different cluster bands. Their positions measured with respect to water absorptions, given in Table A.1, are compared to the positions measured by Lafferty with a high resolution Fourier-transform spectrometer (Bomem) calibrated against these water transitions (Lafferty 1988).

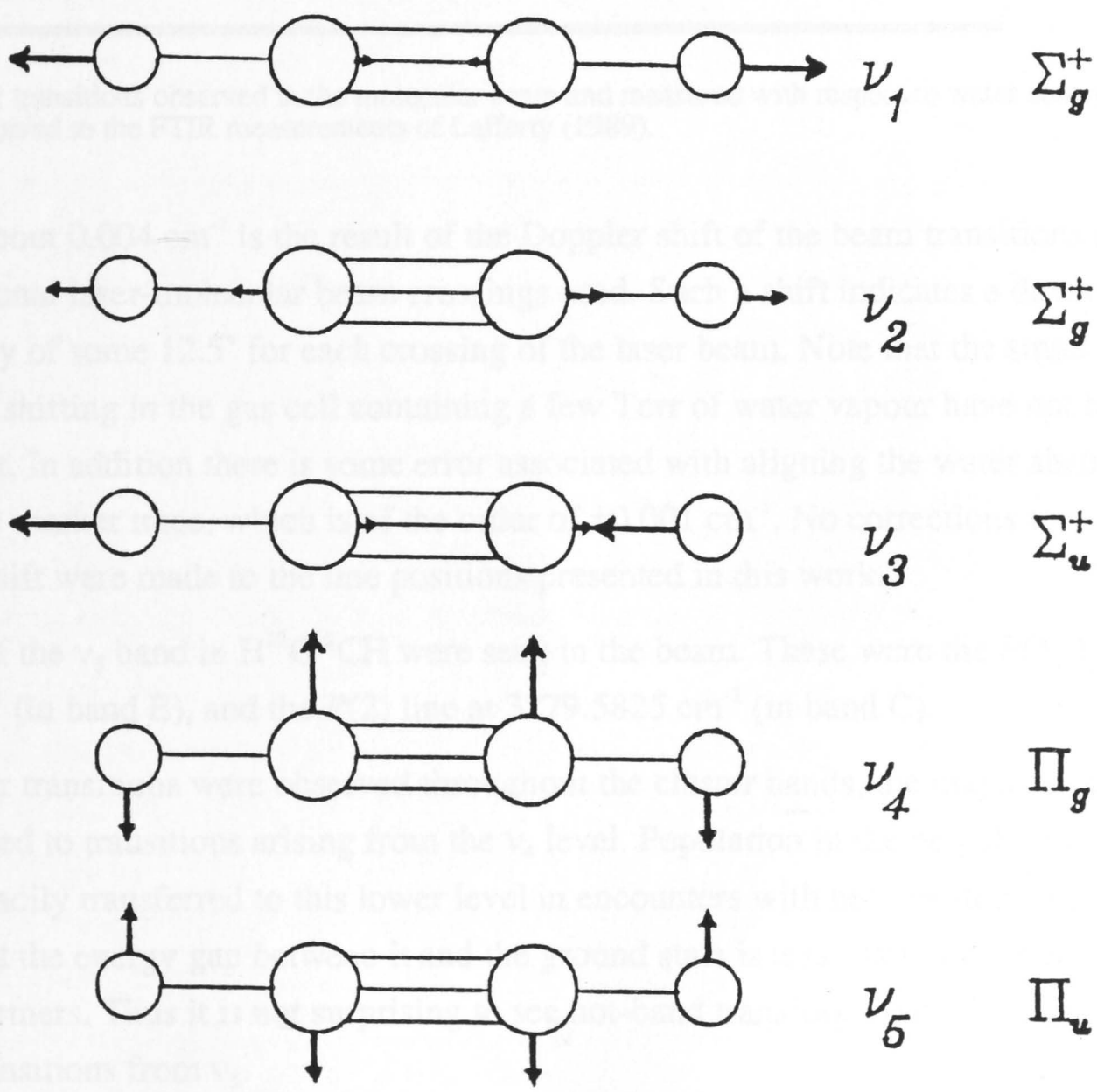


**Figure A.1:** The atomic displacements and symmetry species of the fundamental vibrations in the acetylene molecule. The frequencies these vibrations are 3374, 1974, 3295, 612 and 729 $cm^{-1}$ respectively.

| Band | Transition | Measured | FTIR | Diff./$10^{-3}$ |
|---|---|---|---|---|
| F | $\nu_{245} R(0)$ | 3284.2418 | 3284.2459 | -4.1 |
| D | $\nu_{245} P(1)$ | 3279.5428 | 3279.5475 | -4.7 |
| C | $\nu_{245} P(4)$ | 3272.4345 | 3272.4378 | -3.3 |
| F | $\nu_3$ $P(4)$ | 3285.3727 | 3285.3767 | -4.0 |
| E | $\nu_3$ $P(5)$ | 3282.9868 | 3282.9897 | -2.9 |

**Table A.1:** Monomer transitions observed in the molecular beam and measured with respect to water absorptions. These are compared to the FTIR measurements of Lafferty (1989).

The red shift of about 0.004 $cm^{-1}$ is the result of the Doppler shift of the beam transitions due to the non-orthogonal laser-molecular beam crossings used. Such a shift indicates a deviation from orthogonality of some 12.5° for each crossing of the laser beam. Note that the small effect of pressure shifting in the gas cell containing a few Torr of water vapour have not been taken into account. In addition there is some error associated with aligning the water absorption peak with the marker trace, which is of the order of $\pm 0.001$ $cm^{-1}$. No corrections to account for this shift were made to the line positions presented in this work.

Two transitions of the $\nu_3$ band in $H^{13}C^{12}CH$ were seen in the beam. These were the $P(1)$ line at 3281.8924 $cm^{-1}$ (in band E), and the $P(2)$ line at 3279.5825 $cm^{-1}$ (in band C).

A number of other transitions were observed throughout the cluster bands, the majority of which are attributed to transitions arising from the $\nu_4$ level. Population in the neighbouring $\nu_5$ level would be readily transferred to this lower level in encounters with helium atoms during the expansion, but the energy gap between it and the ground state is less easily imparted to these collision partners. Thus it is not surprising to see hot-band transitions out of $\nu_4$, but no corresponding transitions from $\nu_5$.

Four transitions in the band assigned to $\nu_2+2\nu_4+\nu_5-\nu_4$ by Rinsland *et.al.* (1982) were observed, and the measured positions are given in Table A.2. At the resolution provided by the laser-molecular beam combination the *l*-splitting of these low-*J* transitions is easily measured. In the case of the $P(4)$ line only one component was apparent.

The intensity alternation observed in the doublets is due to the spin-statistiacl weights of the lower levels, and can be used to fix the sign of the *l*-doubling constant. The splitting in each doublet is given by

$$\Delta\nu = (q'+q'')m + (q'-q'')m^2$$

| Band | Transition | Position | Intensity |
|---|---|---|---|
| D | R(3) | 3278.9188 | w |
| | | 3278.8459 | s |
| B | P(2) | 3264.8281 | w |
| | | 3264.8102 | s |
| A | P(3) | 3262.4568 | s |
| | | 3262.4348 | w |
| A | P(4) | 3260.0561 | s |
| | | - | - |

**Table A.2:** Transitions in the $010(21)^1$-$0001^10$ hot band observed in the molecular beam. w:weak, s:strong

where $q'$ and $q''$ are the $l$-doubling constants of the upper and lower states respectively, and $m$ takes the usual meaning. Note that this ignores the higher-order $J$-dependence of the $l$-doubling, which is reasonable for low $J$. The three values of $\Delta\nu/m$ lie on a straight line, with a slope and intercept that lead to values of -0.00679 and -0.00524 for $q'$ and $q''$ respectively. The latter agrees well with the value for $q_4$ determined by Horneman *et.al.* (1989) to be -0.005232(1).

The remainder are isolated rotational transitions from various vibrational bands, and these are summarised in Table A.3. It is interesting to note that several transitions from the $2\nu_4^0$ and $2\nu_5^0$ levels have been assigned. Approximately 1.7% of all HCCH molecules would be in the $2\nu_4/\nu_4+\nu_5/2\nu_5$ levels at room temperature, and presumably this population would remain in the lowest of these levels after expansion from the nozzle source.

| Band | Position | Assignment |
|---|---|---|
| A | 3260.7944 | $R(0)$ $010(31)_+^0$-$0002^20^0$ |
| D | 3279.2821 | $R(1)$ $0011^10$-$0001^10$ |
| | 3279.2605 | ($H^{13}CCH$) |
| E | 3282.3188 | $R(1)$ $0012^00$-$0002^00$ |

**Table A.3:** Other hot-band transitions observed in the cluster bands.

## A.2 Low Temperature Solutions and Matrices

The infrared spectra of solutions of acetylene in liquid nitrogen (77K) and liquid oxygen (90-120K) have been examined by Borgest and Kolomiitsova (1969). The $\nu_3$ vibrational frequency was found to be red-shifted, while the bending vibrations are shifted to the blue. As a result, the unperturbed positions of the levels $\nu_3$ and $\nu_{245}$ are reversed from that found in the free molecule: in oxygen the level separation ($\nu_{245}$-$\nu_3$) is 4 $cm^{-1}$, and in nitrogen it is 18 $cm^{-1}$, which should be compared with -0.55 $cm^{-1}$ in gaseous acetylene. As a result the Fermi resonance between the two levels is considerably weaker in these phases, since, assuming the coupling of the levels remains unchanged upon dissolution, the strength of the interaction will depend directly upon the separation of the levels. In the case of the liquid nitrogen solutions, the combination band is much weaker than the fundamental.

Similar effects have been seen in the spectra of acetylene in nitrogen and oxygen matrices at 20K (Bagdanskis 1972), while in an argon matrix the shifts in acetylene vibrational frequencies are relatively small, and the similarity in the intensities of the two bands observed in free molecule is also seen here.

## A.3 Crystalline Acetylene

Acetylene has two solid forms (at ambient pressures): between 133 and 193K the crystal structure is cubic, while below 133K it is orthorhombic. The unit cell for the low temperature structure is given in Figure A.2 (Koski 1975).

The infrared spectrum of polycrystalline samples of the orthorhombic phase of acetylene have been studied by Bottger and Eggers (1964). A weak band near 3331 $cm^{-1}$ was assigned to $\nu_{245}$, while the fundamental was found near 3226 $cm^{-1}$, red-shifted some 66 $cm^{-1}$ from the unperturbed gas-phase frequency. No absorptions due to the *g* molecular fundamentals were observed.

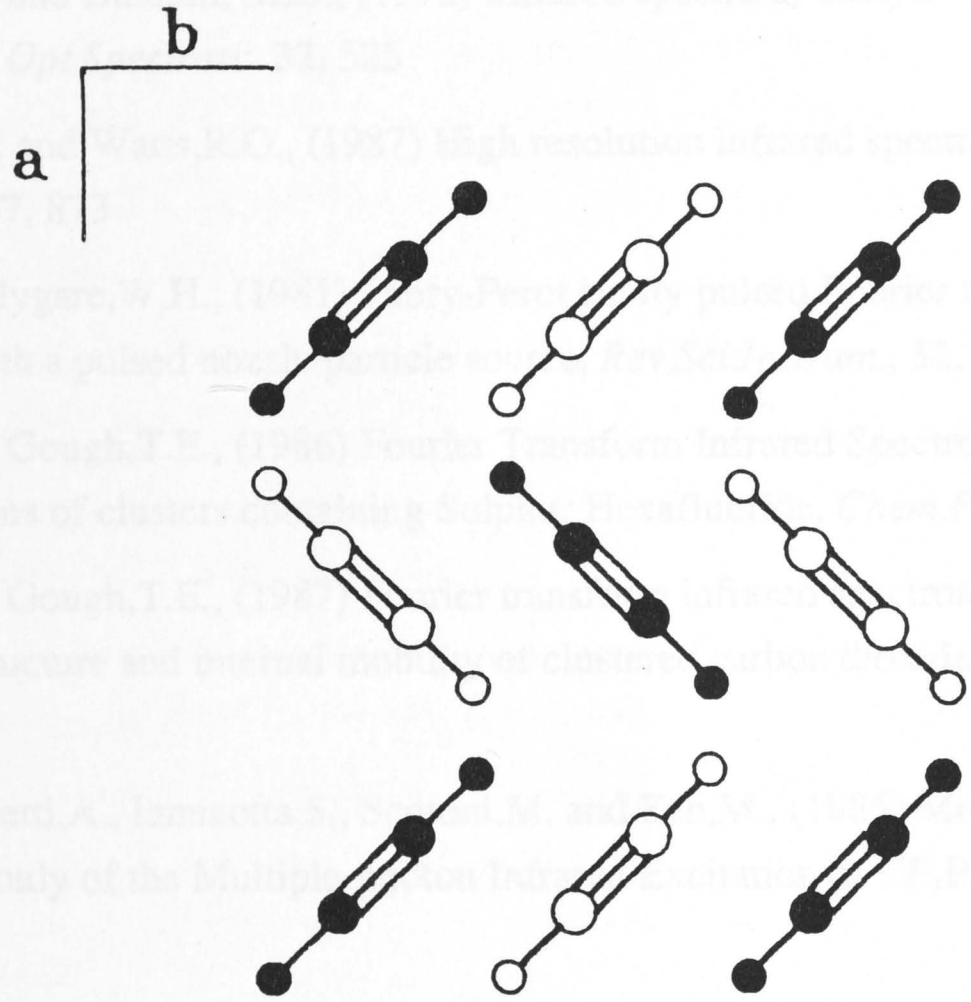


**Figure A.2:** The unit cell in the low temperature phase of crystalline acetylene. **a:** 6.188, **b:** 6.001, and **c:** 5.546 Å (Koski 1975).

# Bibliography


Alberts,I.L., Rowlands,T.W. and Handy,N.C., (1988) Stationary points on the potential energy surfaces of $(C_2H_2)_2$, $(C_2H_2)_3$ and $(C_2H_4)_2$, *J.Chem.Phys.* **88**, 3811

Aoyama,T., Matsuoka,O. and Nakagawa,N., (1979) Ab Initio Hartree-Fock Calculations on Acetylene Dimer, *Chem.Phys.Letts.*, **67**, 508

Bagdanskis,N.I. and Bulanin, M.O., (1972) Infrared spectra of acetylene in matrices at low temperatures II, *Opt.Spectrosc.* **32**, 525

Baldwin,K.G.H. and Watts,R.O., (1987) High resolution infrared spectra of ethylene clusters, *J.Chem.Phys.*, **87**, 873

Balle,T.J. and Flygare,W.H., (1981) Fabry-Perot cavity pulsed Fourier transform microwave spectrometer with a pulsed nozzle particle source, *Rev.Sci.Instrum.*, **52**, 33

Barnes,J.A. and Gough,T.E., (1986) Fourier Transform Infrared Spectroscopy of Supersonic Jets: Observations of clusters containing Sulphur Hexafluoride, *Chem.Phys.Letts.*, **130**, 297

Barnes,J.A. and Gough,T.E., (1987) Fourier transform infrared spectroscopy of molecular clusters: The structure and internal mobility of clustered carbon dioxide, *J.Chem.Phys.*, **86**, 6012

Bassi,D., Boschetti,A., Iannaotta,S., Scotoni,M. and Zen,M., (1985) Molecular Beam Opto-thermal Study of the Multiple-photon Infrared Excitation of $CF_3Br$, *Laser Chem.*, **5**, 143

Bender,D., Eliades,M., Danzeiser,D.A., Jackson,M.W. and Bevan,J.W., (1987) The gas-phase infrared spectrum of $\nu_1$ and $\nu_1$-$\nu_4$ HCN-HF, *J.Chem.Phys.*, **86**, 1225

Beswick,J.A. and Jortner,J., (1981) Intramolecular Dynamics of van der Waals Molecules, *Adv.Chem.Phys.* **47**, part1, 363

Blass,W.E. and Halsey,G.W., (1981) Deconvolution of Absorption Spectra, Academic Press, New York

Bordé,Ch.J., Salomon,Ch., Avriller,S.,Van Lerberghe,A., Bréant,Ch., Bassi,D. and Scoles,G., (1984) Optical Ramsey fringes with travelling waves, *Phys.Rev.*, **A30**, 1836

Borgest,V.A. and Kolomiitsova,T.D. (1969) Fermi resonance in the infrared spectra of acetylene in solution, *Opt.Spectrosc.*, **27**, 128

Bottger,G.L. and Eggers,D.F., (1964) Infrared Spectra of Crystalline $C_2H_2$,$C_2HD$ and $C_2D_2$, *J.Chem.Phys.*, **40**, 2010

Boughton,C.V., Miller,R.E., Vorhalik,P.F. and Watts,R.O., (1986) The helium-hydrogen fluoride differential scattering cross section, *Mol.Phys.*, **58**, 827

Boughton,C.V., Miller,R.E. and Watts,R.O., (1982) Infrared Laser Spectroscopy of Molecular Beams, *Aust.J.Phys.*, **35**, 611

Boughton,C.V., Miller,R.E. and Watts,R.O., (1985) The methane-methane total differential scattering cross section, *Mol.Phys.*, **56**, 363

Brand, J.C.D., (1972) Band Contour Analysis, in Spectroscopy, Ramsay,D.A. (Ed), Physical Chemistry Series One, **3**, 155, MTP International Reviews of Science, Butterworths.

Brumer,P. and Shapiro,M., (1985) Theoretical Aspects of Photodissociation and Intramolecular Dynamics, *Adv.Chem.Phys.*, **60**, 371

Bryant,G.W., Eggers,D.F. and Watts,R.O., (1988) High-resolution infrared spectroscopy of acetylene clusters, *J.Chem.Soc.Farad.Trans.2*, **84**, 1443

Bryant,G.W., Eggers,D.F. and Watts,R.O., (1988) High-resolution infrared spectrum of acetylene tetramer, *Chem.Phys.Letts.* **151**, 309

Buck,U. and Meyer,H., (1986a) Electron bombardment fragmentation of Ar van der Waals clusters by scattering analysis, *J.Chem.Phys.*, **84**, 4854

Buck,U., Kesper,J., Miller,R.E., Rudolph,A. and Vigue,J., (1986b) Laser bolometric detection of long-lived and predissociating electronically excited states, *Chem.Phys.Letts.*, **125**, 257

Buckingham,A.D., Fowler,P.W. and Stone,A.J., (1986) Electrostatic predictions of shapes and properties of Van der Waals molecules, *Int.Rev.Phys.Chem.*, **5**, 107

Camy-Peyret,C., Flaud,J.M., Guelachvili,G. and Amiot,C., (1973) High-resolution Fourier transform spectrum of water between 2930 and 4255 $cm^{-1}$, *Mol.Phys.*, **26**, 825

Cartwright,G.J. and Mills,I.M., (1970) *l*-Resonance Perturbations in Infrared Perpendicular Bands, *J.Mol.Spectrosc.*, **34**, 415

Casassa,M.P., Stephenson,J.C. and King,D.S., (1986) Vibrational Predissociation of the Nitric Oxide Dimer, *Faraday Discuss.Chem.Soc.*, **82**, 251

Casassa,M.P. (1988) Direct time-resolved observations of vibrational energy flow in weakly bound complexes, *Chem.Rev.* **88**, 215

Castleman,A.W. and Keesee,R.G., (1986) Clusters: Properties and Formation, *Ann.Rev.Phys.Chem.*, **37**, 525

Cavallini,M., Gallinaro,G. and Scoles,G., (1967) High Sensitivity Bolometer Detector for Molecular Beams, *Z.Naturf.*, **A22**, 413

Celii,F.G. and Janda,K.C., (1986) Vibrational Spectroscopy, Photochemistry and Photophysics of Molecular Clusters, *Chem.Rev.*, **86**, 507

Coker,D.F., Miller,R.E. and Watts,R.O., (1985) The infrared predissociation spectra of water clusters, *J.Chem.Phys.*, **82**, 3554

Coulombe,M.J. and Pine,A.S., (1979) Linear scan control of tunable lasers using a scanning Fabry-Perot, App.Optics, **18**, 1505

Dam,N., Liedenbaum,C., Stolte,S. and Reuss,J., (1987) Rotational Distributions in Seeded Molecular Beams, *Chem.Phys.Letts.*, **136**, 73

Danielson,L.J., McLeod,K.M. and Keil,M., (1987) Damping of total differential cross sections: Observations and empirical anisotropic potentials for $HeC_2H_2$ and HeOCS, *J.Chem.Phys.*, **87**, 239

DeLeon,R.L. and Muenter,J.S., (1984) Vibrational predissociation in the hydrogen fluoride dimer, *J.Chem.Phys.*, **80**, 6092

Demtröder,W., (1982) Laser Spectroscopy,Basic Concepts and Instrumentation, Springer-Verlag, Berlin

Douketis,C., Anex,D., Ewing,G. and Reily,J.P., (1985) High Resolution Overtone Spectroscopy of $H_2O$ in a Molecular Beam, *J.Phys.Chem.*, **89**, 4173

Dyke,T.R., (1984) Microwave and Radiofrequency Spectra of Hydrogen-Bonded Complexes, Top.Curr.Chem., **120**, 85

Dyke,T.R., Howard,B.J. and Klemperer,W., (1972) Radiofrequency and Microwave Spectrum of the Hydrogen Fluoride Dimer: a Nonrigid Molecule , *J.Chem.Phys.*, **56**, 2442

Eggers,D.F. (1986) private communication

Ewing,G., (1982) Relaxation Channels of Vibrationally Excited Van der Waals Molecules, *Faraday Discuss.Chem.Soc.*, **73**, 325

Fischer,G., Miller,R.E., Vorhalik,P.F. and Watts,R.O., (1985) Molecular beam infrared spectra of dimers formed from acetylene, methyl acetylene and ethene as a function of source pressure and concentration, *J.Chem.Phys.*, **83**, 1471

Fraser,G.T., Nelson,Jr.,D.D., Charo,A. and Klemperer,W., (1985) Microwave and infrared characterisation of several weakly bound $NH_3$ complexes, *J.Chem.Phys.*, **82**, 2535

Fraser,G.T. and Pine,A.S., (1986) van der Waals potentials from the infrared spectra of rare gas-HF complexes, *J.Chem.Phys.*, **85**, 2502

Fraser,G.T., Pine,A.S., Lafferty,W.J. and Miller,R.E., (1987) Sub-Doppler infrared spectrum of the carbon dioxide trimer, *J.Chem.Phys.*, **87**, 1502

Fraser,G.T., Suenram,R.D., Lovas,F.J., Pine,A.S., Hougen,J.T., Lafferty,W.J. and Muenter,J.S., (1988) Infrared and microwave investigations of interconversion tunnelling in the acetylene dimer, *J.Chem.Phys.* **89**, 6028

Fraser,G.T. (1989) Vibrational exchange upon interconversion tunnelling in $(HF)_2$ and $(HCCH)_2$, *J.Chem.Phys.* **90**, 2097

German,K.R., (1986) Optimization of $F_A$(II) and $F_B$(II) color-center lasers, *J.Opt.Soc.Am.B.*, **3**, 149

Ghersetti,S., Baldacci,A., Giorgianni,S., Barnes,R. and Rao,K.N., (1975) Infrared Spectra of the carbon-13 isotopic varieties of acteylene, monodeuteroacetylene and dideuteroacetylene, *Gazz.Chim.Italiana*, **105**, 875

Gough,T.E., Miller,R.E. and Scoles,G., (1977) Infrared laser spectroscopy of molecular beams, *Appl.Phys.Letts.*, **30**, 338

Gough,T.E., Miller,R.E. and Scoles,G., (1978) Photo-induced vibrational predissociation of the van der Waals molecule $(N_2O)_2$, *J.Chem.Phys.* **69**, 1588

Gough,T.E., Miller,R.E. and Scoles,G., (1981a) Infrared Spectra and Vibrational Predissociation of $(CO_2)_n$ Clusters Using Laser-Molecular Beam Techniques, *J.Phys.Chem.* **85**, 4041

Gough,T.E., Miller,R.E. and Scoles,G., (1981b) Sub-Doppler Resolution Infrared Molecular-beam Spectroscopy, *Faraday Discuss.Chem.Soc.*, **71**, 77

Gough,T.E., Gravel,D. and Miller,R.E., (1981c) Multiple crossing devices for laser-molecular beam spectroscopy, *Rev.Sci.Instrum.*, **52**, 802

Gough,T.E., Orr,B.J. and Scoles,G., (1983) Laser-Stark Spectroscopy of Carbon Dioxide in a Molecular Beam, *J.Mol.Spectrosc.*, **99**, 143

Gutowsky,H.S., Klots,T.D., Carl Chuang, Schuttenmaer,C. and Emilsson,T., (1987) Rotational spectra and structures of the $Ar_2$-H/DF trimers, *J.Chem.Phys.*, **86**, 569

Halberstadt,N., Brechignac,Ph., Beswick,J.A. and Shapiro,M., (1985) Theory of mode specific vibrational predissociation: the HF dimer, *J.Chem.Phys.*, **84**, 170

Hartung,C. and Jurgeit,R., (1979) Laser Spectroscopy using an Optothermal Reciever, *Opt.Spectrosc.*, **46**, 660

Herzberg,G., (1945) Molecular Spectra and Molecular Structure II.Infrared and Raman Spectra of Polyatomic Molecules, D.Van Nostrand, New York

Horneman,V.M., Alanko,S. and Hietaner,J. (1989) Difference band $\nu_5$-$\nu_4$ of acetylene $C_2H_2$, *J.Mol.Spectrosc.*, **135**, 191

Howard,B.J. and Pine,A.S., (1985) Rotational Predissociation and Libration in the Infrared Spectrum of Ar-HCl, *Chem.Phys.Letts.* **122**, 1

Huang,Z.S. and Miller,R.E., (1987) Infrared spectroscopy and vibrational predissociation of $C_2H_2$-HF, *J.Chem.Phys.*, **86**, 6059

Huang,Z.S. and Miller,R.E. (1988) Sub-Doppler resolution infrared spectroscopy of water dimer, *J.Chem.Phys.* **88**, 8008

Huisken,F. and Pertsch,T., (1987) Infrared photodissociation and cluster-specific detection of internally cold $(C_2H_4)_n$ van der Waals complexes, *J.Chem.Phys.*, **86**, 106

Jackson,D.J., Gerhardt,H. and Hänsch,T.W., (1981) Doppler-free optogalvanic spectroscopy using an infrared color center laser, *Opt.Comm.*, **37**, 23

Jackson,M.W., Wofford,B.A. and Bevan,J.W., (1987) Predissociating fundamental vibrations of DCN-DF, *J.Chem.Phys.*, **86**, 2518

Janda,K.C., (1985) Predissociation of Polyatomic van der Waals Molecules, *Adv.Chem.Phys.*, **60**, 201

Jucks,J.W., Huang,Z.S, Dayton,D., Miller,R.E. and Lafferty,W.J., (1987a) The structure of the carbon dioxide dimer from near infrared spectroscopy, *J.Chem.Phys.*, **86**, 4341

Jucks,K.W. and Miller,R.E., (1987b) The effect of vibrational state mixing on the predissociation lifetime of $\nu_1$ excited OC-HF, *J.Chem.Phys.*, **86**, 6637

Jucks,K.W., Huang,Z.S., Miller,R.E., Fraser,G.T., Pine,A.S. and Lafferty,W.J. (1988a) Structure and vibrational dyynamics of the $CO_2$ dimer from the sub-Doppler infrared spectrum of the 2.7μm Fermi diad, *J.Chem.Phys.* **88**, 2185

Jucks,K.W. and Miller,R.E. (1988b) Infrared spectroscopy of the hydrogen cyanide dimer, *J.Chem.Phys.* **88**, 6059

Jucks,K.W. and Miller,R.E. (1988c) Near-infrared spectroscopic observation of the linear and cyclic isomers of the hydrogen cyanide trimer, *J.Chem.Phys.* **88**, 2196

Kaspar,J.V.V., Pollock,C.R., Curl,R.F. and Tittel,F.K., (1982) Computer control of broadly tunable lasers: conversion of a color center laser into a high resolution laser spectrometer, *App.Optics*, **21**, 236

Kidd,I.F. and Baltini-Kurti,G.G., (1986) Infrared Predissociation of the Ar-HD van der Waals Molecule, *Faraday Discuss.Chem.Soc.*, **82**, 241

Klemperer,W., (1974) Molecular Spectroscopy of Loosely Bound Complexes, *Ber.Bunsenges.Phys.Chem.*, **78**, 128

Kolenbrander,K.D. and Lisy,J.M., (1986) Vibrational Predissocistion Spectroscopy of binary HF-base complexes, *J.Chem.Phys.*, **85**, 2463

Kolenbrander,K.D., Dykstra,C.E. and Lisy,J.M., (1988) Torsional vibrational modes of $(HF)_3$: IR-IR double resonance spectroscopy and electrical interaction theory, *J.Chem.Phys.*, **88**, 5995

Kornilov,S.T., Ostreikovskii,I.V. and Protsenko,E.D., (1985) Optothermal spectroscopy of ethylene using a tunable waveguide $CO_2$ laser, *Sov.J.Quantum Electron.*, **15**, 1574

Koski,H.K. and Sándor,E. (1975) The low-temperature phase of solid acetylene-$d_2$, *Acta Cryst.*, **B31**, 487

Kyrö,E.K., Shoja-Chagervand,P., Eliades,M., Danzeiser,D. and Bevan,J.W., (1986) Simple color center laser optothermal molecular beam spectrometer for high resolution infrared spectroscopy, *Rev.Sci.Instrum.*, **57**, 1

Kyrö,E.K., Warren,R., McMillan,K., Eliades,M., Danzeiser,D., Shoja-Chaghervand,P., Lieb,S.G. and Bevan,J.W., (1983) Preliminary rovibrational analysis of the $n\nu_6+\nu_1-n\nu_6$ vibration in HCN-HF, *J.Chem.Phys.*, **78**, 5881

Lafferty,W.J. (1988) unpublished results

Lafferty,W.J. and Thibault,R.J., (1964) High Resolution Infrared Spectra of $^{12}C_2H_2$, $^{12}C^{13}CH_2$ and $^{13}C_2H_2$, *J.Mol.Spectrosc.*, **14**, 79

Legon,A.C., (1983) Pulsed-Nozzle Fourier Transform Microwave Spectroscopy of Weakly Bound Dimers, *Ann.Rev.Phys.Chem.*, **34**, 275

Legon,A.C. and Millen,D.J., (1986) Gas-Phase Spectroscopy and the Properties of Hydrogen-Bonded Dimers: HCN-HF as the Spectroscopic Prototype, *Chem.Rev.*, **86**, 635

LeRoy,R.J., Corey,G.C. and Hutson,J.M., (1982) Predissociation of Weak-anisotropy Van der Waals Molecules:Theory, Approximations and Practical Predictions, *Faraday Discuss.Chem.Soc.*, **73**, 339

LeRoy,R.J. and Hutson,J.M., (1987) Improved potential energy surfaces for the interaction of $H_2$ with Ar,Kr and Xe, *J.Chem.Phys.*, **86**, 837

LeSar,R. (1987) Calculated high-pressure properties of solid acetylene and possible polymerization paths, *J.Chem.Phys.*, **86**, 1485

Levy,D.H., (1981) Van der Waals Molecules, *Adv.Chem.Phys.*, **47**, 323

Liu,Shi-Yi, Michael,D.W., Dykstra,C.E. and Lisy,J.M., (1986a) The stabilities of the hydrogen fluoride trimer and tetramer, *J.Chem.Phys.*, **84**, 5032

Liu,Shi-Yi and Dykstra,C.E., (1986b) A Theory of Vibrational Transition Frequency Shifts Due to Hydrogen Bonding, *J.Phys.Chem.*, **90**, 3097

Li,C., Mu,G. and Bao,Y., (1984) A New Optothermal Detector of Infrared Multiple Photon Absorption, *Chem.Phys.Letts.*, **106**, 356

Lovejoy,C.M., Schuder,M.D. and Nesbitt,D.J., (1986) High sensitvity,high-resolution IR laser spectroscopy in slit supersonic jets : Application to $N_2HF$ $\nu_1$ and $\nu_5+\nu_1-\nu_5$, *J.Chem.Phys.*, **85**, 4890

Lovejoy,C.M. and Nesbitt,D.J., (1987a) High resolution IR laser spectroscopy of van der Waals complexes in slit supersonic jets:Observation and analysis of $\nu_1$, $\nu_1+\nu_2$ and $\nu_1+2\nu_3$ in ArHF, *J.Chem.Phys.*, **86**, 3151

Lovejoy,C.M., Schuder,M.D. and Nesbitt,D.J., (1987b) Direct IR laser absorption spectroscopy of jet-cooled $CO_2HF$ complexes:Analysis of the $\nu_1$ HF stretch and a surprisingly low frequency $\nu_6$ intermolecular $CO_2$ bend, *J.Chem.Phys.*, **86**, 5337

Low,F.J., (1961) Low-Temperature Germanium Bolometer, *J.Opt.Soc.Am.*, **51**, 1300

Marchi,M. and Righini,R., (1985), Intermolecular potential and lattice dynamics of orthorhombic acetylene, *Chem.Phys.*, **94**, 465

Maroncelli,M., Hopkins,G.A., Nibler,J.W. and Dyke,T.R., (1985) Coherent Raman and infrared spectroscopy of HCN complexes in free jet expansions and in equilibrium samples, *J.Chem.Phys.*, **83**, 2129

Marshall,M.D., Charo,A., Leung,H.O. and Klemperer,W., (1985) Characterization of the lowest $\Pi$ bending state of Ar-HCI by far infrared laser-stark spectroscopy and molecular beam electric resonance, *J.Chem.Phys.* **83**, 4924

McKellar,A.R.W., (1982) Infrared Spectra of Hydrogen-rare-gas Van der Waals Molecules, *Faraday Discuss.Chem.Soc.*, **73**, 89

Michael,D.W. and Lisy,J.M., (1986) Vibrational predissociation spectroscopy of $(HF)_3$, *J.Chem.Phys.*, **85**, 2528

Miller,R.E., (1982) Infrared laser spectroscopy of molecular beams using a room-temperature beam detector:Application to the study of translational freezing in free-jet expansions, *Rev.Sci.Instrum.*, **53**, 1719

Miller,R.E., Watts R.O. and Ding,A.D., (1984a) Vibrational Predissociation Spectra of Nitrous Oxide Clusters, *Chem.Phys.*, **83**, 155

Miller,R.E., Vorhalik,P.F. and Watts,R.O., (1984b) Sub-Doppler resolution infrared spectroscopy of the acetylene dimer:A direct measure of the predissociation lifetime, *J.Chem.Phys.*, **80**, 5453

Miller,R.E., (1986) Infrared Laser Photodissociation and Spectroscopy of van der Waals Molecules, *J.Phys.Chem.*, **90**, 3301

Miller,R.E. (1988) The vibrational spectroscopy and dynamics of weakly bound neutral complexes, *Science*, **240**, 447

Mills,I.M., (1972) Vibration-Rotation Structure in Asymmetric and Symmetric Top Molecules, in Molecular Spectroscopy: Modern Research, **3**, Rao,K.N. and Mathews,C.W. (Ed.), Academic Press, New York

Mitchell,A., McAuliffe,M.J., Giese,C.F. and Gentry,W.R., (1985) A new upper limit to the vibrational predissociation lifetime of the ethylene dimer excited at 950 $cm^{-1}$, *J.Chem.Phys.*, **83**, 4271

Mollenauer,L.F., (1985) Color Center Lasers, in Laser Handbook, Stitch,M.L. and Bass,M. (Eds.), North-Holland, **4**, 143

Nelson,D.D., Schiffman,A., Lykke,K.R. and Nesbitt,D.J. (1988) A simple F-center laser spectrometer for continuous single-frequency scans, *Chem.Phys.Letts.* **153**, 105

Nemes,I. (1981) Sum Rules for Vibration-Rotation Interaction Coefficients, in Vibrational Spectra and Structure, **10**, 395

Nesbitt,D.J. (1988) High-resolution infrared spectroscopy of weakly bound molecular complexes, *Chem.Rev.*, **88**, 815

Ohashi,N. and Pine,A.S., (1984) High resolution spectrum of the HCl dimer, *J.Chem.Phys.*, **81**, 73

Ohshima,Y., Matsumoto,Y., Takami,M. and Kuchitsu,K. (1988) The structure and tunnelling motion of acetylene dimer studied by free-jet infrared absorption spectroscopy in the 14μm region, *Chem.Phys.Letts.*, **147**, 1

Palmer,K.F., Mickelson,M.E. and Rao,K.N., (1972) Investigations of Several Infrared Bands of $^{12}C_2H_2$ and Studies of the Effects of Vibrational Rotational Interactions, *J.Mol.Spectrosc.*, **44**, 131

Peet,A.C., Clary,D.C. and Hutson,J.M., (1986) Vibrational Predissociation of the Ethylene Dimer, *Faraday Discuss.Chem.Soc.*, **82**, 327

Pendley,R.D. and Ewing,G.E., (1983) The infrared absorption spectra of $(HCCH)_2$ and $(DCCD)_2$, *J.Chem.Phys.* **78**, 3531

Peterson,K.I., Fraser,G.T., Nelson,D.D.Jr. and Klemperer,W., (1985) Intermolecular interactions involving the first row hydrides: Spectroscopic studies of complexes of HF, $H_2O$, $NH_3$ and HCN, in Comparison of Ab-Initio Quantum Chemistry with Experiment for Small Molecules - The State of the Art., Bartlett,R.J.(Ed.), Reidel, Holland

Pine,A.S., Lafferty,W.J. and Howard,B.J., (1984) Vibrational predissociation,tunneling and rotational saturation in the HF and DF dimers, *J.Chem.Phys.*, **81**, 2939

Pine,A.S. and Fraser,G.T. (1988a) Vibrational, rotational and tunnelling dependence of vibrational predissociation in the HF dimer, *J.Chem.Phys.* **89**, 6636

Pine,A.S. and Fraser,G.T., (1988b) Vibrational predissociation in the $CO_2$ dimer and trimer and rare gas $CO_2$ complexes, *J.Chem.Phys.*, **89**, 100

Pine,A.S. and Howard,B.J., (1986) Hydrogen bond energies of the HF and HCl dimers from absolute infrared intensities, *J.Chem.Phys.*, **84**, 590

Pritchard,D., Muenter,J. and Howard,B.J., (1987) Infrared Vibration-Rotation Spectrum of Acetylene Trimer, *Chem.Phys.Letts.*, **135**, 9

Pritchard,D.G., Nandi,R.N. and Muenter,J.S. (1988) Microwave and infrared studies of acetylene dimer in a T-shaped configuration, *J.Chem.Phys.*, **89**, 115

Pubanz,G.A., Maroncelli,M. and Nibler,J.W., (1985) CARS spectra of van der Waals Complexes:The Structure of the $CO_2$ Dimer, *Chem.Phys.Letts.*, **120**, 313

Rinsland,C.P., Baldacci,A. and Rao,K.N., (1982) Acetylene bands observed in carbon stars: A laboratory study and an illustrative example of its application to IRC+10216, *Astrophys.J.Supp.*, **49**, 487

Ruoff,R.S., Emilsson,T., Klots,T.D., Chuang,C. and Gutowsky,H.S. (1988) Rotational spectrum and structure of the linear hydrogen cyanide trimer, *J.Chem.Phys.*, **89**, 138

Sakai,K., Koide,A. and Kihara,T., (1977) Intermolecular Forces for Hydrogen, Nitrogen and Acetylene, *Chem.Phys.Letts.*, **47**, 416

Sandorfy,C., (1984) Vibrational Spectra of Hydrogen Bonded Systems in the Gas Phase, *Top.Curr.Chem.*, **120**, 41

Saykally,R. and Gudeman,C.S., (1984) Velocity Modulation Infrared Laser Spectroscopy of Molecular Ions, *Ann.Rev.Phys.Chem.*, **35**, 387

Scott,J.F. and Rao,K.N., (1966) Infrared Absorption Bands of Acetylene. Part III Analysis of the Bands at 3μm, *J.Mol.Spectrosc.*, **20**, 438

Snels,M., Fantoni,R., Zen,M., Stolte,S. and Reuss,J., (1986) van der Waals Modes and Rotational Fine Structure in $C_2H_4$ Dimers, *Chem.Phys.Letts.*, **124,** 1

Takami,M., Ohshima,Y., Yamamoto,S. and Matsumoto,Y., (1988) Free-jet Absorption Spectroscopy of Stable and Unstable Molecular Species, *Faraday Discuss.Chem.Soc.*, **84**, 1

Truhlar,D.G., (1984) Resonances in Electron-Molecule Scattering, van der Waals Complexes and Reactive Chemical Dynamics, American Chemical Society, Washington DC, ACS Symp.Ser.No.263

Vernon,M.F., Lisy,J.M., Krajnovich,D.J., Tramer,A., Kwok,H.S., Shen,Y.R. and Lee,Y.T., (1982) Vibrational Predissociation Spectra and Dynamics of Small Molecular Clusters of $H_2O$ and HF, *Faraday Discuss.Chem.Soc.*, **73**, 387

Vernon,M.F., Lisy,J.M., Kwok,H.S., Krajnovich,D.J., Tramer,A., Shen,Y.R. and Lee,Y.T., (1981) Vibrational Predissociation of Benzene Dimers and Trimers by the Crossed Laser-Molecular Beam Technique, *J.Phys.Chem.*, **85**, 3327

Vorhalik,P.F., (1986) Structure and Dynamics from Molecular Beam Experiments, Thesis, Research School of Physical Sciences, Australian National University

Wallenstein,R. and Hänsch,T.W., (1974) Linear Pressure Tuning of a Multielement Dye Laser Spectrometer, *App.Optics*, **13**, 625

Walsh,M.A., England,T.H., Dyke,T.R. and Howard,B.J., (1987) Pulsed molecular beam infrared absorption spectroscopy of carbon dioxide dimer, *Chem.Phys.Letts.*, **142**, 265

Weber,A., (1980) Ro-vibronic species, overall allowed species,and nuclear spin statistical weights for symmetric top molecules belonging to the $D_{nd}$ and $D_{nh}$ ($n \leq 6$) point-groups, *J.Chem.Phys.*, **73**, 3952

Weber,A., (1982) Ro-vibronic species, overall allowed species, and nuclear spin statistical weights for symmetric top molecules.II.Point Groups $C_{nv}$ and $C_{nh}$ ($n \leq 6$), *J.Chem.Phys.*, **76**, 3694

Weber,A. (1987) ed., Structure and Dynamics of Weakly Bound Molecular Complexes, NATO ASI Series, **C212**, Reidel, Dordrecht

Weber,A. (1988) Nuclear spin statistical weights for the trimers and tetramers of $C_2H_2$ and $C_2HD$ and $CO_2$, *J.Chem.Phys.* **88**, 3428

Wofford,B.A., Bevan,J.W., Olson,W.B. and Lafferty,W.J., (1986a) Rotational Analysis of the $\nu_5^1$ Band in the HCN-HF Hydrogen Bonded Cluster, *Chem.Phys.Letts.*, **124**, 579

Wofford,B.A., Bevan,J.W., Olson,W.B. and Lafferty,W.J., (1986b) Rotational analysis and vibrational predissociation in the $\nu_2$ band of HCN dimer, *J.Chem.Phys.*, **85**, 105

Wollrab,J.E. (1967) Rotational Spectra and Molecular Structure, Academic Press, New York

Zwerdling,S., Smith,R.A. and Theriault,J.P., (1968) A fast,high-responsivity bolometer detector for the very-far infrared, *Infrared Phys.*, **8**, 271